Farey Sequences and the Riemann Hypothesis

Darrell Cox

Abstract

Relationships between the Farey sequence and the Riemann hypothesis other than the Franel-Landau theorem are discussed.

1 Introduction

The Farey sequence F_x of order x is the ascending series of irreducible fractions between 0 and 1 whose denominators do not exceed x. In this article, the fraction 0/1 is not considered to be in the Farey sequence. The number of fractions in F_x is $A(x) := \sum_{i=1}^{x} \phi(i)$ where ϕ is Euler's totient function. For $v = 1, 2, 3, ..., A(x)$ let δ_v denote the amount by which the vth term of the Farey sequence differs from $v/A(x)$. Franel (in collaboration with Landau) [1] proved that the Riemann hypothesis is equivalent to the statement that $|\delta_1| + |\delta_2| + ... + |\delta_{A(x)}| = o(x^{\frac{1}{2}+\epsilon})$ for all $\epsilon > 0$ as $x \to \infty$. Let $M(x)$ denote the Mertens function ($M(x) := \sum_{i=1}^{x} \mu(i)$ where $\mu(i)$ is the Möbius function). Littlewood [2] proved that the Riemann hypothesis is equivalent to the statement that for every $\epsilon > 0$ the function $M(x)x^{-(1/2)-\epsilon}$ approaches zero as $x \to \infty$. Mertens conjectured that $|M(x)| < \sqrt{x}$. This was disproved by Odlyzko and te Riele [3]. The Stieltjes hypothesis states that $M(x) = O(x^{\frac{1}{2}})$.

2 An Upper Bound of $|M(x)|$

Lehman [4] proved that $\sum_{i=1}^{x} M(\lfloor x/i \rfloor) = 1$. In general, $\sum_{i=1}^{x} M(\lfloor x/(in) \rfloor) = 1$, $n = 1, 2, 3, ..., x$ (since $\lfloor \lfloor x/n \rfloor / i \rfloor = \lfloor x/(in) \rfloor$). Let R' denote a square matrix where element (i, j) equals 1 if j divides i or 0 otherwise. (In a Redheffer matrix, element (i, j) equals 1 if i divides j or if $j = 1$. Redheffer [5] proved that the determinant of such a x by x matrix equals $M(x)$.) Let T denote the matrix obtained from R' by element-by-element multiplication of the columns by $M(\lfloor x/1 \rfloor)$, $M(\lfloor x/2 \rfloor)$, $M(\lfloor x/3 \rfloor)$, ..., $M(\lfloor x/x \rfloor)$. Let U denote the matrix obtained from T by element-by-element multiplication of the columns by $\phi(j)$. The sum of the columns of U then equals $A(x)$. $i = \sum_{d|i} \phi(d)$, so $\sum_{i=1}^{x} M(\lfloor x/i \rfloor) i$ (the sum of the rows of U) equals $A(x)$.

Theorem (1) $\sum_{i=1}^{x} M(\lfloor x/i \rfloor) i = A(x)$

By the Schwarz inequality, $A(x)/\sqrt{x(x+1)(2x+1)/6}$ is a lower bound of $\sqrt{\sum_{i=1}^{x} M(\lfloor x/i \rfloor)^2}$. See Figure 1 for a plot of $\sum_{i=1}^{x} M(\lfloor x/i \rfloor)^2$ for $x = 2, 3, 4, ..., 10000$. Let $\Lambda(i)$ denote the Mangoldt function ($\Lambda(i)$ equals $\log(p)$ if $i = p^m$ for some prime p and some $m \geq 1$ or 0 otherwise). Mertens [6] proved that $\sum_{i=1}^{x} M(\lfloor x/i \rfloor) \log(i) = \psi(x)$ where $\psi(x)$ denotes the second Chebyshev function ($\psi(x) := \sum_{i \leq x} \Lambda(i)$). Let $\sigma_x(i)$ denote the sum of positive divisors function ($\sigma_x(i) := \sum_{d|i} d^x$). Replacing $\phi(j)$ with $\log(j)$ in the U matrix gives a similar result.

Theorem (2) $\sum_{i=1}^{x} M(\lfloor x/i \rfloor) \log(i) \sigma_0(i)/2 = \log(x!)$

The following conjecture is based on data collected for $x \leq 10000$.

Conjecture (1) $\log(x!) \geq \sum_{i=1}^{x} M(\lfloor x/i \rfloor)^2 \geq \psi(x)$

By Stirling's formula, $\log(x!) = x\log(x) - x + O(\log(x))$. Since $\log(x)$ increases more slowly than any positive power of x, this is a better upper bound of $\sum_{i=1}^{x} M(\lfloor x/i \rfloor)^2$ than $x^{1+\epsilon}$ for any $\epsilon > 0$.

3 Shorter Intervals of Farey Points

Let $r_1, r_2, ..., r_{A(x)}$ denote the terms of the Farey sequence of order x and let $h(\xi)$ denote the number of r_v less than or equal to ξ. Kanemitsu and Yoshimoto [7] proved that each of the estimates $\sum_{r_v \leq 1/3}(r_v - h(1/3)/(2A(x)) = O(x^{1/2+\epsilon})$ and $\sum_{r_v \leq 1/4}(r_v - h(1/4)/(2A(x)) = O(x^{1/2+\epsilon})$ is equivalent to the Riemann hypothesis. Let $n = 4, 5, 6, ...$, and let $j = \lfloor n/2 \rfloor$. Let $y_x(n)$ denote the number of fractions less than $1/n$ and let $z_x(n)$ denote the number of fractions greater than $1/n$ and less than $2/n$ in a Farey sequence of order x. (If $x \leq n$, set y_x to 0. If $x \leq j$, set z_x to 0. If $x > j$ and $x < n$, set z_x to $x - j$. If $x = n$, set z_x to $j - 1$ if n is even or j if n is odd.) Franel proved that $M(x) = \sum_{v=1}^{A(x)} e^{2\pi i r_v}$, so there should be some discernible relationship between $M(x)$ and $y_x(4) - z_x(4)$. The "curve" of $y_x(4) - z_x(4)$ values resembles that of $M(x)$ in that the peaks and valleys occur roughly at the same places and have about the same heights and depths. See Figure 2 for a plot of $M(x)$ for $x = 1, 2, 3, ..., 5000$. See Figure 3 for a plot of $y_x(4) - z_x(4)$ for $x = 1, 2, 3, ..., 5000$. Let $h_x(n)$ denote $\sum_{i=1}^{x}(z_{\lfloor x/i \rfloor}(n) - y_{\lfloor x/i \rfloor}(n))$.

Theorem (3) $h_{x+n}(n) = h_x(n) + \lfloor (n-1)/2 \rfloor$

The value of $h_x(4) - h_{x-1}(4)$ is determined by the distribution of the fractions $1/x, 2/x, 3/x, ..., \lfloor (x-1)/2 \rfloor/x$ about $1/4$. The difference in the number of fractions after $1/4$ and before $1/4$ is 0 unless 4 divides $x + 1$, in which case it is 1. Similar arguments are applicable for $n > 4$.

While $\sum_{i=1}^{x} M(\lfloor x/i \rfloor)$ has only one value (1), $\sum_{i=1}^{x}(y_{\lfloor x/i \rfloor}(n) - z_{\lfloor x/i \rfloor}(n) + \lfloor (n-1)/2 \rfloor / n)$ has up to n values. (For $n = 4$, these values are 1/2, 1/4, 0, or $-1/4$.) Additional comparisons of $M(x)$ and $y_x(n) - z_x(n)$ can then be made by replacing $M(\lfloor x/i \rfloor)$ by $y_{\lfloor x/i \rfloor}(n) - z_{\lfloor x/i \rfloor}(n) + \lfloor (n-1)/2 \rfloor / n$ in formulas such as $\sum_{i=1}^{x} M(\lfloor x/i \rfloor) \log(i) = \psi(x)$. See Figure 4 for a plot of $\psi(x)$ and $\sum_{i=1}^{x}(y_{\lfloor x/i \rfloor}(4) - z_{\lfloor x/i \rfloor}(4) + 1/4) \log(i)$ for $x = 2, 3, 4, \ldots, 5000$ (the prime number theorem is equivalent to the limit relation $\lim_{x\to\infty} \psi(x)/x = 1$). For a linear least-squares fit of $\sum_{i=1}^{x}(y_{\lfloor x/i \rfloor}(4) - z_{\lfloor x/i \rfloor}(4) + 1/4) \log(i)$ for $x = 2$, 3, 4, ..., 5000, $p_1 = 0.2188$ with a 95% confidence interval of (0.2186, 0.219), $p_2 = 0.9646$ with a 95% confidence interval of (0.3782, 1.551), SSE=5.582e+5, R-square=0.9989, and RMSE=10.57. See Figure 5 for a plot of $\log(x!)$ and $4.38 \sum_{i=1}^{x}(y_{\lfloor x/i \rfloor}(4) - z_{\lfloor x/i \rfloor}(4) + 1/4) \log(i) \sigma_0(i)/2$ (superimposed on each other) for $x = 2, 3, 4, \ldots, 1000$.

Let $\lambda(i)$ denote the Liouville function ($\lambda(1) := 1$ or if $i = p_1^{a_1} \cdots p_k^{a_k}$, $\lambda(i) = (-1)^{a_1+\cdots+a_k}$). Let $L(x) := \sum_{i \le x} \lambda(i)$. Let $H(x) := \sum_{i \le x} \mu(i) \log(i)$. ($H(x)/(x \log(x)) \to 0$ as $x \to \infty$ and $\lim_{x\to\infty}(M(x)/x - H(x)/(x \log(x))) = 0$.) Other relationships that are useful for comparing $M(x)$ and $y_x(n) - z_x(n)$ are;

Theorem (4) $\sum_{i=1}^{x} M(\lfloor x/i \rfloor) \sigma_0(i) = x$

Theorem (5) $\sum_{i=1}^{x} M(\lfloor x/i \rfloor) \sigma_1(i) = x(x+1)/2$

Theorem (6) $\sum_{i=1}^{x} M(\lfloor x/i \rfloor) \sigma_2(i) = x(x+1)(2x+1)/6$

Theorem (7) $\sum_{i=1}^{x} M(\lfloor x/i \rfloor) \Lambda(i) = -H(x)$

Theorem (8) $\sum_{i=1}^{x} M(\lfloor x/i \rfloor)$ where the summation is over i values that are perfect squares equals $L(x)$

See Figure 6 for a plot of $\sum_{i=1}^{x}(y_{\lfloor x/i \rfloor}(5) - z_{\lfloor x/i \rfloor}(5) + 2/5) \sigma_0(i)$ for $x = 2, 3, 4, \ldots, 1000$. For a linear least-squares fit of $\sum_{i=1}^{x}(y_{\lfloor x/i \rfloor}(5) - z_{\lfloor x/i \rfloor}(5) + 2/5) \sigma_0(i)$ for $x = 2, 3, 4, \ldots, 1000$, $p_1 = 0.3734$ with a 95% confidence interval of (0.3731, 0.3738), $p_2 = 0.1253$ with a 95% confidence interval of (-0.08557, 0.3362), SSE=2863, R-square=0.9998, and RMSE=1.695. See Figure 7 for a plot of $\sum_{i=1}^{x}(y_{\lfloor x/i \rfloor}(6) - z_{\lfloor x/i \rfloor}(6) + 1/3) \sigma_1(i)$ for $x = 2, 3, 4, \ldots, 200$. For a quadratic least-squares fit of $\sum_{i=1}^{x}(y_{\lfloor x/i \rfloor}(6) - z_{\lfloor x/i \rfloor}(6) + 1/3) \sigma_1(i)$ for $x = 2, 3, 4, \ldots, 200$, SSE=2.531e+4, R-square=1, and RMSE=11.36. See Figure 8 for a plot of $\sum_{i=1}^{x}(y_{\lfloor x/i \rfloor}(7) - z_{\lfloor x/i \rfloor}(7) + 3/7) \sigma_2(i)$ for $x = 2, 3, 4, \ldots, 100$. For a cubic least-squares fit of $\sum_{i=1}^{x}(y_{\lfloor x/i \rfloor}(7) - z_{\lfloor x/i \rfloor}(7) + 3/7) \sigma_2(i)$ for $x = 2, 3, 4, \ldots, 100$, SSE=1.454e+6, R-square=1, and RMSE=123.7. See Figure 9 for a plot of $1/(x \log(x)) \sum_{i=1}^{x}(y_{\lfloor x/i \rfloor}(4) - z_{\lfloor x/i \rfloor}(4) + 1/4) \Lambda(i)$ for $x = 2, 3, 4, \ldots, 5000$. See Figure 10 for a plot of $L(x)$ and $\sum_{i=1}^{x}(y_{\lfloor x/i \rfloor}(4) - z_{\lfloor x/i \rfloor}(4) + 1/4)$ where the summation is over i values that are perfect squares for $x = 2, 3, 4, \ldots, 1000$. (Pólya conjectured that $L(x) \le 0$ for $x \ge 2$. This was disproved by Haselgrove [8].)

See Figure 11 for a plot of $y_x(65) - z_x(65)$ for $x = 2, 3, 4, ..., 1625$. See Figure 12 for a plot of $y_x(200) - z_x(200)$ for $x = 2, 3, 4, ..., 5000$. See Figure 13 for a plot of $y_x(200) - z_x(200)$ for $x = 100, 200, 300, ..., 5000$. Note that the values of $y_x(200) - z_x(200)$ in the x intervals of (100, 200), (200, 300), (300, 400), ..., can be approximated by linear interpolation. For even n, the limits of $(y_{n/2}(n) - z_{n/2}(n))/n$, $(y_n(n) - z_n(n))/n$, $(y_{3n/2}(n) - z_{3n/2}(n))/n$, ..., as $n \to \infty$ appear to be $-1/2$, $-1/4$, $-1/3$, $-1/6$, $-2/5$, $-2/15$, $-31/105$, $-29/140$, $-19/42$, $-41/420$, $-76/385$, $-201/1540$, $-751/1430$, $-1109/4004$, $-803/2718$, $-857/13411$, $-3577/11807$, $-721/17163$, $-738/2897$, ... Let $\delta_1(1)$, $\delta_1(2)$, $\delta_1(3)$, ..., denote these limits and let $\delta_m(x)$, $m = 2, 3, 4, ...$, denote the limits and $m-1$ values that have been linearly interpolated between successive limits. See Figure 14 for a plot of $-\sum_{i=1}^{x} \delta_4(\lfloor x/i \rfloor)$ for $x = 1, 2, 3, ..., 76$ (19 limits were used). For a linear least-squares fit of $-\sum_{i=1}^{x} \delta_4(\lfloor x/i \rfloor)$ for $x = 1, 2, 3, ..., 76$, $p_1 = 0.1278$ with a 95% confidence interval of (0.1266, 0.1291), $p_2 = -0.05671$ with a 95% confidence interval of $(-0.1116, -0.001796)$, SSE=0.979, R-square=0.9983, and RMSE=0.1158. See Figure 15 for a plot of $\sum_{i=1}^{x}(\delta_4(\lfloor x/i \rfloor) + 0.1278)\log(i)$ for $x = 1, 2, 3, ..., 76$. For a linear least-squares fit of $\sum_{i=1}^{x}(\delta_4(\lfloor x/i \rfloor) + 0.1278)\log(i)$ for $x = 1, 2, 3, ..., 76$, SSE=2.233, R-square=0.9945, and RMSE=0.1749. See Figure 16 for a plot of $\sum_{i=1}^{x}(\delta_4(\lfloor x/i \rfloor) + 0.1278)\sigma_1(i)$ for $x = 1, 2, 3, ..., 76$. For a quadratic least-squares fit of $\sum_{i=1}^{x}(\delta_4(\lfloor x/i \rfloor) + 0.1278)\sigma_1(i)$ for $x = 1, 2, 3, ..., 76$, SSE=81.03, R-square=0.9999, and RMSE=1.061. See Figure 17 for a plot of $\sum_{i=1}^{x}(\delta_4(\lfloor x/i \rfloor) + 0.1278)\sigma_2(i)$ for $x = 1, 2, 3, ..., 76$. For a cubic least-squares fit of $\sum_{i=1}^{x}(\delta_4(\lfloor x/i \rfloor) + 0.1278)\sigma_2(i)$ for $x = 1, 2, 3, ..., 76$, SSE=5210, R-square=1, and RMSE=8.567.

See Figure 18 for a plot of $-\sum_{i=1}^{x} \delta_1(\lfloor x/i \rfloor)$ and $-\sum_{i=1}^{x} \delta_1(\lfloor x/i \rfloor)\Lambda(i)$ for $x = 2, 3, 4, ..., 999$ (these values were computed using 1000 approximate limits accurate to about 6 decimal places). For a linear least-squares fit of $-\sum_{i=1}^{x} \delta_1(\lfloor x/i \rfloor)$ for $x = 2, 3, 4, ..., 999$, $p_1 = 0.1704$ with a 95% confidence interval of (0.1073, 0.1706), $p_2 = -0.04484$ with a 95% confidence interval of $(-0.1291, 0.03936)$, SSE=455.6, R-square=0.9998, and RMSE=0.6763. For a linear least-squares fit of $-\sum_{i=1}^{x} \delta_1(\lfloor x/i \rfloor)\Lambda(i)$ for $x = 2, 3, 4, ..., 999$, $p_1 = 0.17$ with a 95% confidence interval of (0.1695, 0.1705), $p_2 = -0.2796$ with a 95% confidence interval of $(-0.5688, 0.009683)$, SSE=5374, R-square=0.9978, and RMSE=2.323. See Figure 19 for a plot of the p_1 values of the linear least-squares fits of $-\sum_{i=1}^{x} \delta_1(\lfloor x/i \rfloor)\Lambda(i)$, $-\sum_{i=1}^{x} \delta_2(\lfloor x/i \rfloor)\Lambda(i)$, $-\sum_{i=1}^{x} \delta_3(\lfloor x/i \rfloor)\Lambda(i)$, ..., $-\sum_{i=1}^{x} \delta_{36}(\lfloor x/i \rfloor)\Lambda(i)$ for respective x values up to 999, 1999, 2999, ..., 35999. See Figure 20 for a plot of $-\sum_{i=1}^{x} \delta_{100}(\lfloor x/i \rfloor)$ and $-\sum_{i=1}^{x} \delta_{100}(\lfloor x/i \rfloor)\Lambda(i)$ (superimposed on each other) for $x = 2, 3, 4, ..., 99999$. For a linear least-squares fit of $-\sum_{i=1}^{x} \delta_{100}(\lfloor x/i \rfloor)$ for $x = 2, 3, 4, ..., 99999$, $p_1 = 0.01936$ with a 95% confidence interval of (0.01936, 0.01936), $p_2 = -0.1094$ with a 95% confidence interval of $(-0.1154, -0.1034)$, SSE=2.347e+4, R-square=1, and RMSE=0.4845. For a linear least-squares fit of $-\sum_{i=1}^{x} \delta_{100}(\lfloor x/i \rfloor)\Lambda(i)$ for $x = 2, 3, 4, ..., 99999$, $p_1 = 0.01936$ with a 95% confidence interval of (0.01936, 0.01936), $p_2 = -0.6391$ with a 95% confidence interval of $(-0.6584, -0.6198)$, SSE=2.415e+4, R-square=1, and RMSE=1.554.

Let $(\alpha \circ F)(x)$ denote $\sum_{i \leq x} \alpha(i)F(\lfloor x/i \rfloor)$ where α is an arithmetical function. (Usually$(\alpha \circ F)(x)$ denotes $\sum_{i \leq x} \alpha(i)F(x/i)$ where F is a real or complex-valued function defined on $(0, +\infty)$ such that $F(x) = 0$ for $0 < x < 1$.) Let $u(x) = 1$ for all x. See Figure 21 for a plot of $(u \circ \delta_1) \circ \delta_1$ for $x = 2, 3, 4, ..., 999$. For a quadratic least-squares fit of $(u \circ \delta_1) \circ \delta_1$ for $x = 2, 3, 4, ..., 999$, $p_1 = 0.008421$ with a 95% confidence interval of (0.008414, 0.008428), $p_2 = 0.001703$ with a 95% confidence interval of $(-0.005279, 0.008684)$, $p_3 = -0.01665$ with a 95% confidence interval of $(-1.53, 1.497)$, SSE=6.483e+4, R-square=1, and RMSE=8.072. See Figure 22 for a plot of $(\Lambda \circ \delta_1) \circ \delta_1$ for $x = 2, 3, 4, ..., 999$. For a quadratic least-squares fit of $(\Lambda \circ \delta_1) \circ \delta_1$ for $x = 2, 3, 4, ..., 999$, $p_1 = 0.00847$ with a 95% confidence interval of (0.008459, 0.008428), $p_2 = -0.09465$ with a 95% confidence interval of $(-0.1054, -0.08319)$, $p_3 = 4.914$ with a 95% confidence interval of (2.586, 7.242), SSE=1.534e+5, R-square=1, and RMSE=12.42.

Let $c_k(x)$ denote Ramanujan's sum $(c_k(x) := \sum_{m \ mod \ k, (m,k)=1} e^{2\pi i m x/k})$.

Conjecture 2 $\sum_{i=1}^{x} (y_{\lfloor x/i \rfloor}(n) - z_{\lfloor x/i \rfloor}(n))c_k(i)$ is a periodic function with period nk.

See Figure 23 for a plot of $\sum_{i=1}^{x} (y_{\lfloor x/i \rfloor}(n) - z_{\lfloor x/i \rfloor}(n) + \lfloor (n-1)/2 \rfloor /n)c_k(i)$ where $n = 13$, $k = 13$, and $x = 1, 2, 3, ..., 169$ and $\sum_{i=1}^{x} (y_{\lfloor x/i \rfloor}(n) - z_{\lfloor x/i \rfloor}(n) + \lfloor (n-1)/2 \rfloor /n)$ where $n = 169$ and $x = 1, 2, 3, ..., 169$. See Figure 24 for a corresponding plot where $n = 12$, $k = 10$, and $x = 1, 2, 3, ..., 120$ and where $n = 120$ and $x = 1, 2, 3, ..., 120$. See Figure 25 for a plot of the real parts of the Fourier coefficients of $\sum_{i=1}^{x} (y_{\lfloor x/i \rfloor}(n) - z_{\lfloor x/i \rfloor}(n) + \lfloor (n-1)/2 \rfloor /n)c_k(i)$ where $n = 4$, $k = 19$, and $x = 1, 2, 3, ..., 76$. The Fourier coefficients resemble those of a triangular pulse. See Figure 26 for a plot of $\sum_{i=1}^{x} M(\lfloor x/i \rfloor)c_k(i)$ where $k = 150$ and $x = 2, 3, 4, ..., 300$. Based on empirical evidence, $\sum_{i=1}^{x} M(\lfloor x/i \rfloor)c_k(i) = \phi(k)$ for $x \geq k$.

4 Similar Convolutions

$\chi_3(n)$ for $n = 1, 2, 3, ..., 7$ (a Dirichlet character mod 7) equal $1, \omega^2, \omega, -\omega, -\omega^2, -1$, and 0 respectively where $\omega = e^{\pi i/3}$. Let $G(n, \chi)$ denote the Gauss sum associated with the Dirichlet character χ $(G(n, \chi) := \sum_{m=1}^{k} \chi(m)e^{2\pi i m n/k})$. See Figure 27 for a plot of the real and imaginary components of $\sum_{i=1}^{x} G(\lfloor x/i \rfloor, \chi)$ for χ_3 mod 7 and $x = 2, 3, 4, ..., 10000$. For a linear least-squares fit of the real components, $p_1 = -0.9076$ with a 95% confidence interval of $(-0.9077, -0.9075)$, $p_2 = -0.5368$ with a 95% confidence interval of $(-1.155, 0.0809)$, SSE=2.481e+6, R-square=1, and RMSE=15.75. For a linear least-squares fit of the imaginary components, $p_1 = 0.8163$ with a 95% confidence interval of (0.8163, 0.8164), $p_2 = 0.4341$ with a 95% confidence interval of (0.0005613, 0.8677), SSE=1.222e+6, R-square=1, and RMSE=11.06. See Figure 28 for a plot of the real components of

$\sum_{i=1}^{x}(G(\lfloor x/i\rfloor,\chi)+0.9076)\log(i)$ for $x=2$, 3, 4, ..., 10000. See Figure 29 for a plot of the imaginary components of $\sum_{i=1}^{x}(G(\lfloor x/i\rfloor,\chi)-0.8163)\log(i)$ for $x=2$, 3, 4, ..., 10000. See Figure 30 for a plot of the real and imaginary components of $\sum_{i=1}^{x}G(\lfloor x/i\rfloor,\chi)\sigma_1(i)$ for $x=2$, 3, 4, ..., 1000. For a quadratic least-squares fit of the real components, SSE=3.689e+8, R-square=1, and RMSE=608.6. For a quadratic least-squares fit of the imaginary components, SSE=1.568e+8, R-square=1, and RMSE=396.8. For a linear least-squares fit of the real components of $\sum_{i=1}^{x}G(\lfloor x/i\rfloor,\chi)$ for a Dirichlet character mod 13 and $x=2$, 3, 4, ..., 10000, $p_1=-1.247$ with a 95% confidence interval of $(-1.247, -1.247)$, $p_2=-0.7447$ with a 95% confidence interval of $(-1.438, -0.05162)$, SSE=3.123e+6, R-square=1, and RMSE=17.68. For a linear least-squares fit of the imaginary components, $p_1=0.08855$ with a 95% confidence interval of (0.08847, 0.08863), $p_2=0.004809$ with a 95% confidence interval of $(-0.4693, 0.4789)$, SSE=1.461e+6, R-square=0.9978, and RMSE=12.09. See Figure 31 for a plot of the real components of $-\sum_{i=1}^{x}(G(\lfloor x/i\rfloor,\chi)+1.247)\log(i)\sigma_0(i)/2$ for the Dirichlet character mod 13, the imaginary components of $-\sum_{i=1}^{x}(G(\lfloor x/i\rfloor,\chi)-0.08855)\log(i)\sigma_0(i)/2$ for the Dirichlet character mod 13, $1.25\log(x!)$, and $0.2289\log(x!)$ for $x=2$, 3, 4, ..., 1000. See Figure 32 for a plot of the real and imaginary components of $\sum_{i=1}^{x}(y_{\lfloor x/i\rfloor}(n)-z_{\lfloor x/i\rfloor}(n)+\lfloor(n-1)/2\rfloor/n)G(i,\chi)$ where $n=200$, χ is a Dirichlet character mod 11, and $x=2$, 3, 4, ..., 2000.

See Figure 33 for a plot of $\sum_{i=1}^{x}c_k(\lfloor x/i\rfloor)$ for $k=17$ and $x=2$, 3, 4, ..., 500. When k is prime, the points fall on parallel lines having a slope of -1. Also, the bottom line persists until $x>k^2$. See Figure 34 for a plot of $\sum_{i=1}^{x}c_k(\lfloor x/i\rfloor)\sigma_1(i)$ for $k=15$ and $x=2$, 3, 4, ..., 1000. For a quadratic least-squares fit, SSE=3.622e+8, R-square=1, and RMSE=603. See Figure 35 for a plot of $\sum_{i=1}^{x}(c_k(\lfloor x/i\rfloor)+1)\log(i)$ for $k=11$ and $x=2$, 3, 4, ..., 1000. See Figure 36 for a plot of $\sum_{i=1}^{x}(c_k(\lfloor x/i\rfloor)+1)M(i)$ for $k=29$ and $x=2$, 3, 4, ..., 1000. See Figure 37 for a plot of $\sum_{i=1}^{x}(c_k(\lfloor x/i\rfloor)+1)(y_i(n)-z_i(n))$ for $k=7$, $n=100$, and $x=2$, 3, 4, ..., 1000.

5 More on an Upper Bound of $|M(x)|$

Let $j(x):=\sum_{i}^{x}M(x/i)^2$ where the summation is over i values where $i|x$. Let l_1, l_2, l_3, ... denote the x values where $j(x)$ is a local maximum (that is, greater than all preceding $j(x)$ values) and let m_1, m_2, m_3, ... denote the values of the local maxima. The local maxima occur at x values that equal products of powers of small primes (Lagarias [9] discusses colossally abundant numbers and their relationship to the Riemann hypothesis). See Figure 38 for a plot of $l_i/(\log(l_i)m_i)$, m_i/l_i, and $1/\log(l_i)$ for $i=1$, 2, 3, ..., 516 (corresponding to the local maxima for $x\le 1000000000$). The first two curves cross frequently, so there are i values where m_i is approximately equal to $l_i/\sqrt{\log(l_i)}$. See Figure 39 for a plot of $j(x)$ and $\sum_{i=1}^{x}M(\lfloor x/i\rfloor)^2$ for $x=2$, 3, 4, ..., 10000. See Figure 40 for a plot of $1/\log(l_i)$ and $1/\log(i+1)-0.11$ for $i=1$, 2, 3, ..., 516. See Figure

41 for a plot of $\log(l_i)$, $\log(M(l_i)^2)$, and $\log(m_i/\sigma_0(l_i))$ for $i = 1, 2, 3, ..., 516$. Note that the vertical distance between the first two curves is roughly constant so that $M(l_i)^2$ increases linearly (roughly) with x. However, the growing deviation of $l_i/(\log(l_i)m_i)$ and m_i/l_i from $l_i/\sqrt{\log(l_i)}$ as shown in Figure 38 indicates that the Stieltjes conjecture is false. See Figure 42 for a plot of $|M(l_i)|/\sqrt{l_i}$ for $i = 1, 2, 3, ..., 516$. The largest known value of $M(x)/\sqrt{x}$ (computed by Kotnik and van de Lune [10] for $x \leq 10^{14}$) is 0.570591 (for $M(7766842813) = 50286$).

Let l_i and m_i be similarly defined for the function $k(x) := \sum_{i=1}^{x} |M(x/i)|$ where the summation is over i values where $i|x$. See Figure 43 for a plot of $\sqrt{l_i}/m_i$, m_i/l_i, and $1/\sqrt{l_i}$ for $i = 1, 2, 3, ..., 180$ (corresponding to the local maxima for $x \leq 400000000$). See Figure 44 for a plot of $1/\log(l_i)$ and $1/\log(i+1) - 0.14$ for $i = 1, 2, 3, ..., 180$. See Figure 45 for a plot of $\log(m_i/\sigma_0(l_i))$ for $i = 1, 2, 3, ..., 180$. For a quadratic least-squares fit of $\log(m_i/\sigma_0(l_i))$ for $i = 1, 2, 3, ..., 180$, $p_1 = -3.242\text{e-}5$ with a 95% confidence interval of (-3.998e-5, -2.486e-5), $p_2 = 0.03064$ with a 95% confidence interval of (0.02923, 0.03206), $p_3 = -0.05244$ with a 95% confidence interval of (-0.1078, 0.00295), SSE=2.728, R-square=0.991, and RMSE=0.1241. See Figure 46 for a plot of $\log(l_i)$, $\log(|M(l_i)|)$, and $\log(m_i/\sigma_0(l_i))$ for $i = 1, 2, 3, ..., 180$. In this case, the locations and values of local maxima are less dependent on $M(x/1)$.

Let l_i and m_i be similarly defined for the function $g(x) := \sum_{i=1}^{x}(y_{\lfloor x/i \rfloor}(10) - z_{\lfloor x/i \rfloor}(10))^2$ where the summation is over i values where $i|x$. See Figure 47 for a plot of $l_i/(\log(l_i)m_i)$ and m_i/l_i for $i = 1, 2, 3, ..., 65$ (corresponding to the local maxima for $x \leq 30000$). See Figure 48 for a plot of $1/\log(l_i)$ and $1/\log(i+1) - 0.13$ for $i = 1, 2, 3, ..., 65$. See Figure 49 for a plot of $\log(l_i)$, $\log((y_{l_i}(10) - z_{l_i}(10))^2)$, and $\log(m_i/\sigma_0(l_i))$ for $i = 1, 2, 3, ..., 65$. Let l_i and m_i be similarly defined for the function $h(x) := \sum_{i=1}^{x}(y_{\lfloor x/i \rfloor}(12) - z_{\lfloor x/i \rfloor}(12))^2$ where the summation is over i values where $i|x$. See Figure 50 for a plot of $l_i/(\log(l_i)m_i)$ and m_i/l_i for $i = 1, 2, 3, ..., 63$ (corresponding to the local maxima for $x \leq 30000$).

Let l_i and m_i be similarly defined for the function $\sigma_0(x)$. For a quadratic least-squares fit of $\log(m_i/l_i)$ for $i = 1, 2, 3, ..., 65$ (corresponding to the local maxima for $x \leq 1000000000$), $p_1 = 0.0009031$ with a 95% confidence interval of (0.0007913, 0.001015), $p_2 = -0.2634$ with a 95% confidence interval of (-0.2711, -0.2558), $p_3 = 0.2064$ with a 95% confidence interval of (0.0976, 0.3153), SSE=1.247, R-square=0.9987, and RMSE=0.1418. For a quadratic least-squares fit of $\log(l_i)$ for $i = 1, 2, 3, ..., 65$, $p_1 = -0.002029$ with a 95% confidence interval of (-0.002256, -0.001802), $p_2 = 0.424$ with a 95% confidence interval of (0.4086, 0.4395), $p_3 = 1.043$ with a 95% confidence interval of (0.8219, 1.264), SSE=5.15, R-square=0.9974, and RMSE=0.2882. Let $b(x, \chi) := \sum_{i=1}^{x} |G(x/i, \chi)|^2$ where the summation is over i values where $i|x$. See Figure 51 for a plot of m_i for $i = 1, 2, 3, ..., 37$ (corresponding to the local maxima for $x \leq 1000000$). For a quadratic least-squares fit of m_i for $i = 1$, 2, 3, ..., 37, $p_1 = 0.188$ with a 95% confidence interval of (0.1773, 0.1987), $p_2 = -0.627$ with a 95% confidence interval of (-1.045, -0.2095), $p_3 = 4.885$ with a 95% confidence interval of (1.445, 8.326), SSE=358.8, R-square=0.9981, and RMSE=3.249. See Figure 52 for a plot of $\log(l_i)$ for $i = 1, 2, 3, ..., 37$. For a quadratic least-squares fit of $\log(l_i)$ for $i = 1, 2, 3, ..., 37$, $p_1 = -0.004631$ with a 95% confidence interval of (-0.005132, -0.004131), $p_2 = 0.5276$ with a 95% confidence interval of (0.508, 0.5472), $p_3 = 0.3631$ with a 95% confidence interval of (0.2015, 0.5246), SSE=0.7912, R-square=0.9985, and RMSE=0.1525. See Figure 53 for a plot of $b(l_i, \chi)/m_i$ for a non-principal Dirichlet character mod 3 and $i = 1, 2, 3, ..., 37$ (the values are 3/1, 3/2, 3/3, 3/4, or 3/5). For $i = 1$ and $i = 2$, $|G(l_i, \chi)|^2 = 3$ and for $i > 2$, $|G(l_i, \chi)|^2 = 0$.

Let l_i and m_i be similarly defined for the function $\sigma_0(x)$ with the additional stipulation that $||G(x, \chi)|^2 - k| < 0.1$ where k is the modulus of the Dirichlet character. When k is prime, there appear to be Dirichlet characters (non-principal) such that $b(l_i, \chi) = m_i k$. (There are also such Dirichlet characters for many composite values of k.) When k is prime, a better stipulation is that k does not divide x (making it unnecessary to compute $|G(x, \chi)|^2$). See Figure 54 for a plot of $\log(m_i/l_i)$ for $k = 2$ and $i = 1, 2, 3, ..., 34$ (corresponding to the local maxima for $x \leq 1000000000$). For a linear least-squares fit of $\log(m_i/l_i)$ for $i = 1, 2, 3, ..., 34$, $p_1 = -0.4037$ with a 95% confidence interval of (-0.4141, -0.3934), $p_2 = -0.6406$ with a 95% confidence interval of (-0.8478, -0.4333), SSE=2.694, R-square=0.995, and RMSE=0.2901. See Figure 55 for a plot of $\log(l_i)$ for $k = 2$ and $i = 1, 2, 3, ..., 34$. For a quadratic least-squares fit of $\log(l_i)$ for $i = 1, 2, 3, ..., 34$, $p_1 = -0.005143$ with a 95% confidence interval of (-0.006254, -0.004032), $p_2 = 0.7344$ with a 95% confidence interval of (0.6943, 0.7745), $p_3 = 0.9003$ with a 95% confidence interval of (0.5959, 1.205), SSE=2.312, R-square=0.9977, and RMSE=0.2731. For a linear least-squares fit of $\log(m_i/l_i)$ for $k = 3$ and $i = 1, 2, 3, ..., 48$ (corresponding to the local maxima for $x \leq 1000000000$), $p_1 = -0.2903$ with a 95% confidence interval of (-0.2964, -0.2842), $p_2 = -0.2597$ with a 95% confidence interval of (-0.4315, -0.08794), SSE=3.897, R-square=0.995, and RMSE=0.291. For a linear least-squares fit of $\log(m_i/l_i)$ for $k = 5$ and $i = 1, 2, 3, ..., 54$ (corresponding to the local maxima for $x \leq 1000000000$), $p_1 = -0.2556$ with a 95% confidence interval of (-0.2574, -0.2538), $p_2 = 0.1686$ with a 95% confidence interval of (0.113, 0.2241), SSE=0.5232, R-square=0.9994, and RMSE=0.1003. For a linear least-squares fit of $\log(m_i/l_i)$ for $k = 7$ and $i = 1, 2, 3, ..., 70$ (corresponding to the local maxima for $x \leq 1000000000$), $p_1 = -0.1941$ with a 95% confidence interval of (-0.1975, -0.1907), $p_2 = -0.5277$ with a 95% confidence interval of (-0.6663, -0.3892), SSE=5.612, R-square=0.9948, and RMSE=0.2873.

Let l_i and m_i be similarly defined for the function $\sigma_0(x)$ with the additional stipulation that $|M(x)| = k$. See Figure 56 for a plot of $\log(m_i/l_i)$ for $k = 1$ and $i = 1, 2, 3, ..., 31$ (corresponding to the local maxima for $x \leq 1000000000$). For a quadratic least-squares fit of $\log(m_i/l_i)$ for $k = 1$ and $i = 1, 2, 3, ..., 31$, $p_1 = -0.008157$ with a 95% confidence interval of (-0.009575, -0.00674),

$p_2 = -0.1901$ with a 95% confidence interval of $(-0.2368, -0.1433)$, $p_3 = -0.02875$ with a 95% confidence interval of $(-0.3533, 0.2958)$, SSE=2.122, R-square=0.9959, and RMSE=0.2753. Let $m'_i = j(l_i)$. See Figure 57 for a plot of $l_i/(\log(l_i)m'_i)$, m'_i/l_i, and $1/\log(l_i)$ for $k = 1$ and $i = 1, 2, 3, ..., 31$. See Figure 58 for a plot of $\log(m'_i)$ for $i = 1, 2, 3, ..., 31$. For a quadratic least-squares fit of $\log(m'_i)$ for $i = 1, 2, 3, ..., 31$, $p_1 = 0.009924$ with a 95% confidence interval of (0.007953, 0.0119), $p_2 = 0.2451$ with a 95% confidence interval of (0.1801, 0.3101), $p_3 = 0.6756$ with a 95% confidence interval of (0.2243, 1.127), SSE=4.103, R-square=0.9949, and RMSE=0.3828. See Figure 59 for a plot of $\log(l_i)$ for $i = 1, 2, 3, ..., 31$. For a quadratic least-squares fit of $\log(l_i)$ for $i = 1, 2, 3, ..., 31$, $p_1 = 0.006226$ with a 95% confidence interval of (0.004778, 0.007673), $p_2 = 0.4393$ with a 95% confidence interval of (0.3916, 0.487), $p_3 = 0.68$ with a 95% confidence interval of (0.3486, 1.011), SSE=2.212, R-square=0.9978, and RMSE=0.2811. See Figure 60 for a plot of $\log(l_i/\sqrt{\log(l_i)})$ and $\log(m'_i)$ for $i = 1, 2, 3, ..., 31$ (the two curves should intersect at about the 42nd maxima [having an estimated l value of about 1.2e+13]). See Figure 61 for a plot of the p_1 values of the quadratic least-squares fits of $\log(m'_i)$ and the p_1 values of the quadratic least-squares fits of $\log(l_1)$ for $k = 0$, 1, 2, ..., 12 and $i = 19$, 31, 28, 25, 29, 28, 23, 26, 28, 25, 26, 24, 23 respectively (corresponding to the local maxima for $x \leq 1000000000$). See Figure 62 for a plot of the p_2 values of the quadratic least-squares fits of $\log(l_i)$ and the p_2 values of the quadratic least-squares fits of $\log(m'_1)$ for $k = 0, 1, 2, ..., 12$. See Figure 63 for a plot of the p_3 values of the quadratic least-squares fits of $\log(l_i)$ and the p_3 values of the quadratic least-squares fits of $\log(m'_1)$ for $k = 0, 1, 2, ...,$ 12. The R-square values for the quadratic least-squares fits of the $\log(m'_i)$ values are 0.9739, 0.9949, 0.9843, 0.9904, 0.9748, 0.991, 0.9867, 0.9872, 0.9859, 0.9903, 0.9836, 0.9957, and 0.9807 respectively. The R-square values for the quadratic least-squares fits of the $\log(l_i)$ values are 0.981, 0.9978, 0.9917, 0.9931, 0.9844, 0.9932, 0.9937, 0.995, 0.991, 0.9926, 0.9856, 0.9944, and 0.9878 respectively. See Figure 64 for a plot of $l_i/(\log(l_i)m'_i)$, m'_i/l_i, and $1/\log(l_i)$ for $k = 2000$ and $i = 1, 2, 3, ..., 17$ (corresponding to the local maxima for $x \leq 1000000000$). See Figure 65 for a plot of $\log(m'_i)$ for $i = 1, 2, 3, ..., 17$. See Figure 66 for a plot of $\log(l_i)$ for $i = 1, 2, 3, ..., 17$. See Figure 67 for a plot of $\log(l_i/\sqrt{\log(l_i)})$ and $\log(m'_i)$ for $i = 1, 2, 3, ..., 17$. These curves are typical for large k values. If the first few maxima are disregarded (in this case the first 11 maxima), the curves of the $\log(m'_i)$ and $\log(l_i)$ values appear to be quadratic (based on the small amount of data available).

Let l_i and m_i be similarly defined for the function $\sigma_0(x)$ with the additional stipulation that $|M(x)| \leq k$. Let $m'_i = j(l_i)$. See Figure 68 for a plot of $l_i/(\log(l_i)m'_i)$, m'_i/l_i, and $1/\log(l_i)$ for $k = 10$ and $i = 1, 2, 3, ..., 46$ (corresponding to the local maxima for $x \leq 1000000000$). See Figure 69 for a plot of $\log(m'_i)$ for $i = 1, 2, 3, ..., 46$. For a quadratic least-squares fit of $\log(m'_i)$ for $i = 1, 2, 3, ..., 46$, $p_1 = 0.002978$ with a 95% confidence interval of (0.002156, 0.0038), $p_2 = 0.2244$ with a 95% confidence interval of (0.1845, 0.2642), $p_3 = 1.03$ with a 95% confidence interval of (0.6242, 1.437), SSE=8.161, R-square=0.9925, and

RMSE=0.4356. See Figure 70 for a plot of $\log(l_i)$ for $i = 1, 2, 3, ..., 46$. For a linear least-squares fit of $\log(l_i)$ for $i = 1, 2, 3, ..., 46$, $p_1 = 0.4093$ with a 95% confidence interval of (0.4018, 0.4168), $p_2 = 0.8728$ with a 95% confidence interval of (0.6691, 1.076), SSE=4.998, R-square=0.9963, and RMSE=0.337. See Figure 71 for a plot of $\log(l_i/\sqrt{\log(l_i)})$ and $\log(m'_i)$ for $i = 1, 2, 3, ..., 46$. See Figure 72 for a plot of the p_1 values of the quadratic least-squares fits of $\log(m'_i)$ and the p_1 values of the quadratic least-squares fits of $\log(l_1)$ for $k = 100, 200, 300, ..., 1000$ and $i = 57, 59, 58, 57, 56, 57, 57, 57, 60$, and 61 respectively (corresponding to the local maxima for $x \leq 950000000$). See Figure 73 for a plot of the p_2 values of the quadratic least-squares fits of $\log(l_i)$ and the p_2 values of the quadratic least-squares fits of $\log(m'_1)$ for $k = 100, 200, 300, ..., 1000$. See Figure 74 for a plot of the p_3 values of the quadratic least-squares fits of $\log(l_i)$ and the p_3 values of the quadratic least-squares fits of $\log(m'_1)$ for $k = 100, 200, 300, ..., 1000$. The R-square values for the quadratic least-squares fits of the $\log(m'_i)$ values are 0.9894, 0.9904, 0.9907, 0.990, 0.9907, 0.9925, 0.9932, 0.9932, 0.9947, and 0.9938 respectively. The R-square values for the quadratic least-squares fits of the $\log(l_i)$ values are 0.9912, 0.9915, 0.9919, 0.9908, 0.9913, 0..9922, 0.9925, 0.9925, 0.9949, and 0.9947 respectively.

Let l_i and m_i be similarly defined for the function $\sigma_0(x)$. Let m'_i denote $j(l_i)$. See Figure 75 for a plot of $l_i/(\log(l_i)m'_i)$, m'_i/l_i, and $1/\log(l_i)$ for $i = 1, 2, 3, ..., 65$ (corresponding to the local maxima for $x \leq 1000000000$). See Figure 76 for a plot of $\log(m'_i)$ for $i = 1, 2, 3, ..., 65$. For a quadratic least-squares fit of $\log(m'_i)$ for $i = 1, 2, 3, ..., 65$, $p_1 = -0.0007068$ with a 95% confidence interval of (-0.001025, -0.0003881), $p_2 = 0.3254$ with a 95% confidence interval of (0.3037, 0.3471), $p_3 = 0.5652$ with a 95% confidence interval of (0.2549, 0.8756), SSE=10.14, R-square=0.9943, and RMSE=0.4045. See Figure 77 for a plot of $\log(l_i)$ for $i = 1, 2, 3, ..., 65$. (A quadratic least-squares fit is given in the above.) See Figure 78 for a plot of $\log(l_i/\sqrt{\log(l_i)})$ and $\log(m'_i)$ for $i = 1, 2, 3, ..., 65$. See Figure 79 for a plot of $\log(l_i) + \log(\log(l_i))$, $\log(l_i)$, and $\log(m_i)$ for $i = 1, 2, 3, ..., 65$. See Figure 80 for a plot of $(\log(l_i) + \log(\log(l_i))) - \log(m'_i)$ for $i = 1, 2, 3, ..., 65$. (This is evidence in support of Conjecture 1.)

Let l_i and m_i be similarly defined for the function $\sigma_0(x)$ with the additional stipulation that $|y_x(8) - z_x(8)| = k$. Let $m'_i = \sum_{n=1}^{l_i} (y_{l_i/n}(8) - z_{l_i/n}(8))^2$ where $n|l_i$. See Figure 81 for a plot of $l_i/(\log(l_i)m'_i)$, m'_i/l_i, and $1/\log(l_i)$ for $k = 3$ and $i = 1, 2, 3, ..., 13$ (corresponding to the local maxima for $x \leq 30000$). See Figure 82 for a plot of $\log(m'_i)$ for $i = 1, 2, 3, ..., 13$. For a quadratic least-squares fit of $\log(m'_i)$ for $i = 1, 2, 3, ..., 13$, $p_1 = 0.00597$ with a 95% confidence interval of (-0.004447, 0.01564), $p_2 = 0.3586$ with a 95% confidence interval of (0.2141, 0.5031), $p_3 = 1.81$ with a 95% confidence interval of (1.37, 2.25), SSE=0.4068, R-square=0.9884, and RMSE=0.2017. See Figure 83 for a plot of $\log(l_i)$ for $i = 1, 2, 3, ..., 13$. For a quadratic least-squares fit of $\log(l_i)$ for $i = 1, 2, 3, ..., 13$, $p_1 = -0.01942$ with a 95% confidence interval of (-0.03464, -0.004204), $p_2 = 0.9339$ with a 95% confidence interval of (0.7149, 0.1.153),

$p_3 = 0.7612$ with a 95% confidence interval of (0.09466, 1.428), SSE=0.934, R-square=0.9885, and RMSE=0.3056. See Figure 84 for a plot of $\log(l_i/\sqrt{\log(l_i)})$ and $\log(m'_i)$ for $i = 1, 2, 3, ..., 13$.

References

[1] J. Franel and E. Landau, Les suites de Farey et le problème des nombres premiers, *Göttinger Nachr.*, 198-206 (1924)

[2] J. E. Littlewood, Quelques conséquences de l'hypothèse que la fonction $\zeta(s)$ n'a pas de zèros dans le demi-plan $\mathrm{Re}(s) > 1/2$. *C. R. Acad. Sci. Paris* **154**, 263-266 (1912)

[3] A. M. Odlyzko and H. J. J. te Riele, Disproof of the Mertens Conjecture, *Journal für die reine und angewandte Mathematik*, **357**:138-160 (1985)

[4] R. S. Lehman, On Liouville's Function, *Math. Comput.* **14**:311-320 (1960)

[5] R. M. Redheffer, Eine explizit lösbare Optimierungsaufgabe, *Internat. Schriftenreine Numer. Math.*, **36** (1977)

[6] F. Mertens, Über eine zahlentheoretische Funktion, *Akademie Wissenschaftlicher Wien Mathematik-Naturlich Kleine Sitzungsber*, **106** (1897) 761-830

[7] S. Kanemitsu and M. Yoshimoto, Farey series and the Riemann hypothesis, *Acta Arith.*, LXXV.4 (1996)

[8] C. B. Haselgrove, A disproof of a conjecture of Pólya, *Mathematika*, **5**(02), 141-145 (1958)

[9] J. C. Lagarias, An elementary problem equivalent to the Riemann hypothesis, *American Mathematical Monthly* 109, 534-543 (2002)

[10] T. Kotnik and J. van de Lune, On the order of the Mertens function, *Experimental Mathematics* **13**, pp. 473-481 (2004)

Figure 1

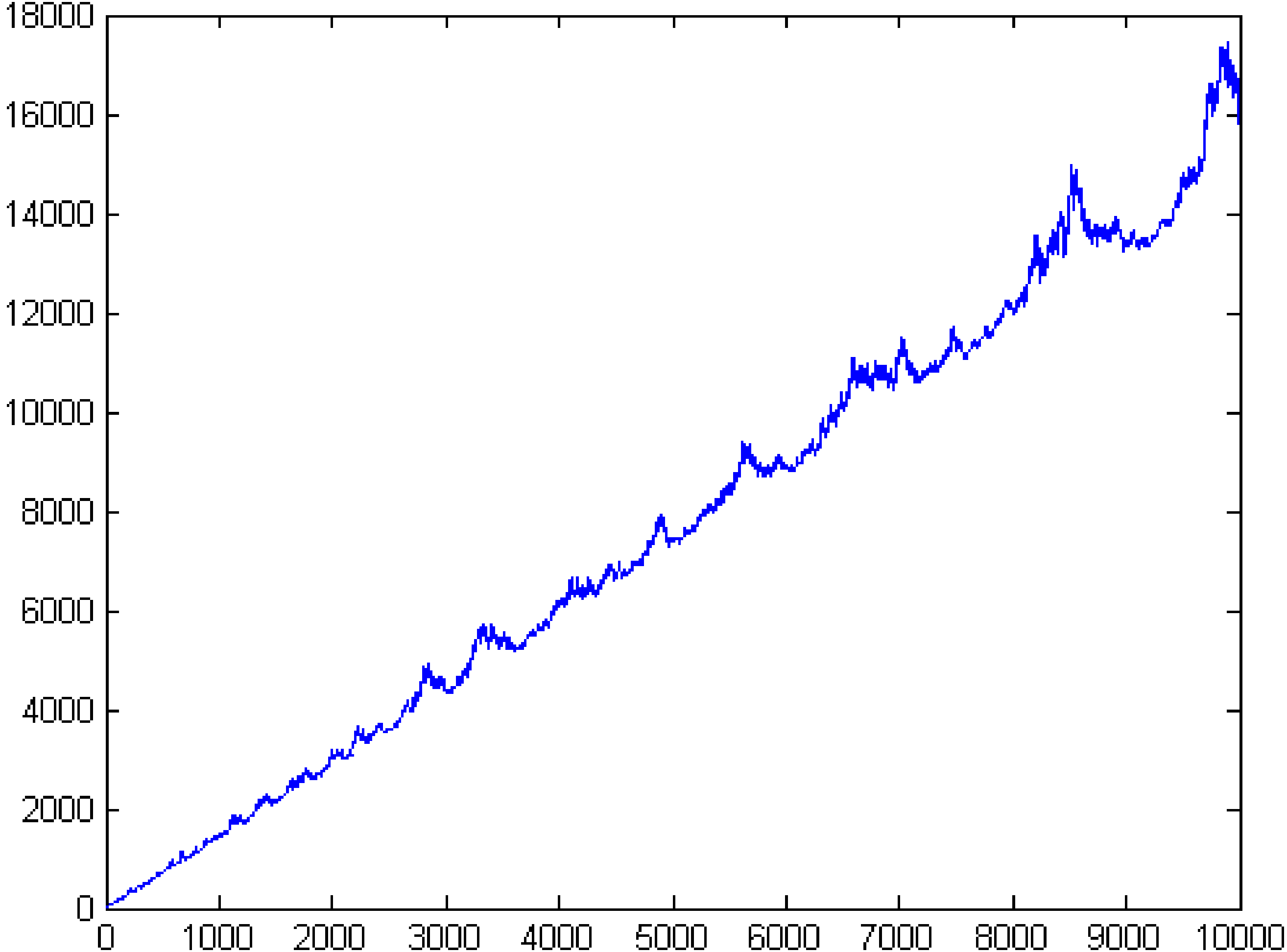

18000
16000
14000
12000
10000
8000
6000
4000
2000
0
0
1000
2000
3000
4000
5000
6000
7000
8000
9000
10000

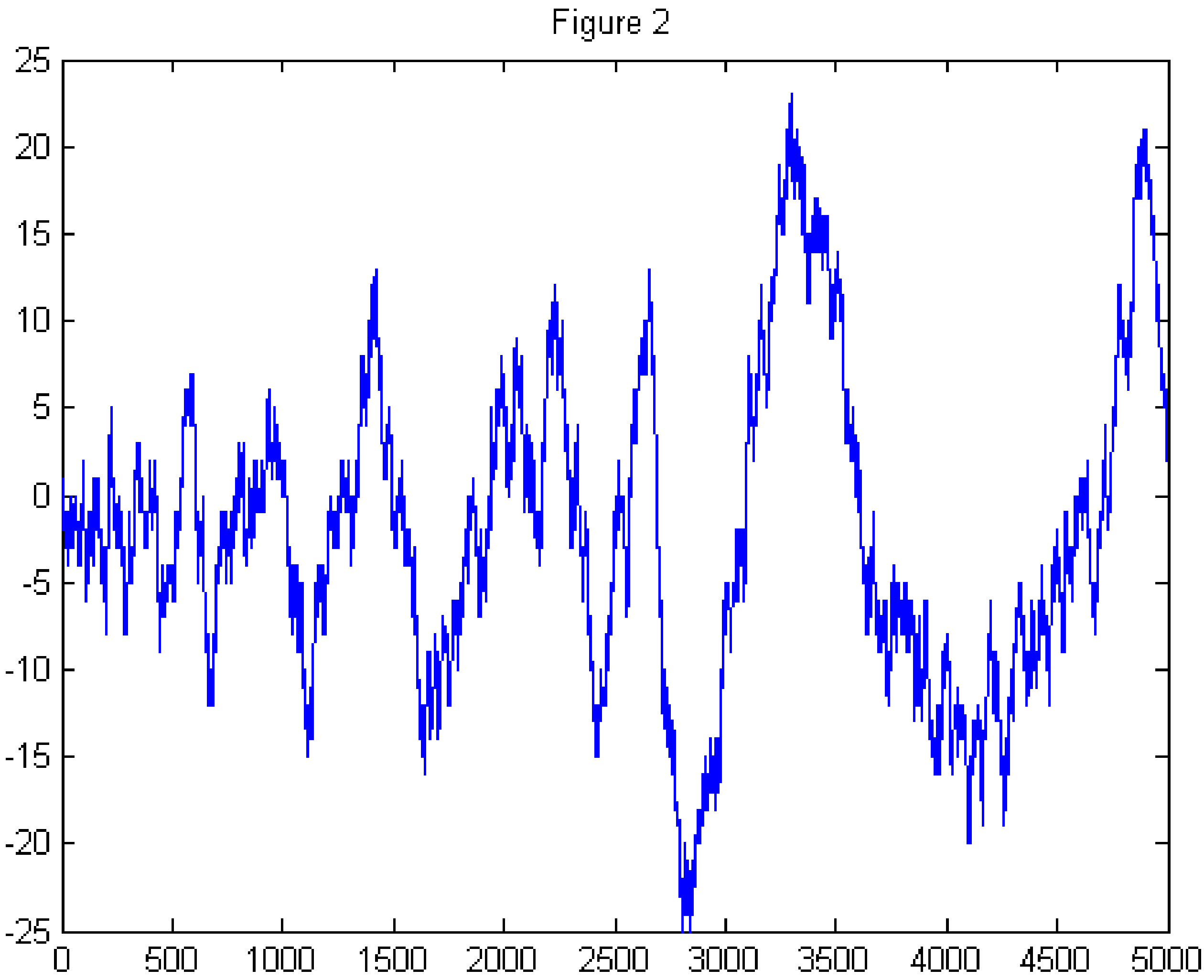
Figure 2
25
20
15
10
5
0
-5
-10
-15
-20
-25
0
500
1000
1500
2000
2500
3000
3500
4000
4500
5000

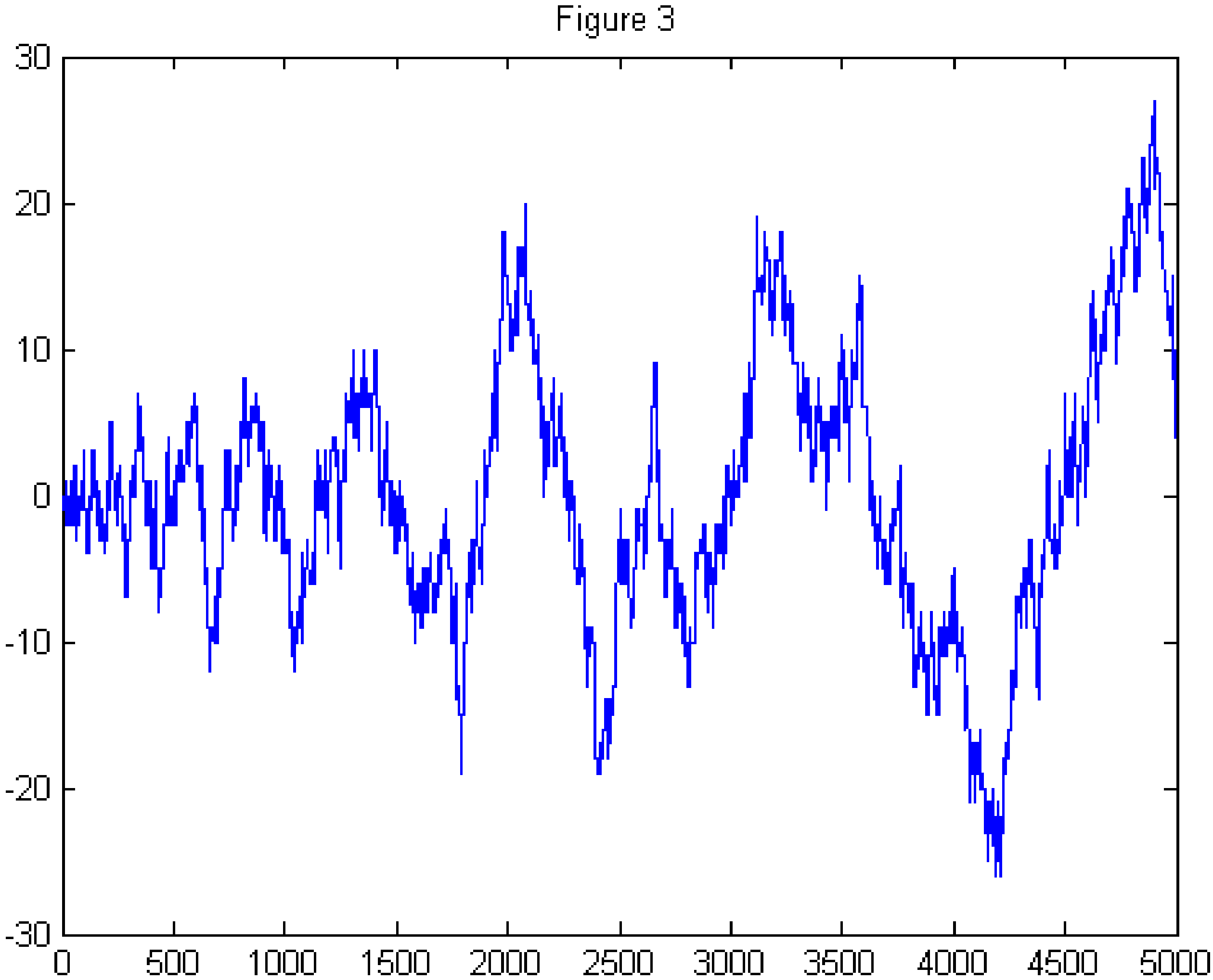
Figure 3
30
20
10
0
-10
-20
-30
0
500
1000
1500
2000
2500
3000
3500
4000
4500
5000

Figure 4

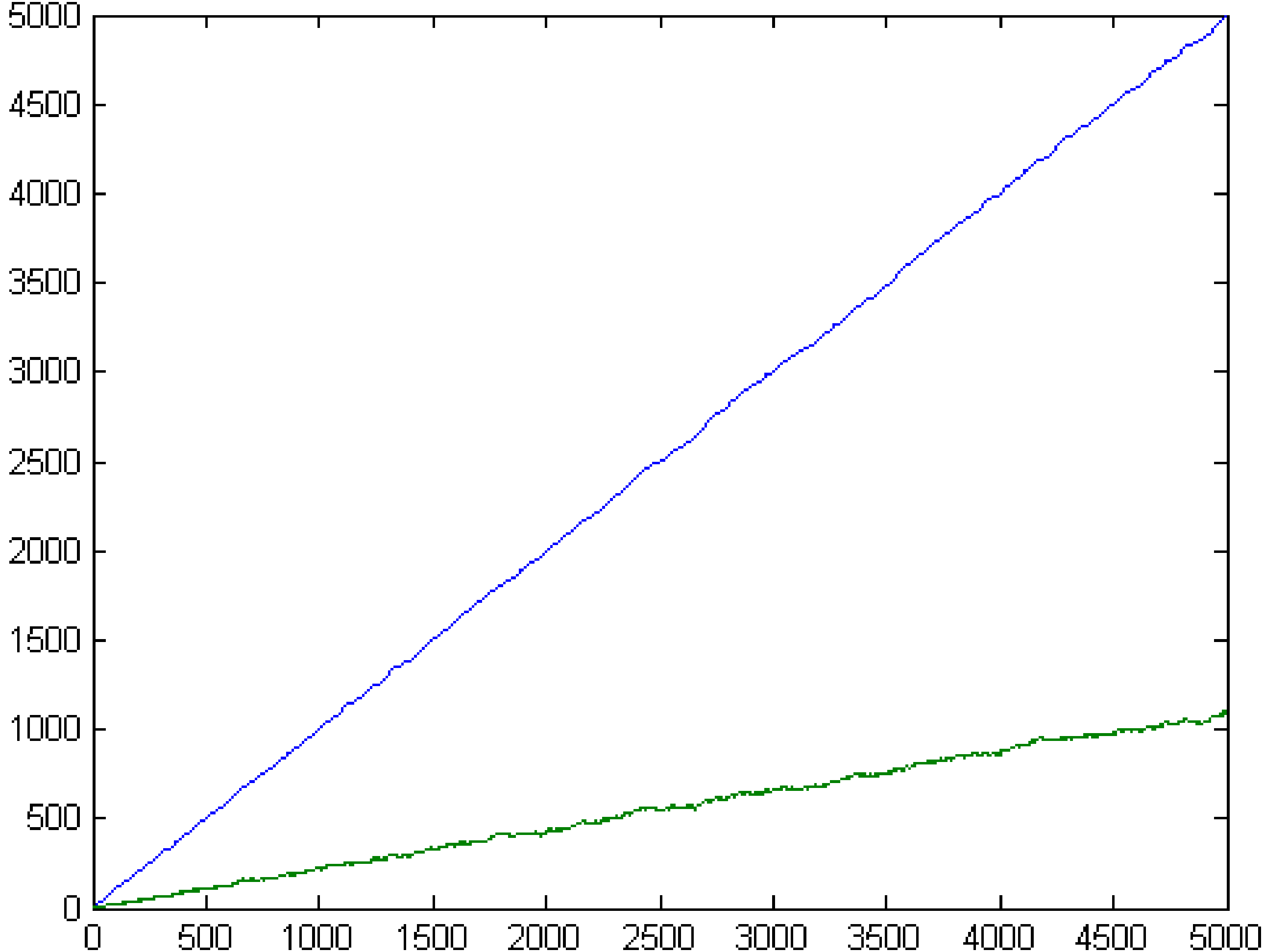
5000
4500
4000
3500
3000
2500
2000
1500
1000
500
0
0
500
1000
1500
2000
2500
3000
3500
4000
4500
5000

Figure 5

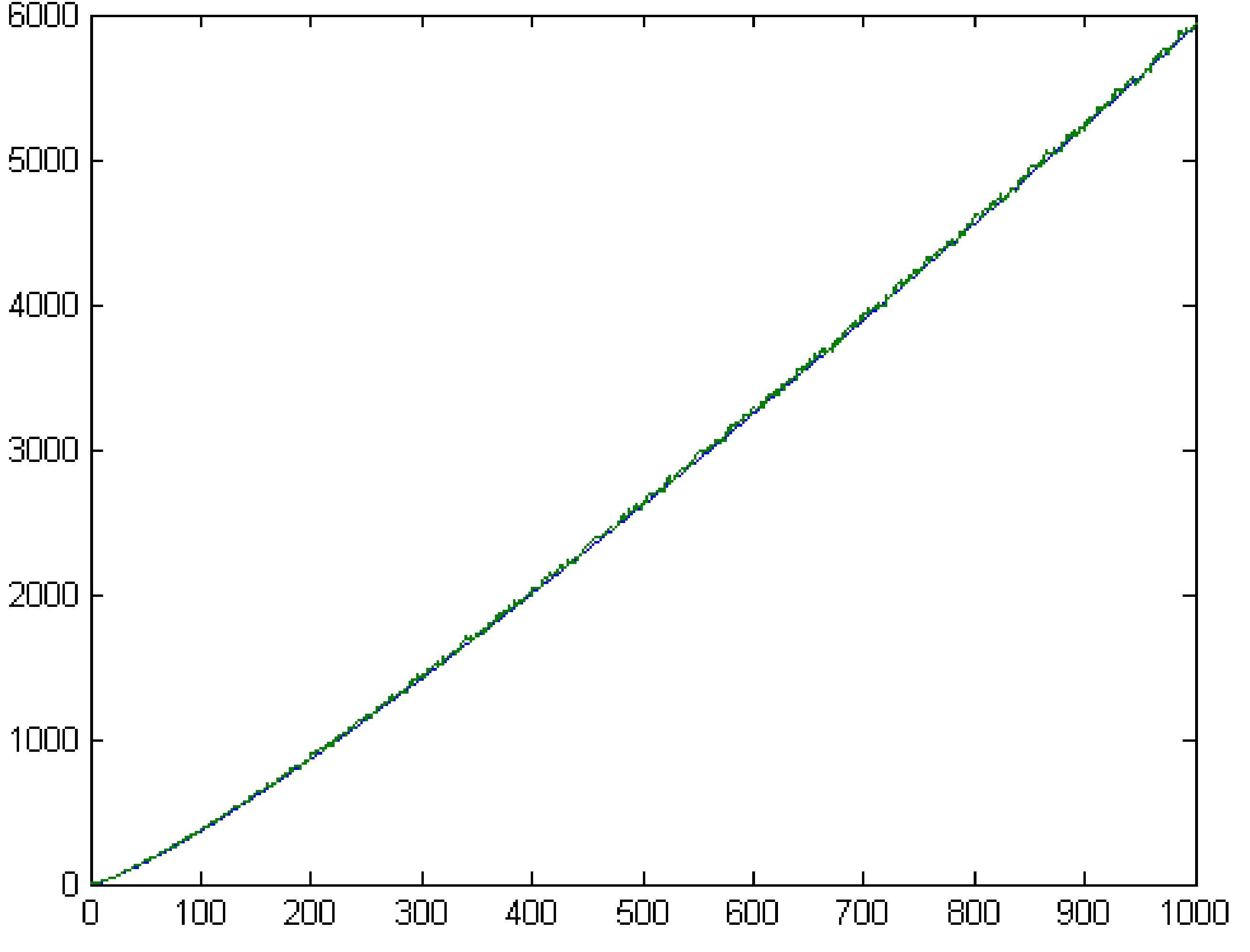

6000
5000
4000
3000
2000
1000
0
0
100
200
300
400
500
600
700
800
900
1000

Figure 6

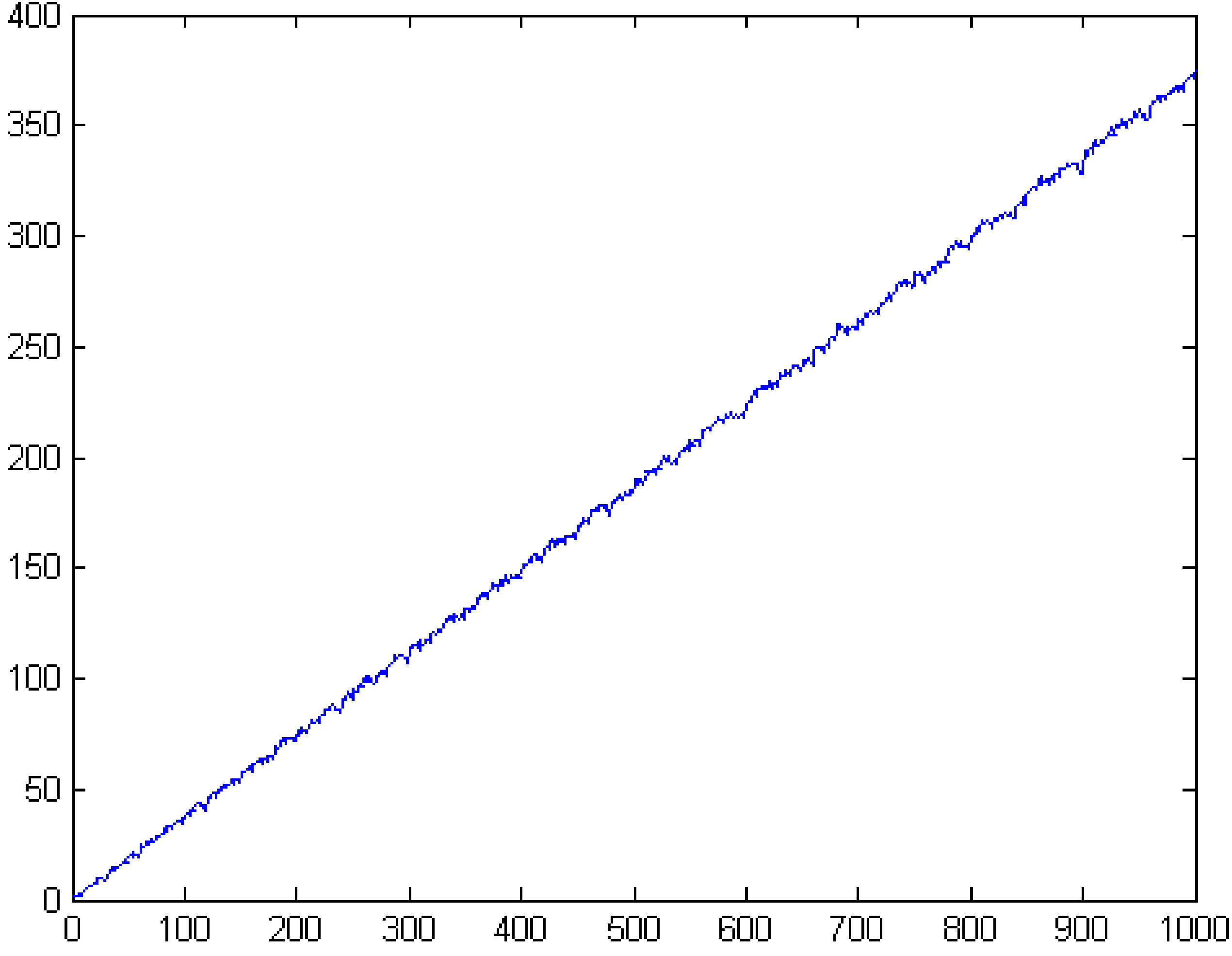

0
50
100
150
200
250
300
350
400
0
100
200
300
400
500
600
700
800
900
1000

Figure 7

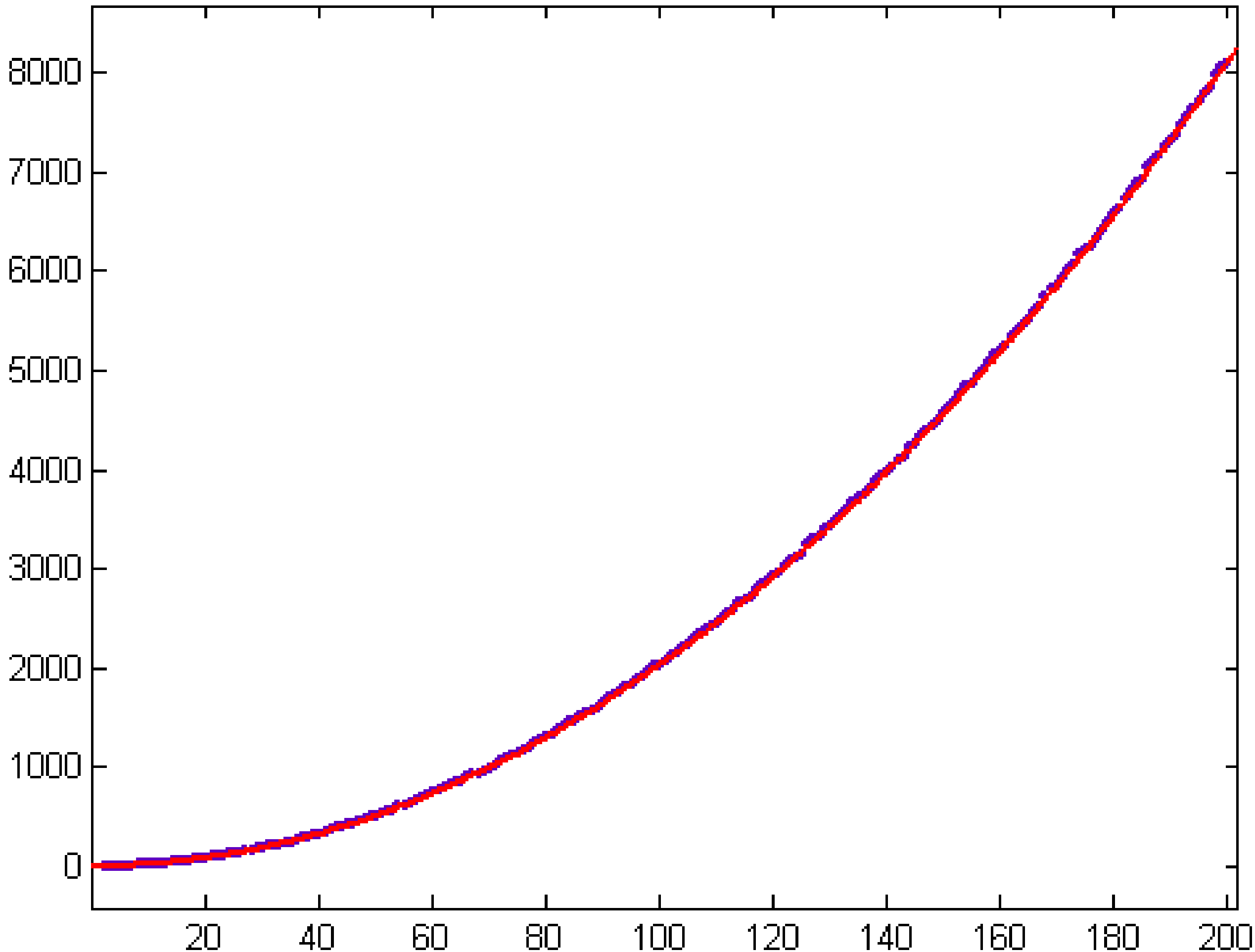

8000
7000
6000
5000
4000
3000
2000
1000
0
20
40
60
80
100
120
140
160
180
200

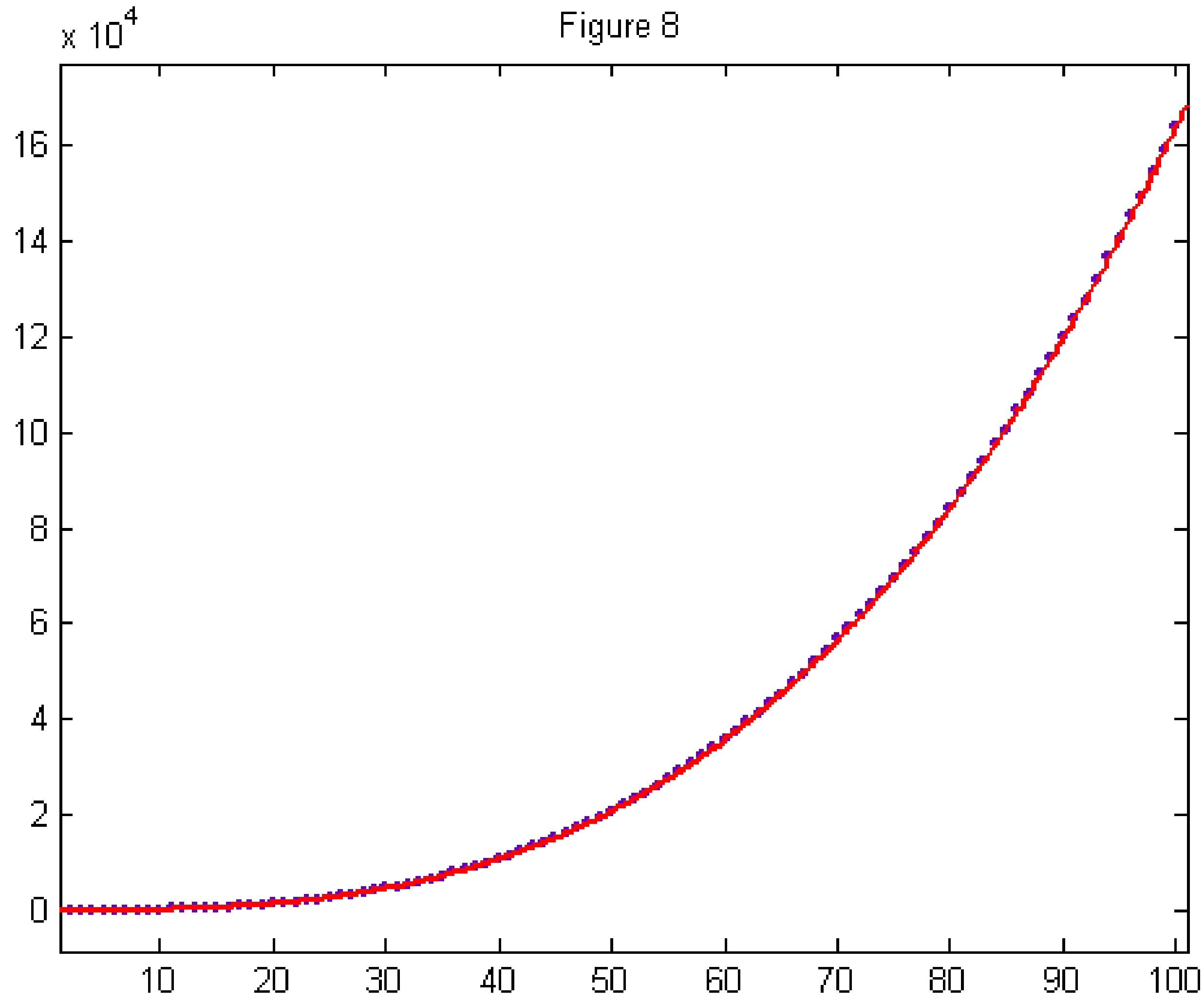
Figure 8
x 10^4
0
2
4
6
8
10
12
14
16
10
20
30
40
50
60
70
80
90
100

Figure 9

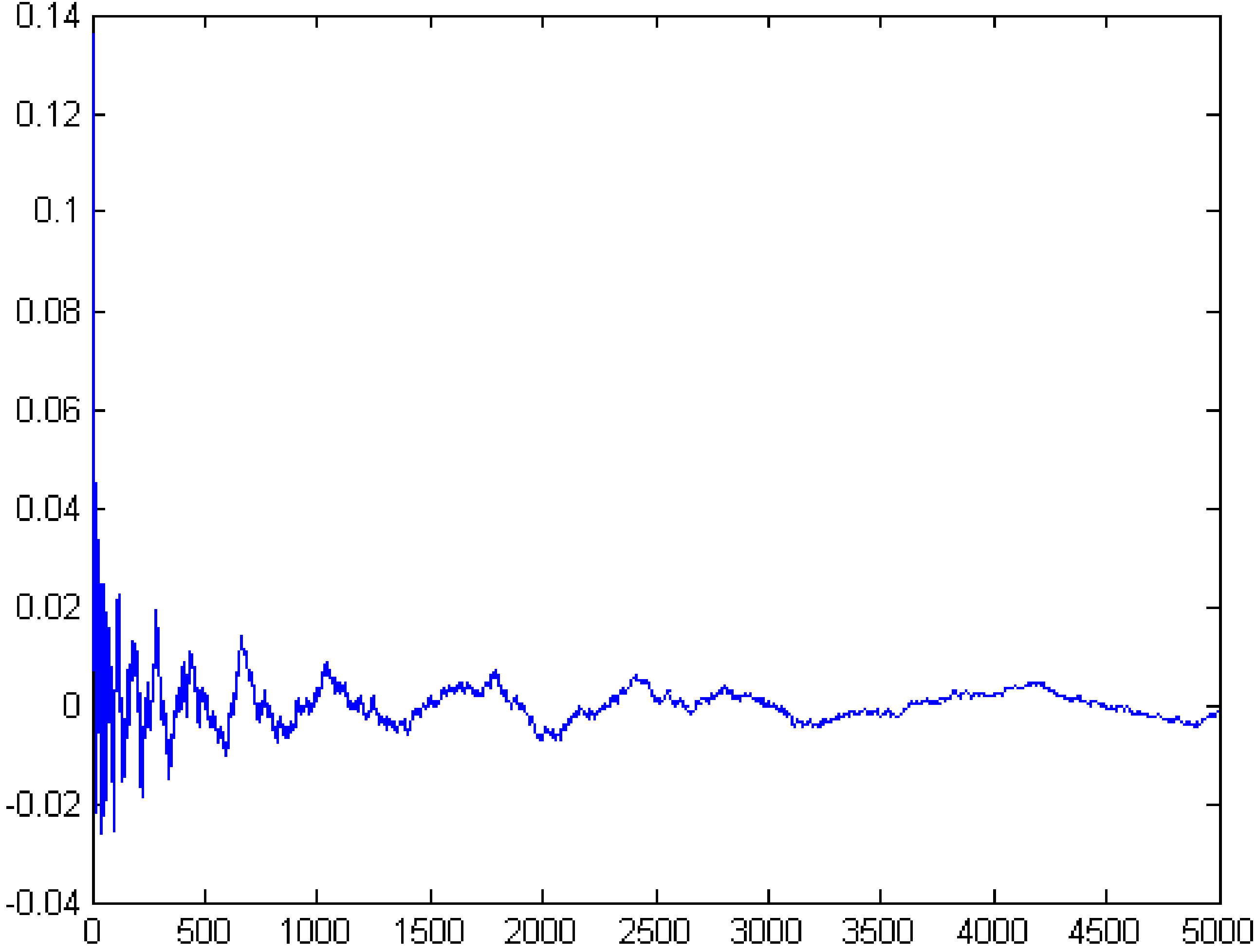

0.14
0.12
0.1
0.08
0.06
0.04
0.02
0
-0.02
-0.04
0
500
1000
1500
2000
2500
3000
3500
4000
4500
5000

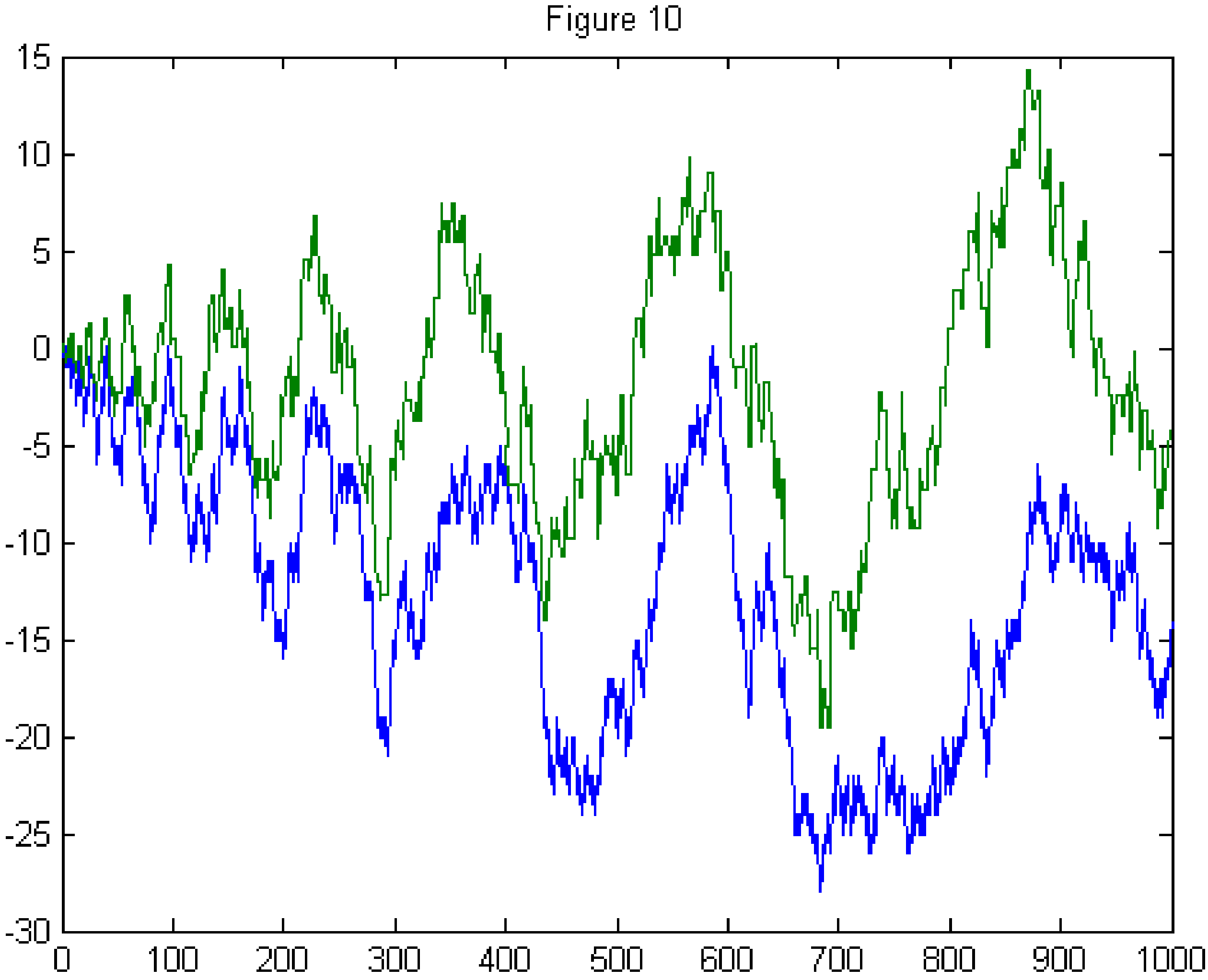
Figure 10
15
10
5
0
-5
-10
-15
-20
-25
-30
0
100
200
300
400
500
600
700
800
900
1000

Figure 11

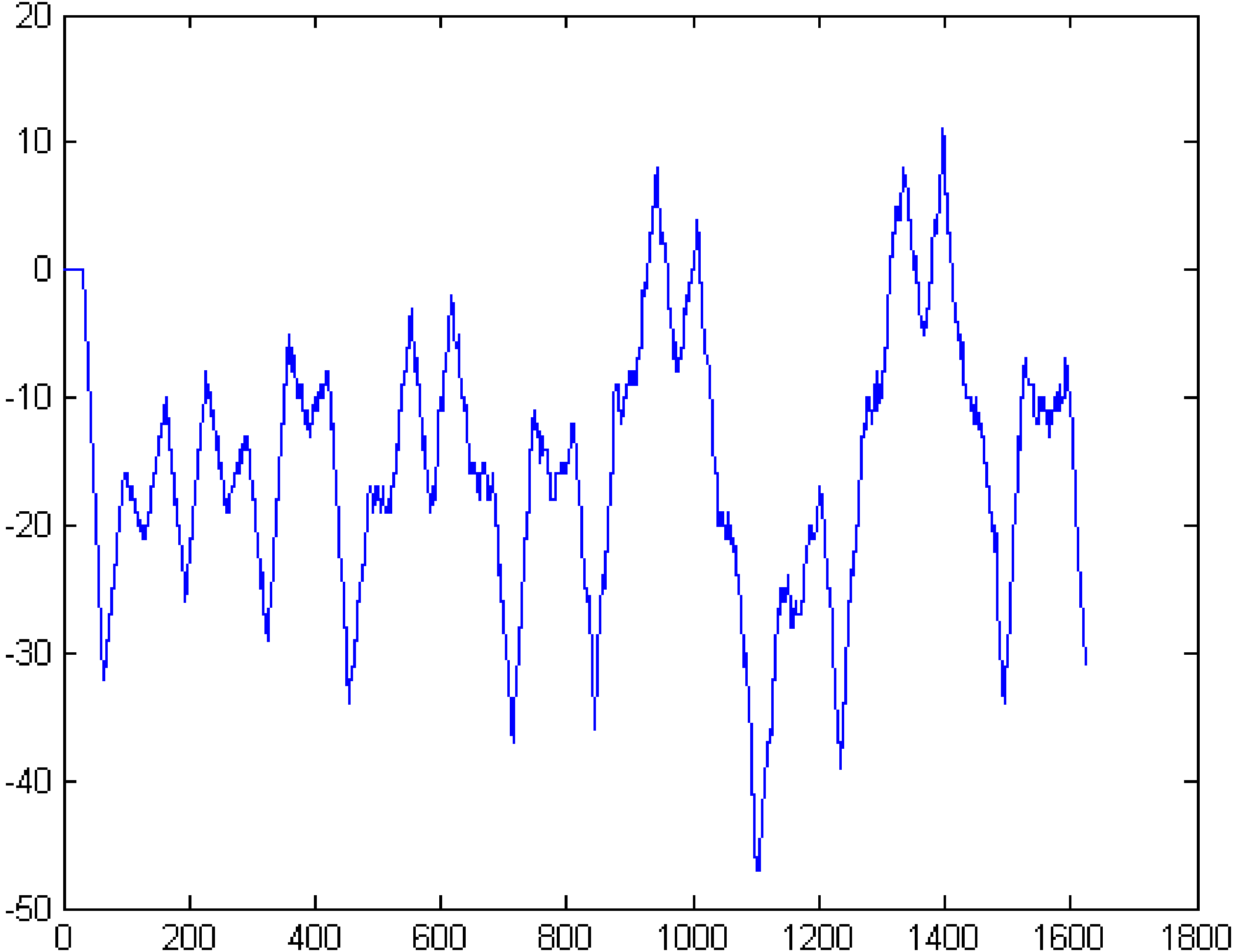

Figure 12

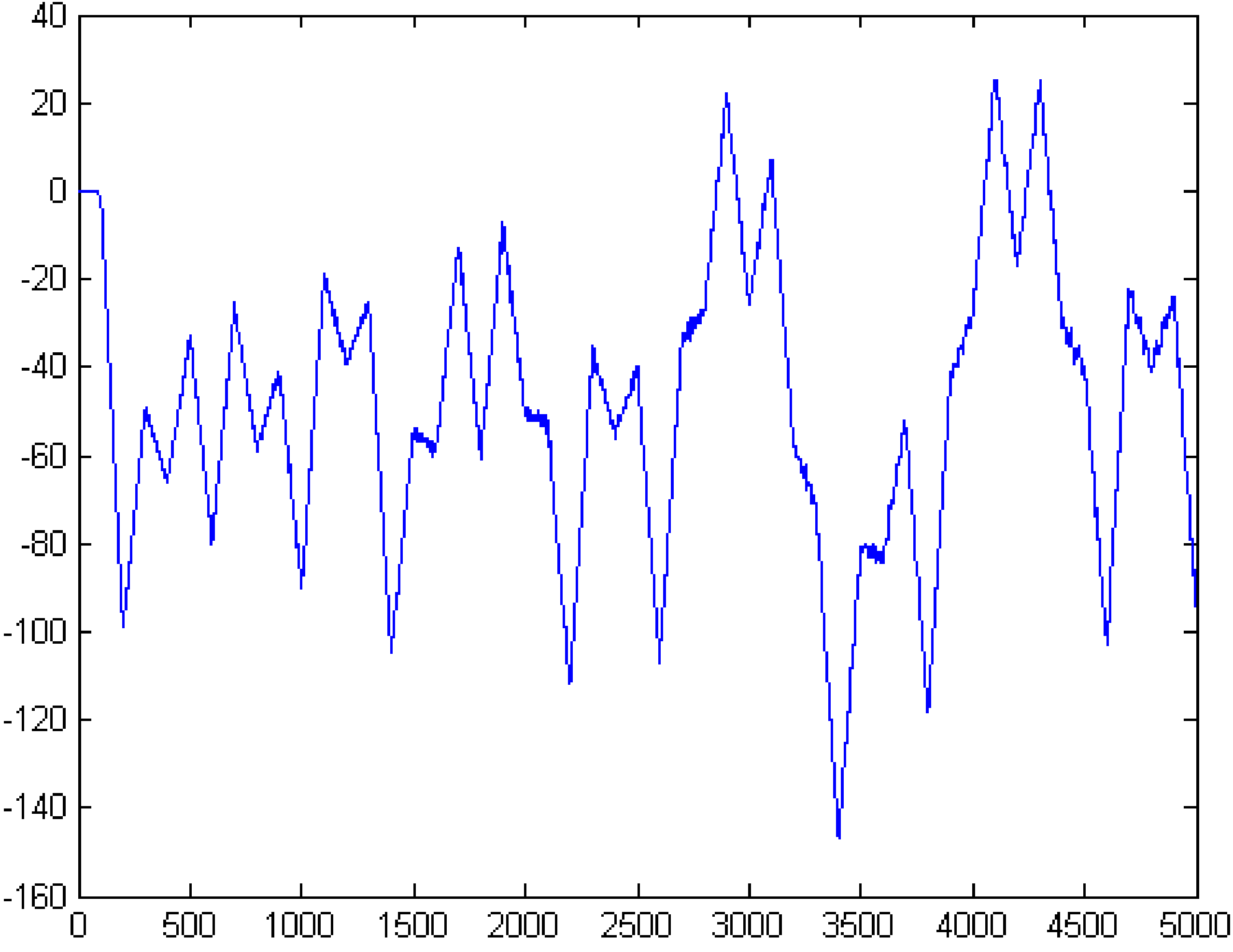

40
20
0
-20
-40
-60
-80
-100
-120
-140
-160
0
500
1000
1500
2000
2500
3000
3500
4000
4500
5000

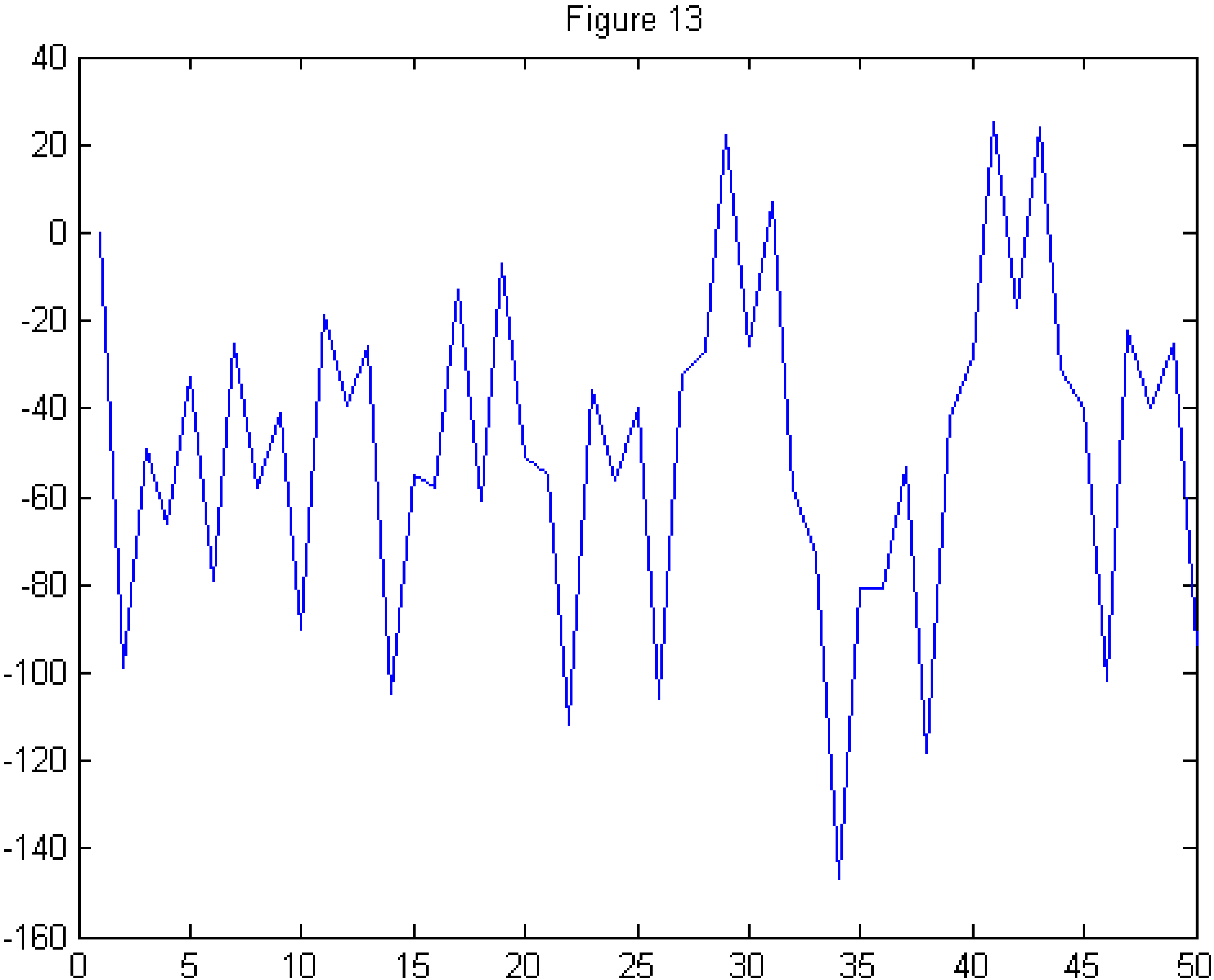
Figure 13
40
20
0
-20
-40
-60
-80
-100
-120
-140
-160
0
5
10
15
20
25
30
35
40
45
50

Figure 14

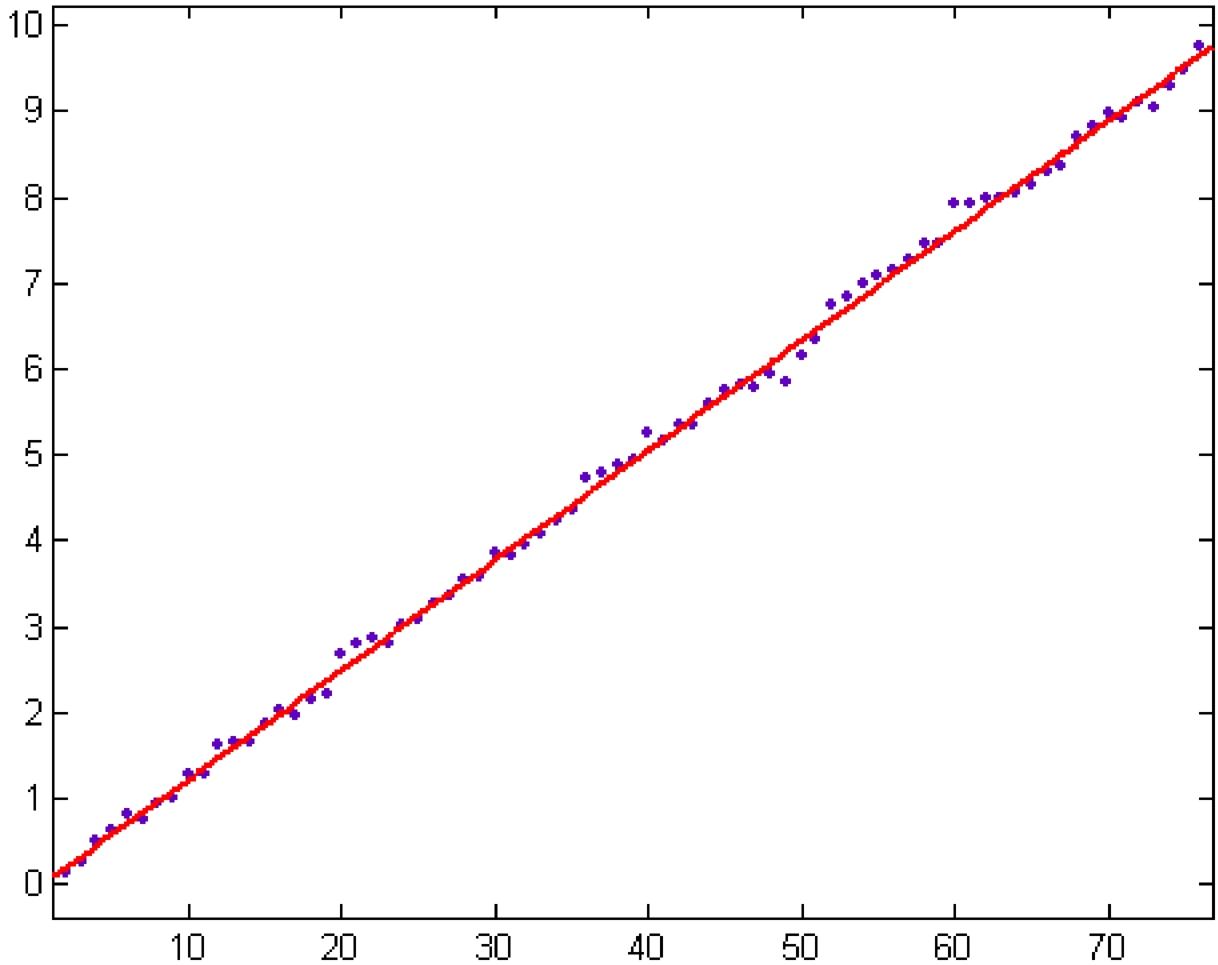

Figure 15

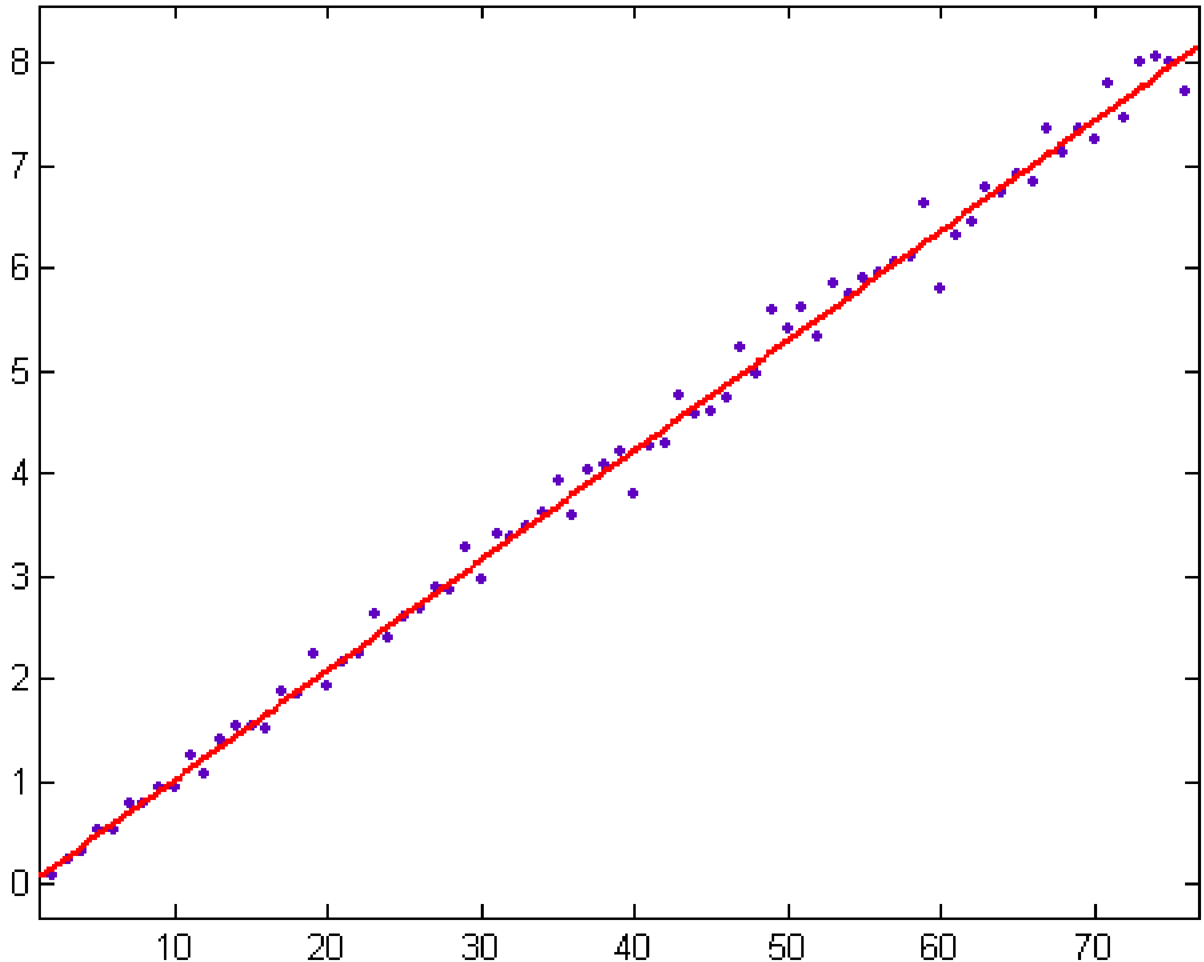

Figure 16

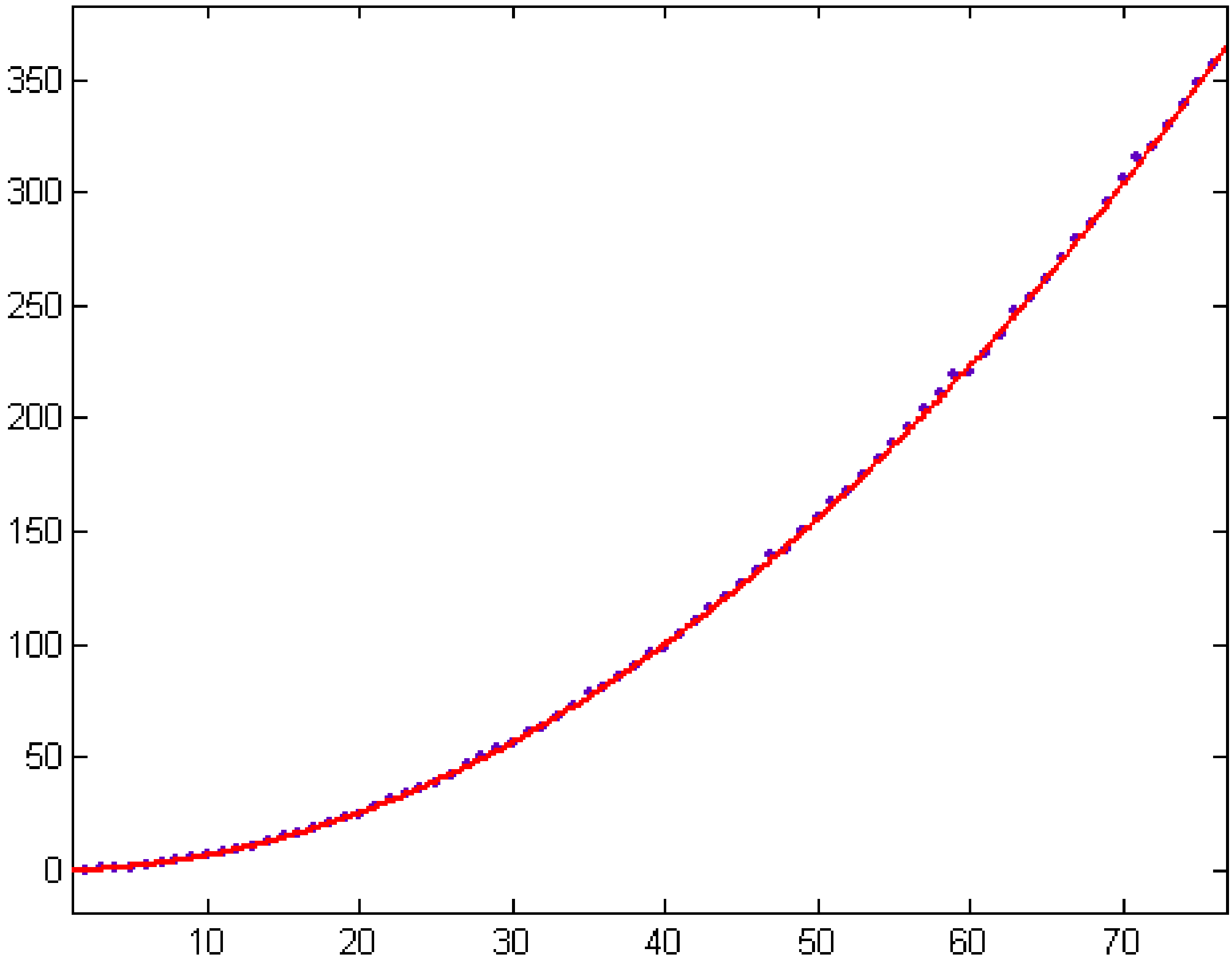

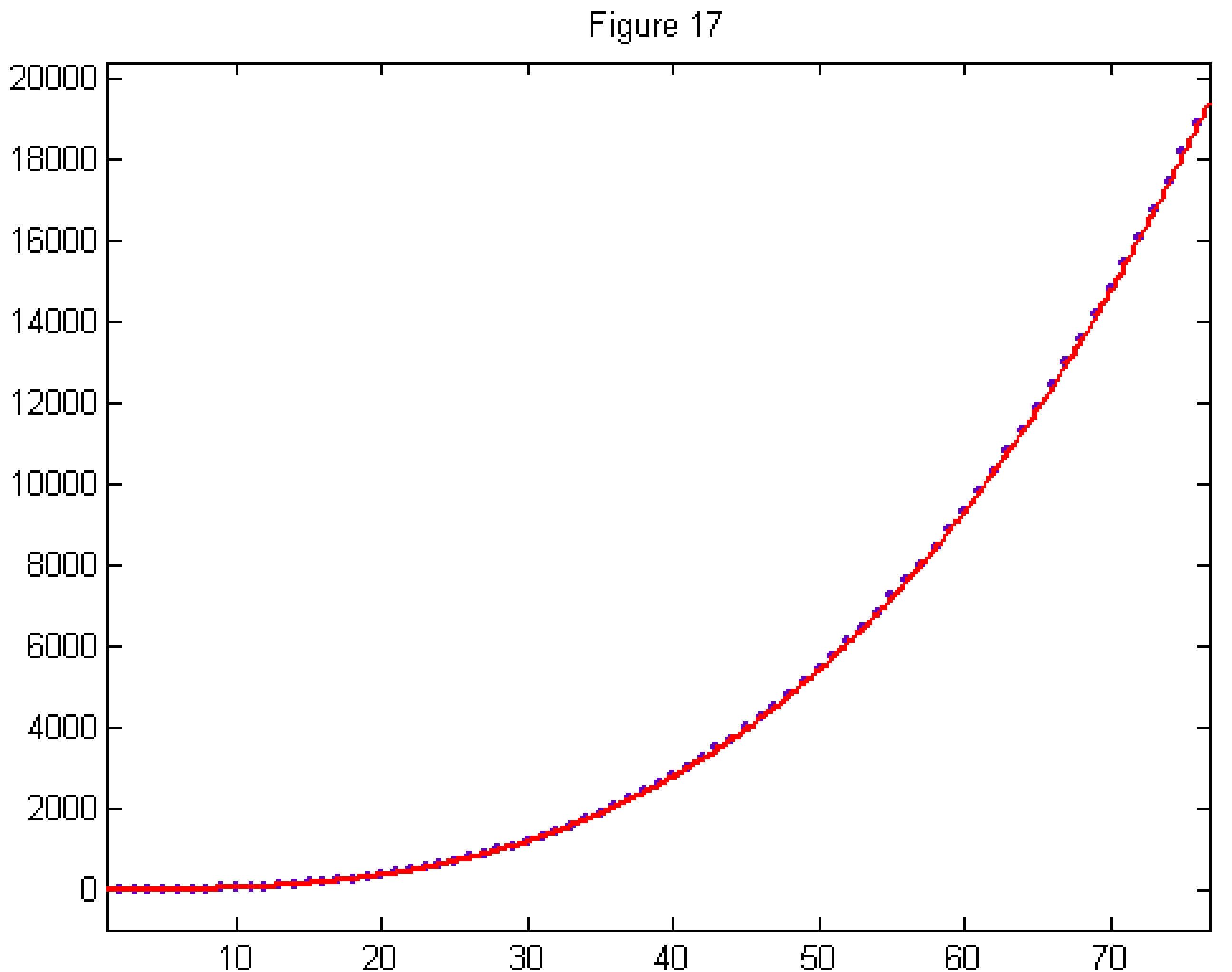
Figure 17
20000
18000
16000
14000
12000
10000
8000
6000
4000
2000
0
10
20
30
40
50
60
70

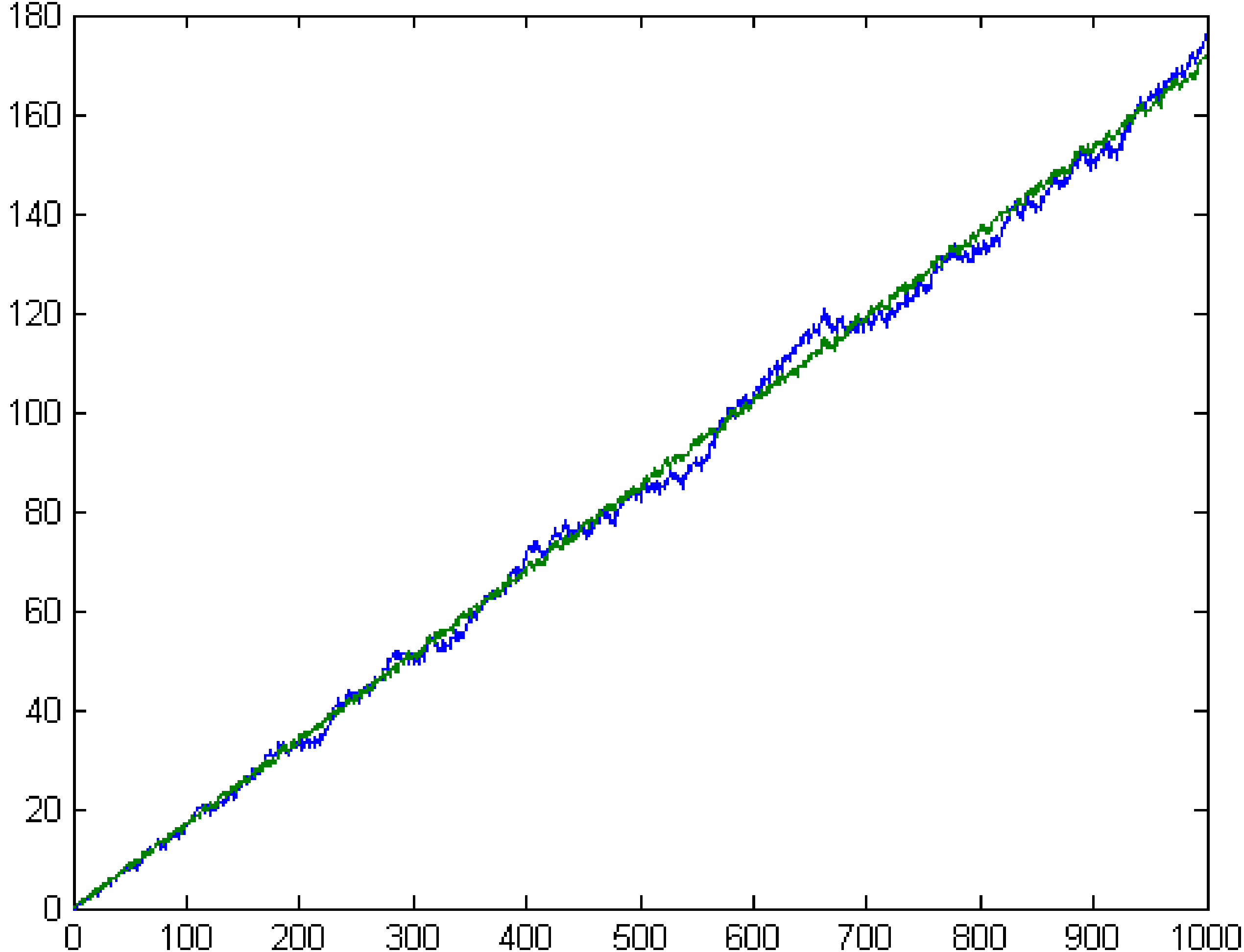
180
160
140
120
100
80
60
40
20
0
0 100 200 300 400 500 600 700 800 900 1000

Figure 18

Figure 19

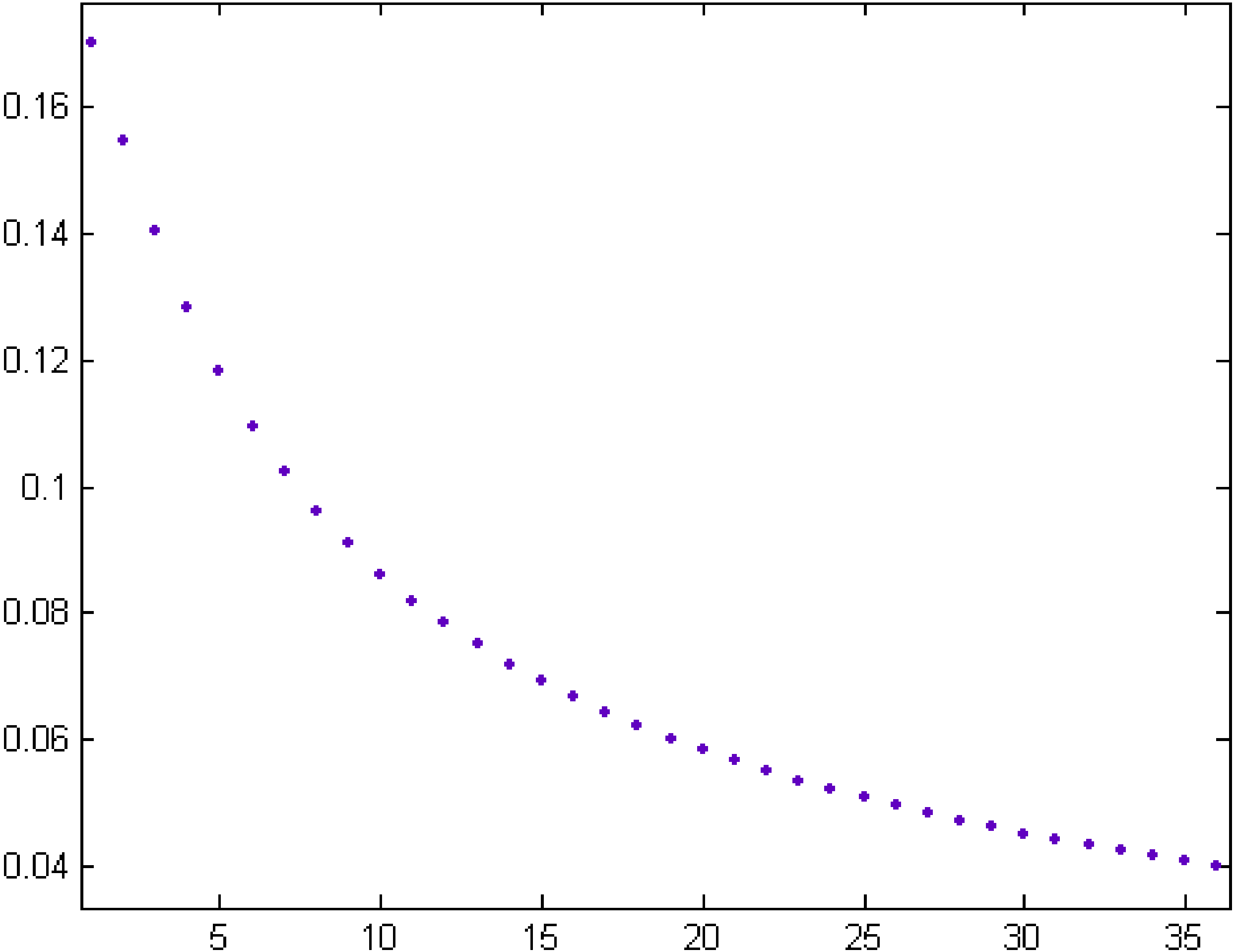

Figure 20

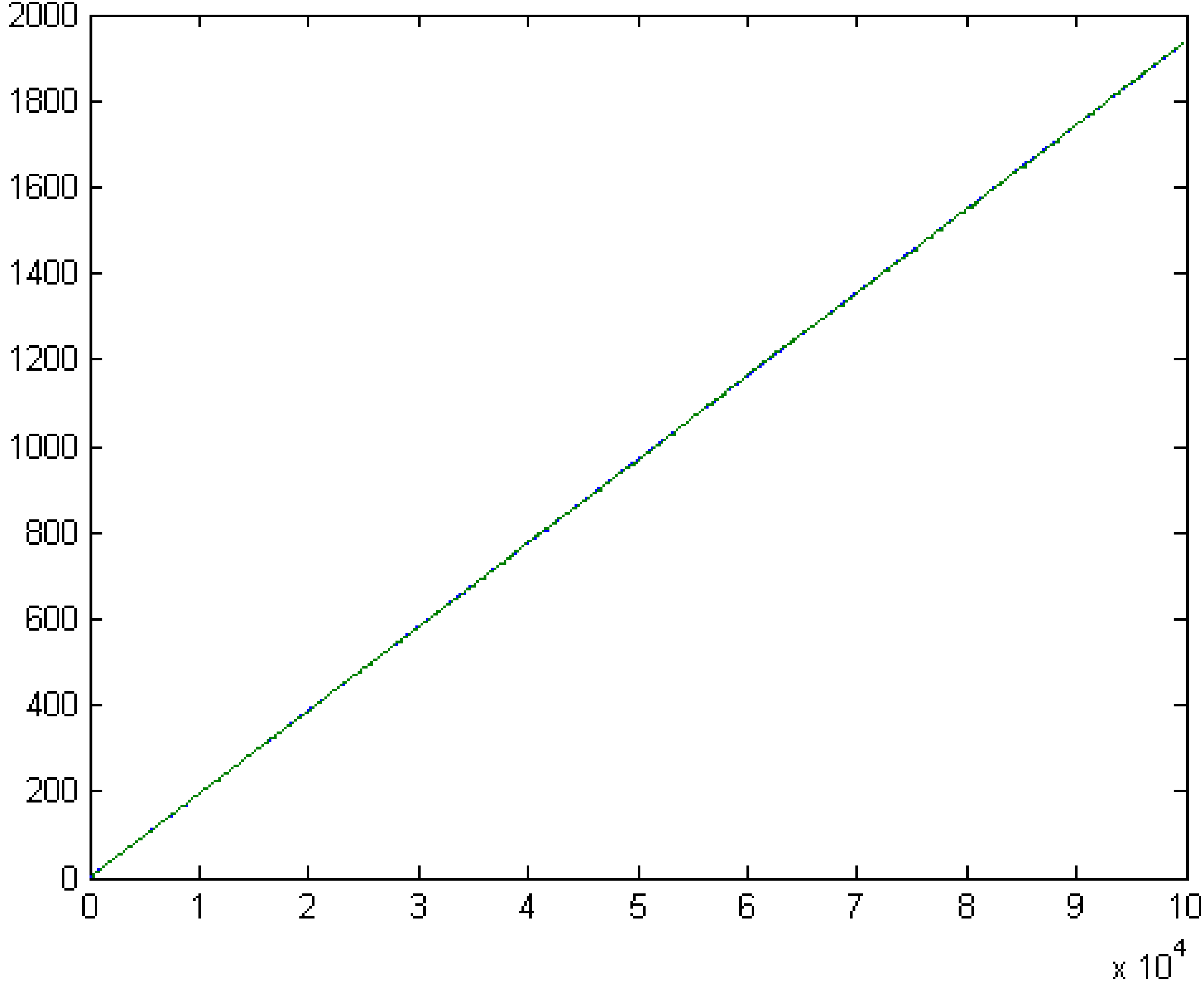

2000
1800
1600
1400
1200
1000
800
600
400
200
0
0
1
2
3
4
5
6
7
8
9
10
x 10^4

Figure 21

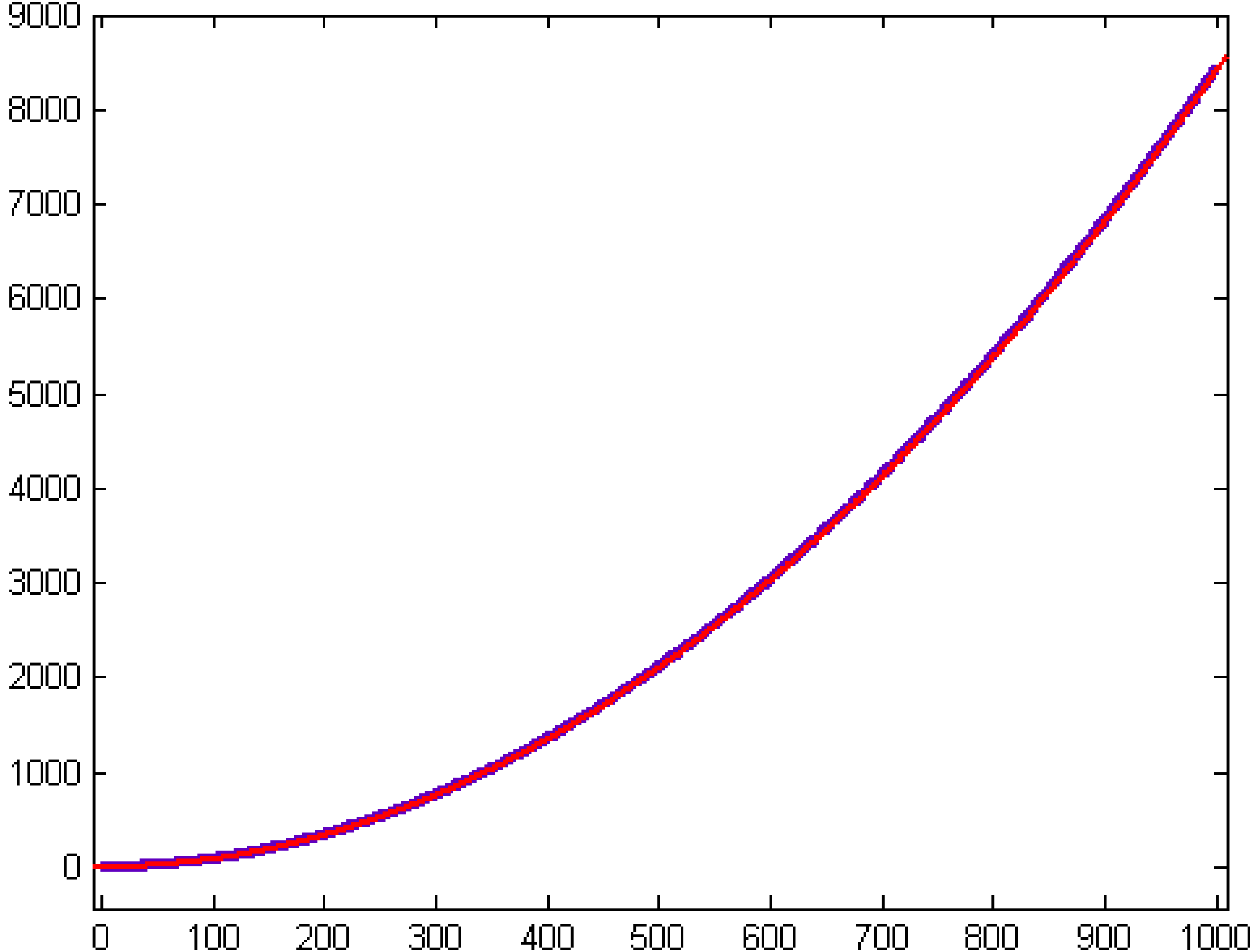

9000
8000
7000
6000
5000
4000
3000
2000
1000
0
0
100
200
300
400
500
600
700
800
900
1000

Figure 22

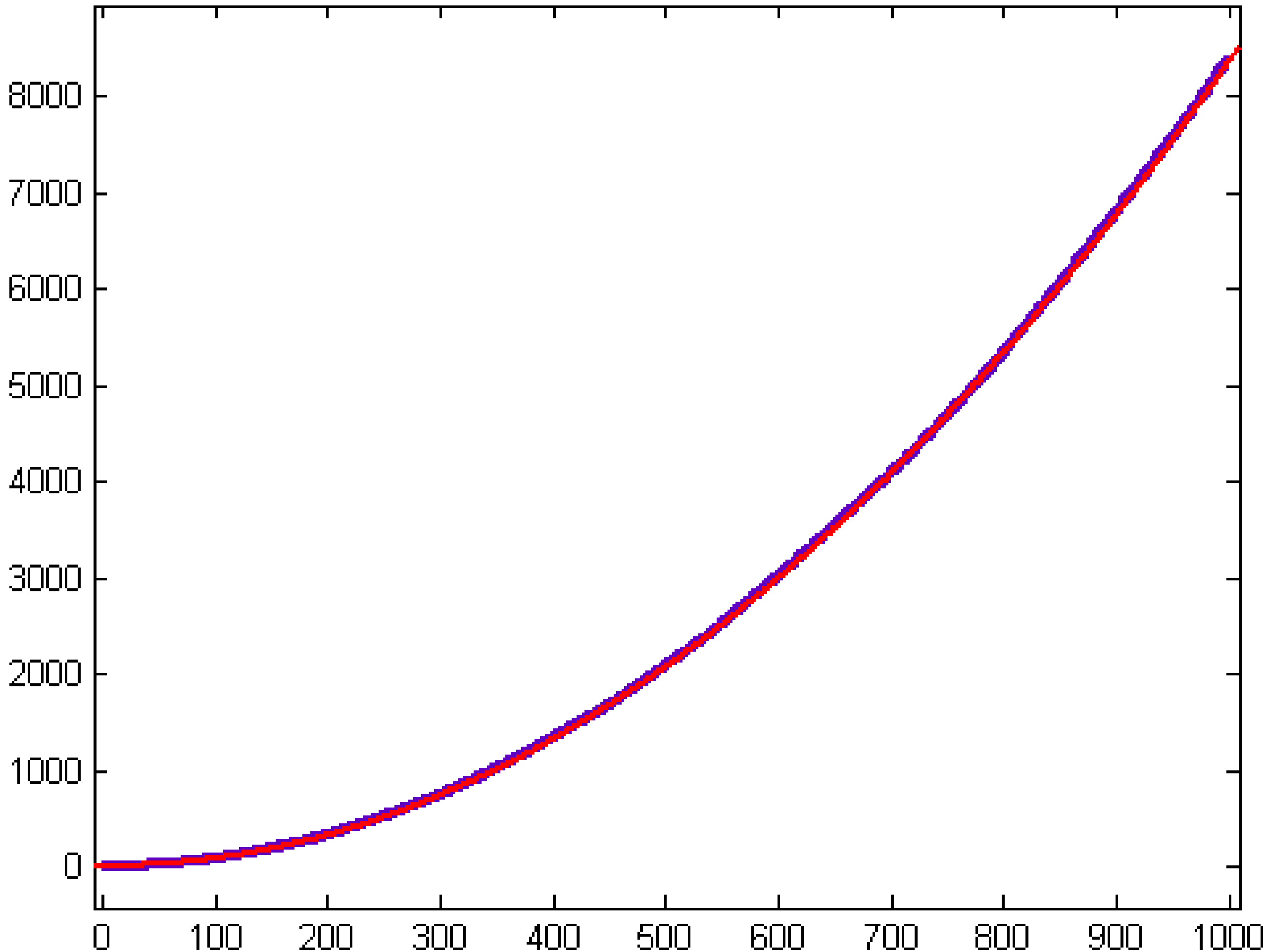
8000
7000
6000
5000
4000
3000
2000
1000
0
0
100
200
300
400
500
600
700
800
900
1000

Figure 23

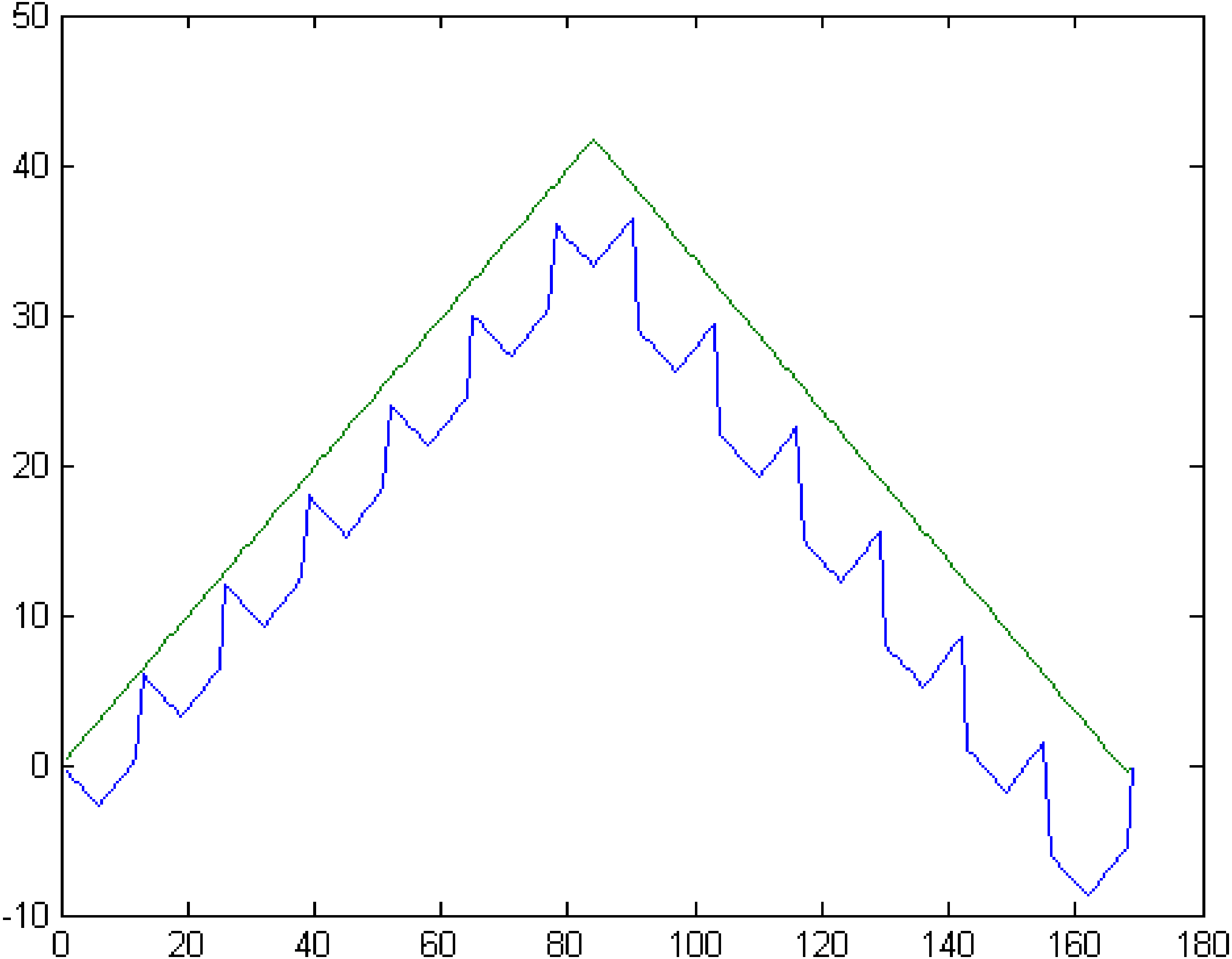

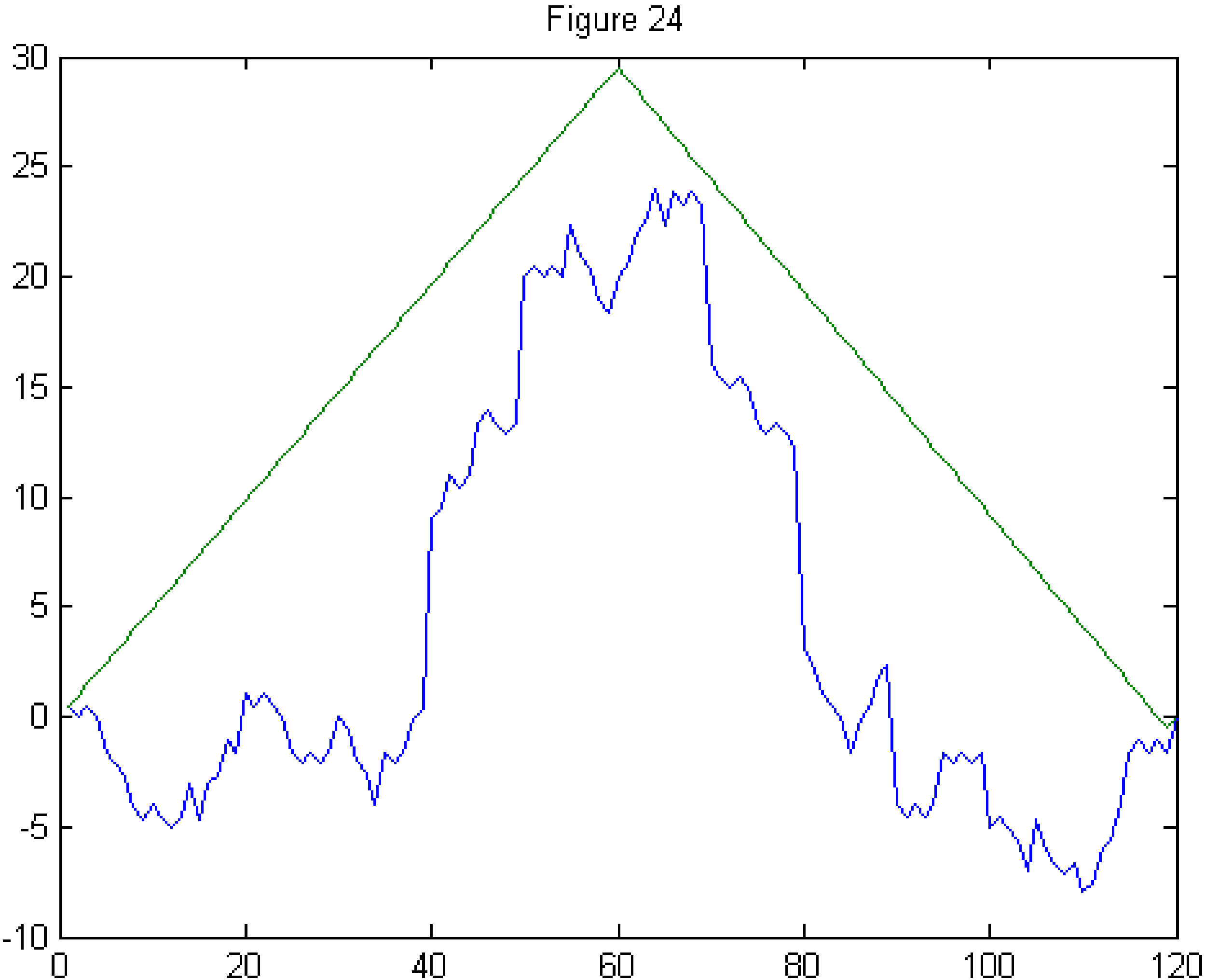
Figure 24
30
25
20
15
10
5
0
-5
-10
0
20
40
60
80
100
120

Figure 25

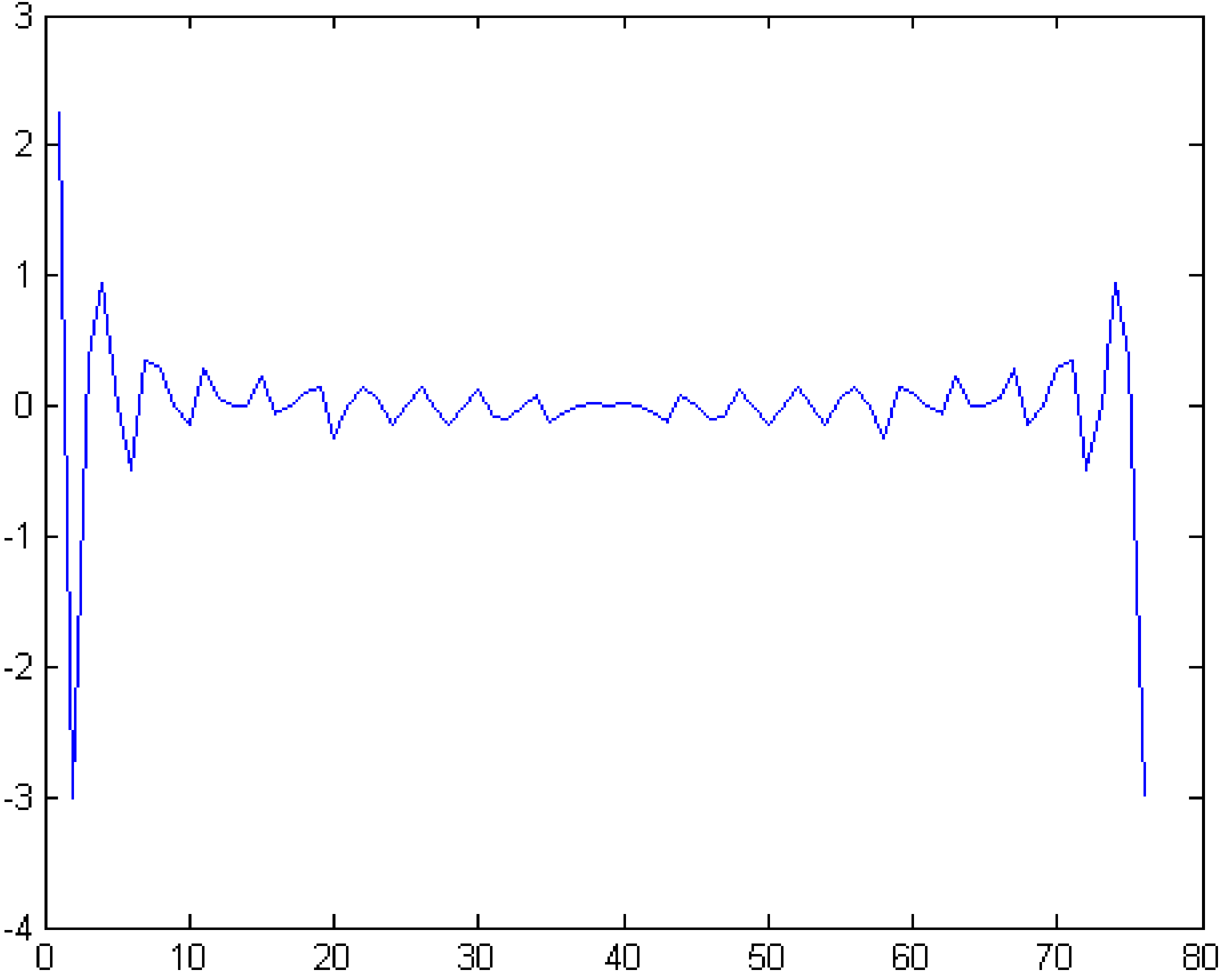

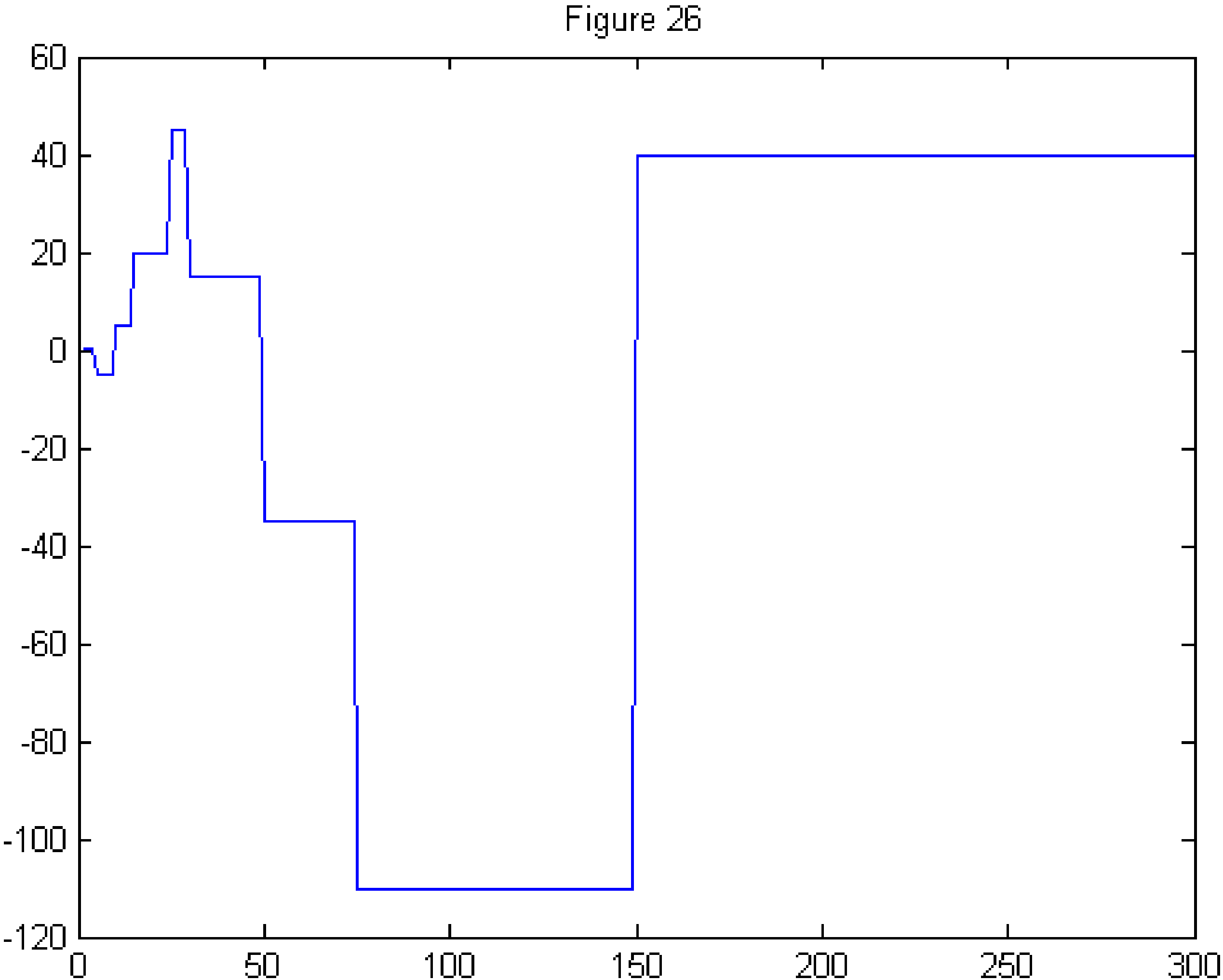
Figure 26
60
40
20
0
-20
-40
-60
-80
-100
-120
0
50
100
150
200
250
300

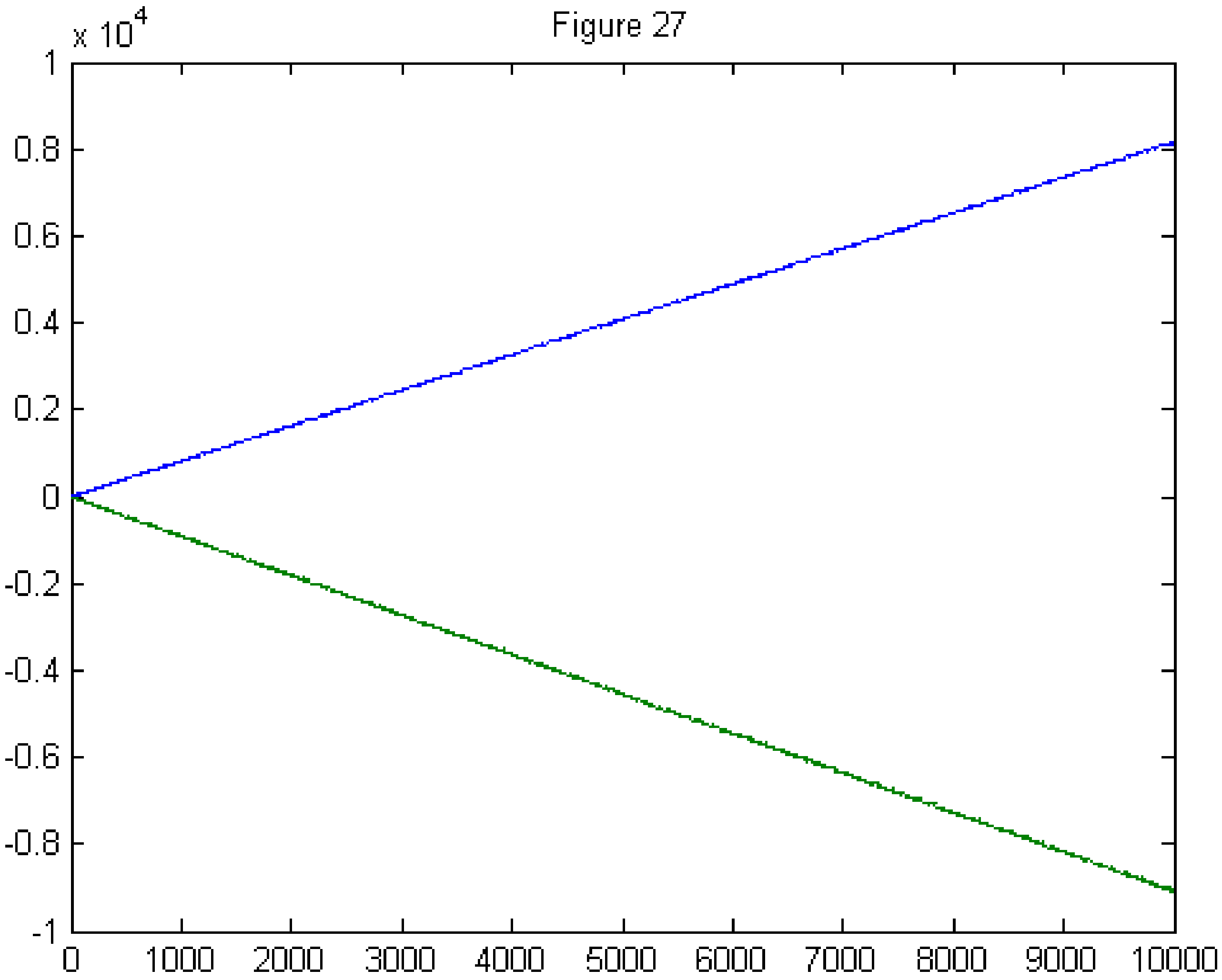
Figure 27
x 10^4
1
0.8
0.6
0.4
0.2
0
-0.2
-0.4
-0.6
-0.8
-1
0
1000
2000
3000
4000
5000
6000
7000
8000
9000
10000

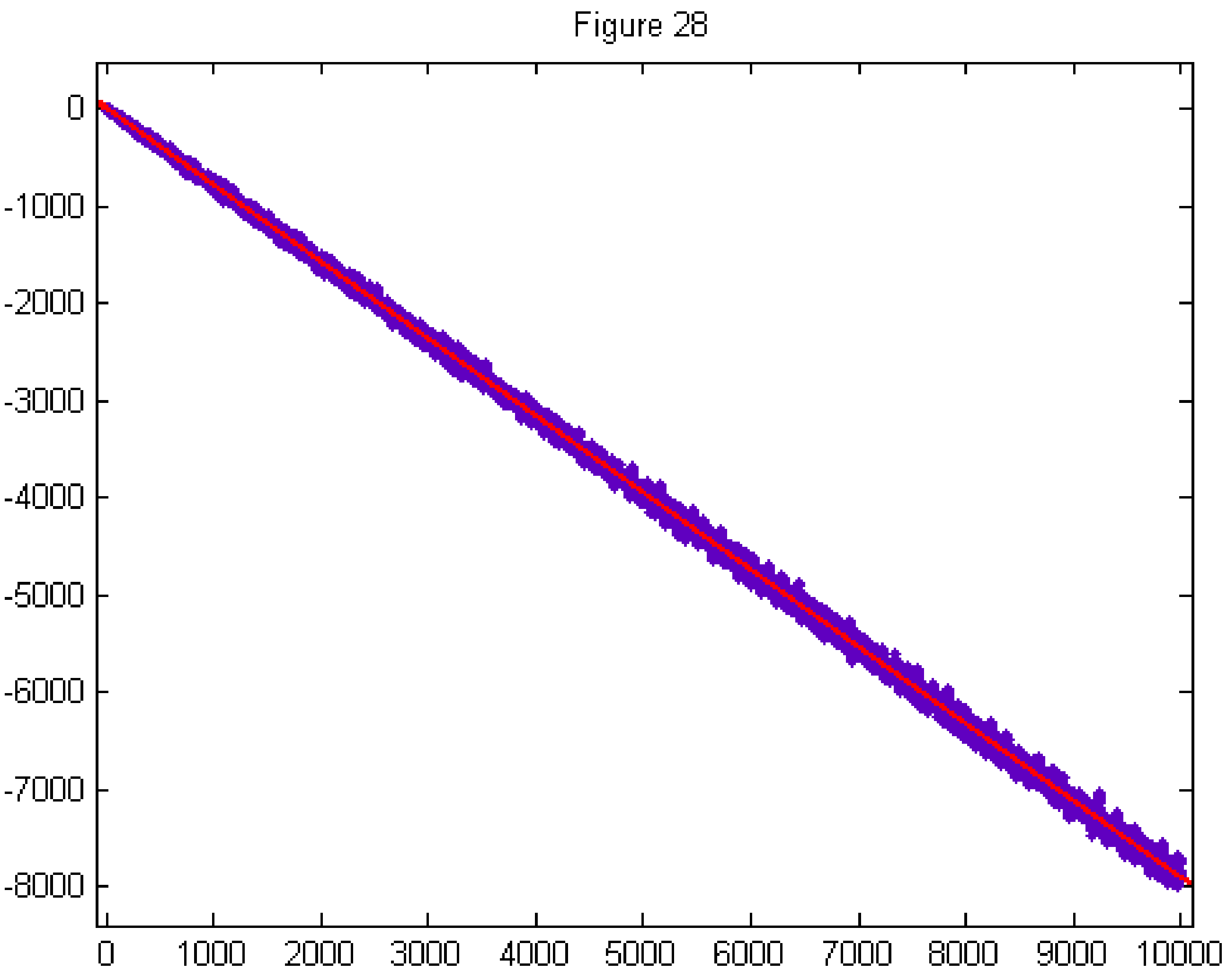
Figure 28
0
-1000
-2000
-3000
-4000
-5000
-6000
-7000
-8000
0
1000
2000
3000
4000
5000
6000
7000
8000
9000
10000

Figure 29

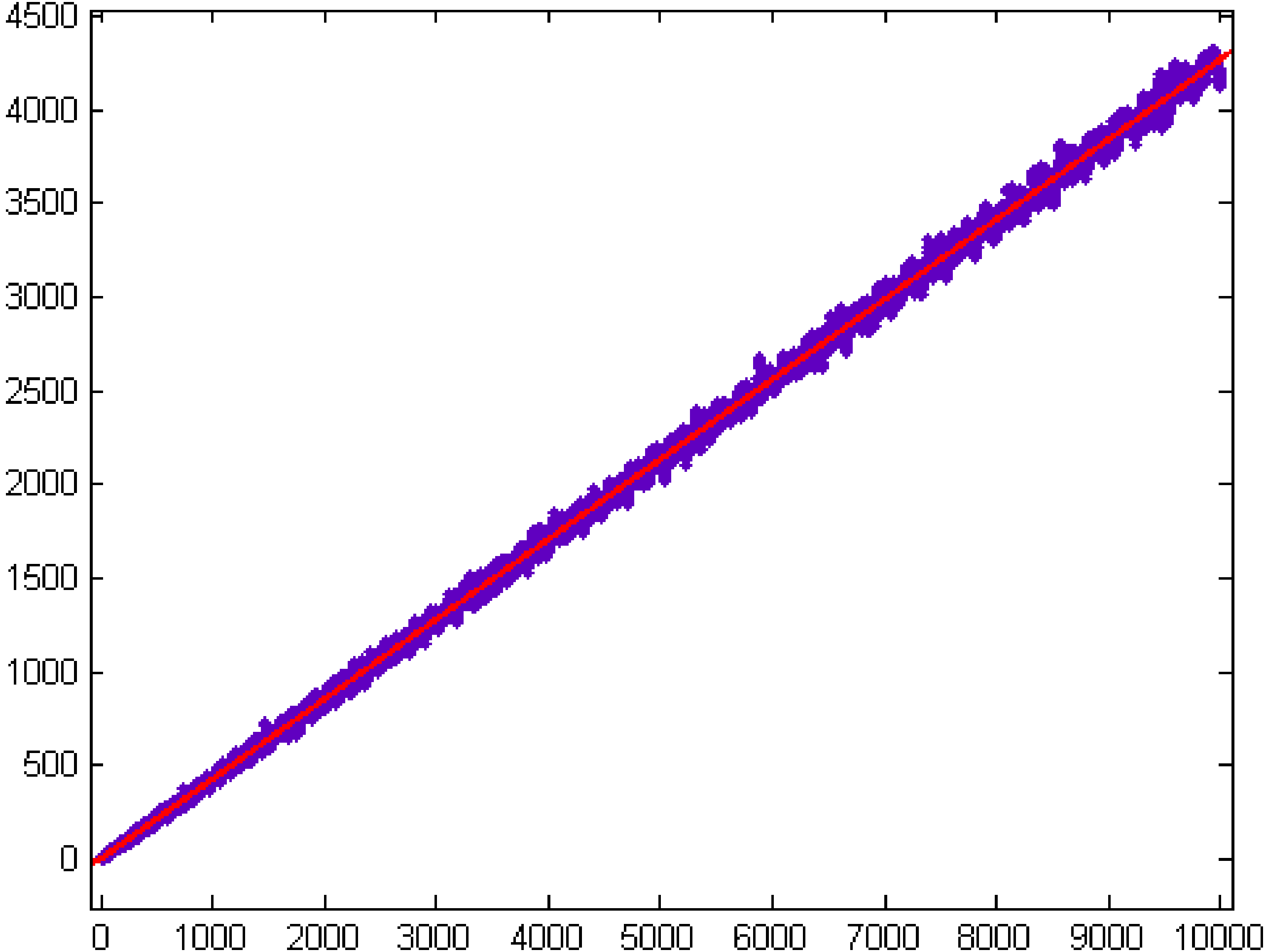
4500
4000
3500
3000
2500
2000
1500
1000
500
0
0
1000
2000
3000
4000
5000
6000
7000
8000
9000
10000

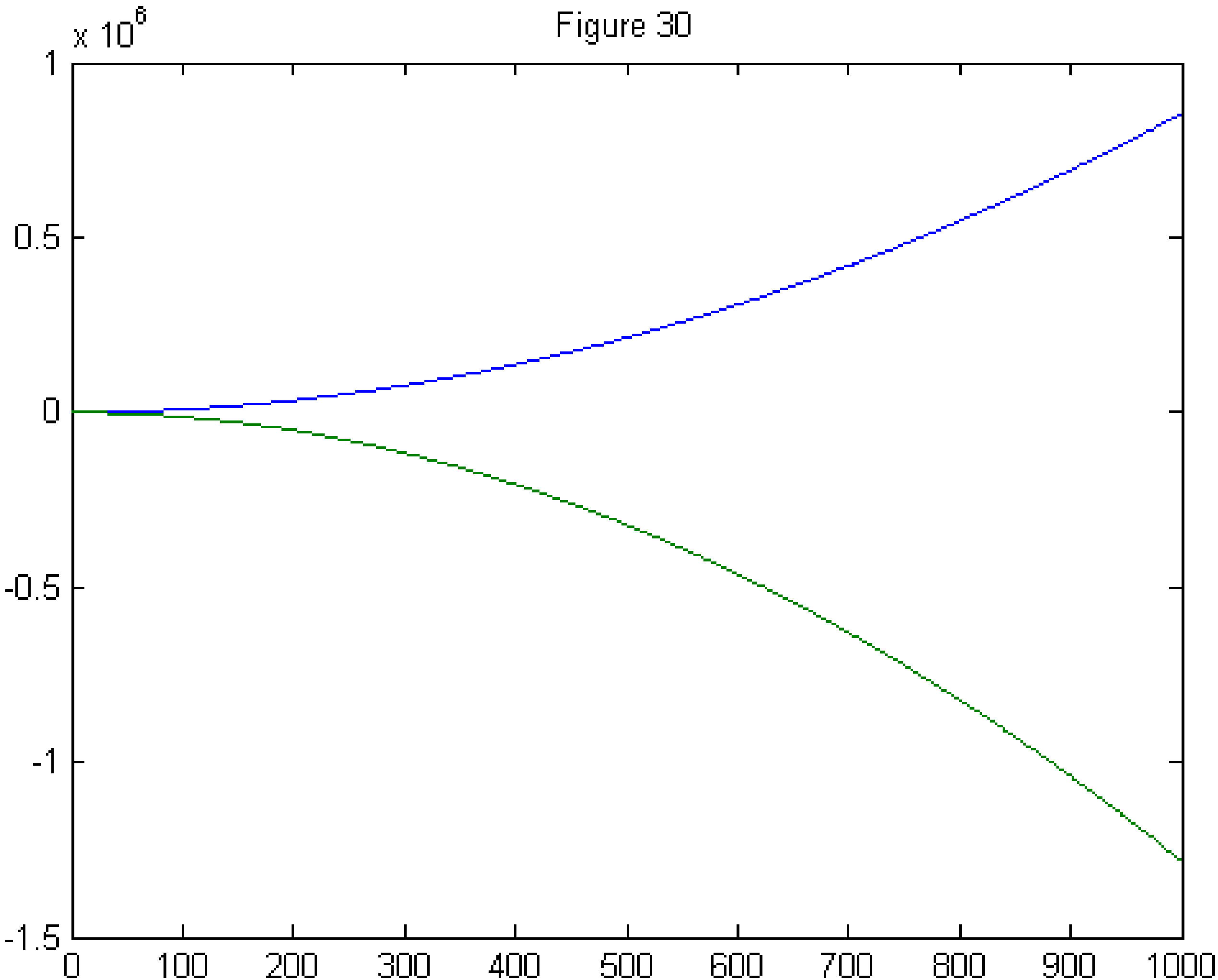

Figure 30
x 10^6
1
0.5
0
-0.5
-1
-1.5
0
100
200
300
400
500
600
700
800
900
1000

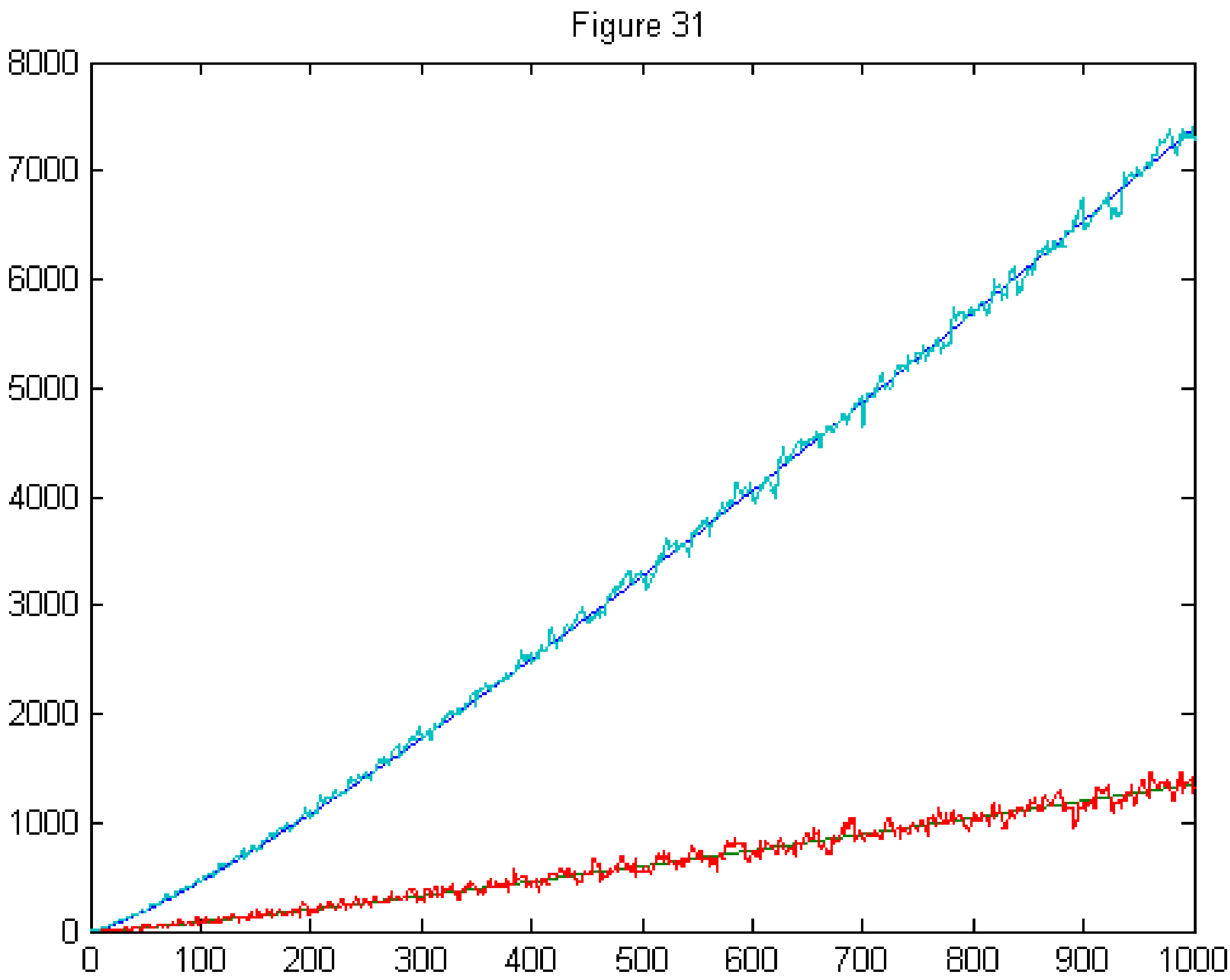
Figure 31
8000
7000
6000
5000
4000
3000
2000
1000
0
0
100
200
300
400
500
600
700
800
900
1000

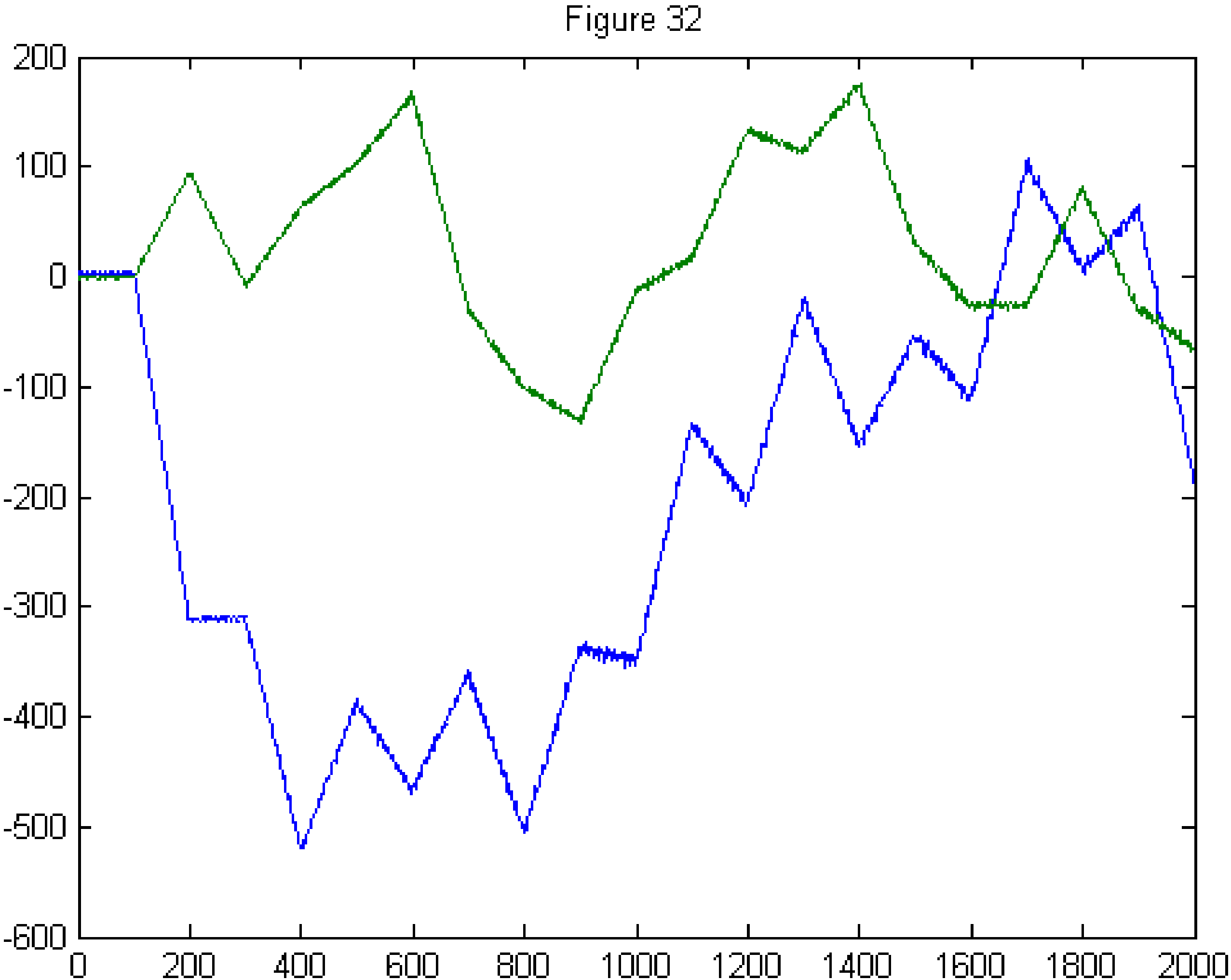
Figure 32
200
100
0
-100
-200
-300
-400
-500
-600
0
200
400
600
800
1000
1200
1400
1600
1800
2000

Figure 33

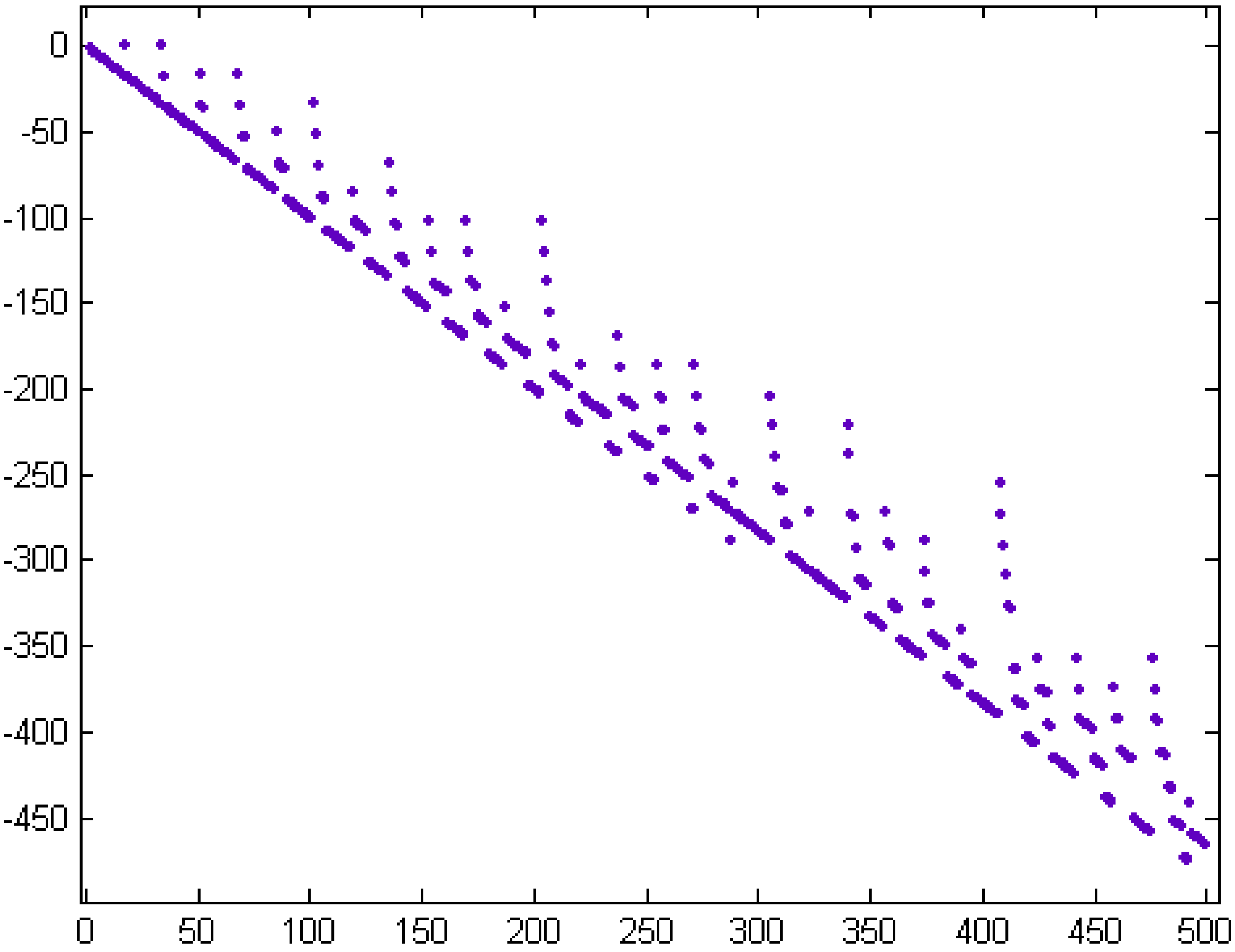
0
-50
-100
-150
-200
-250
-300
-350
-400
-450
0
50
100
150
200
250
300
350
400
450
500

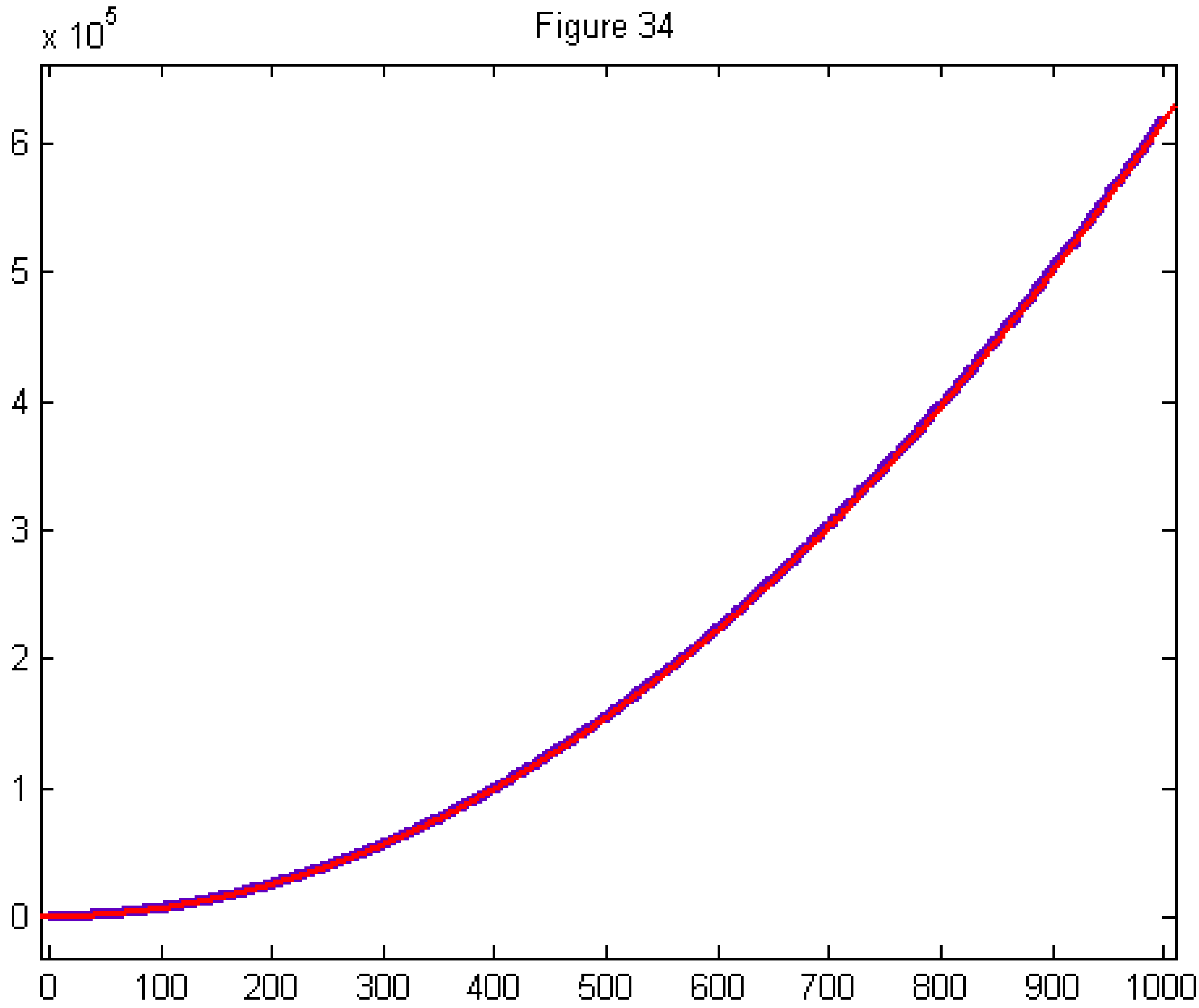
Figure 34
x 10^5
0
1
2
3
4
5
6
0
100
200
300
400
500
600
700
800
900
1000

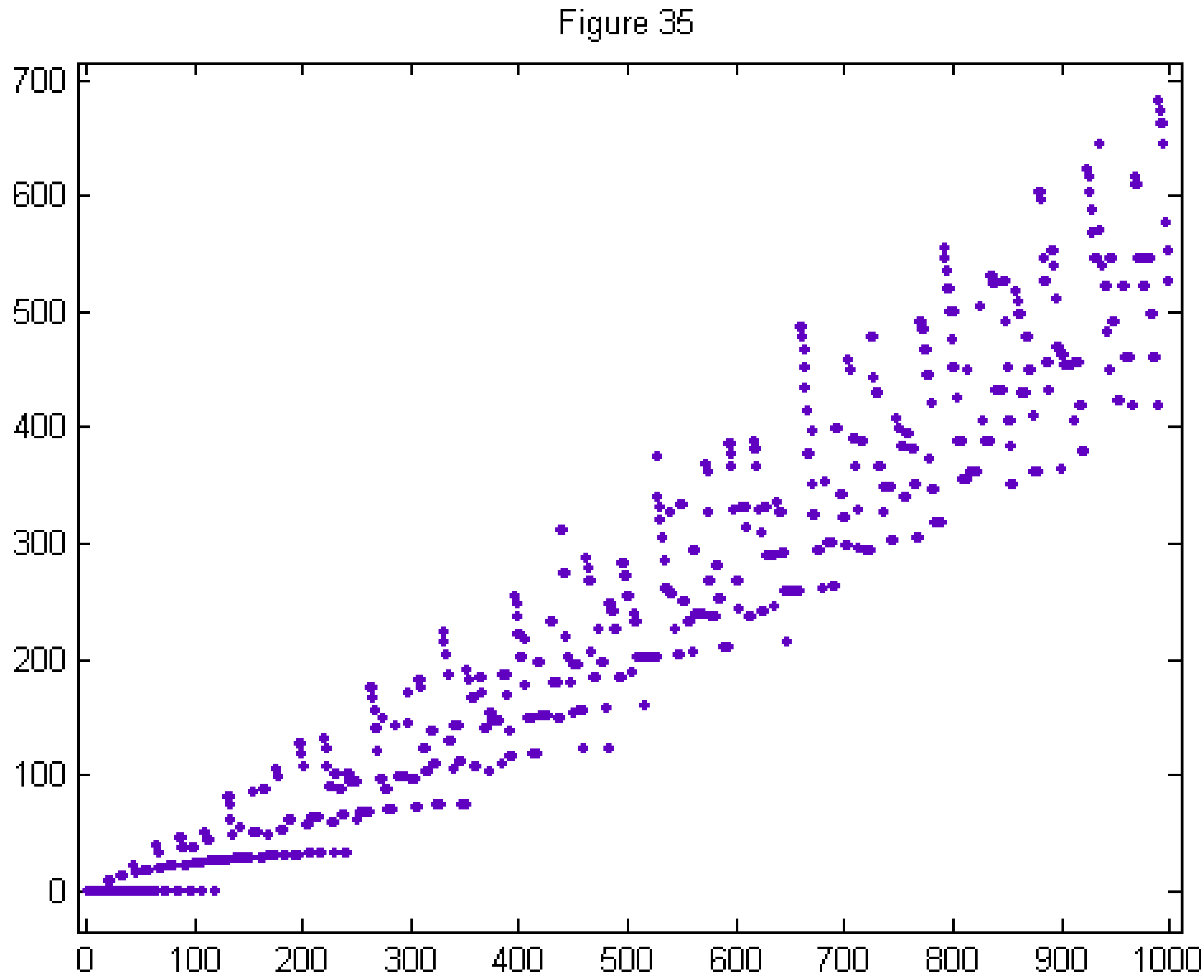
Figure 35
700
600
500
400
300
200
100
0
0
100
200
300
400
500
600
700
800
900
1000

Figure 36

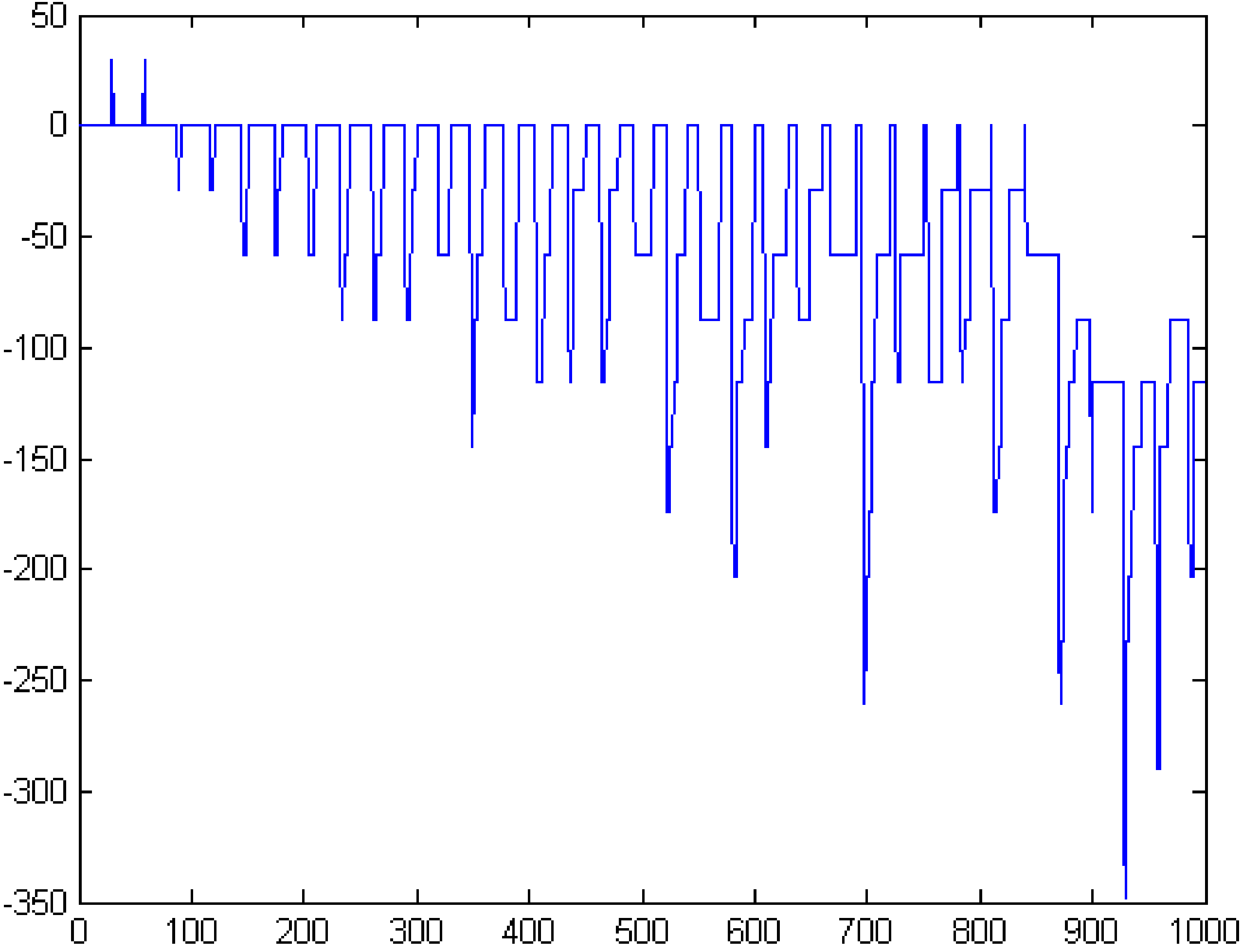

50
0
-50
-100
-150
-200
-250
-300
-350
0
100
200
300
400
500
600
700
800
900
1000

Figure 37

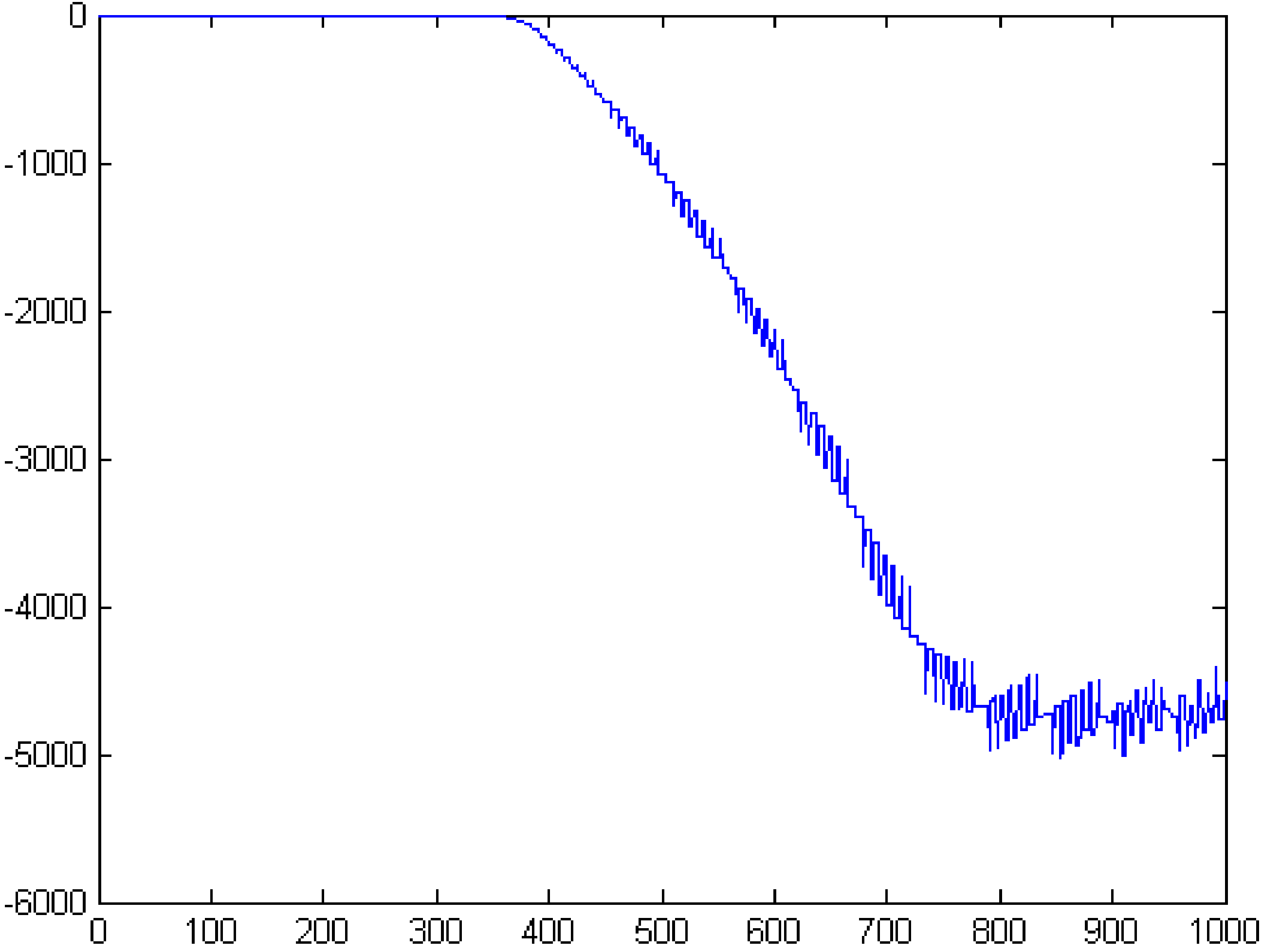
0
-1000
-2000
-3000
-4000
-5000
-6000
0
100
200
300
400
500
600
700
800
900
1000

Figure 38

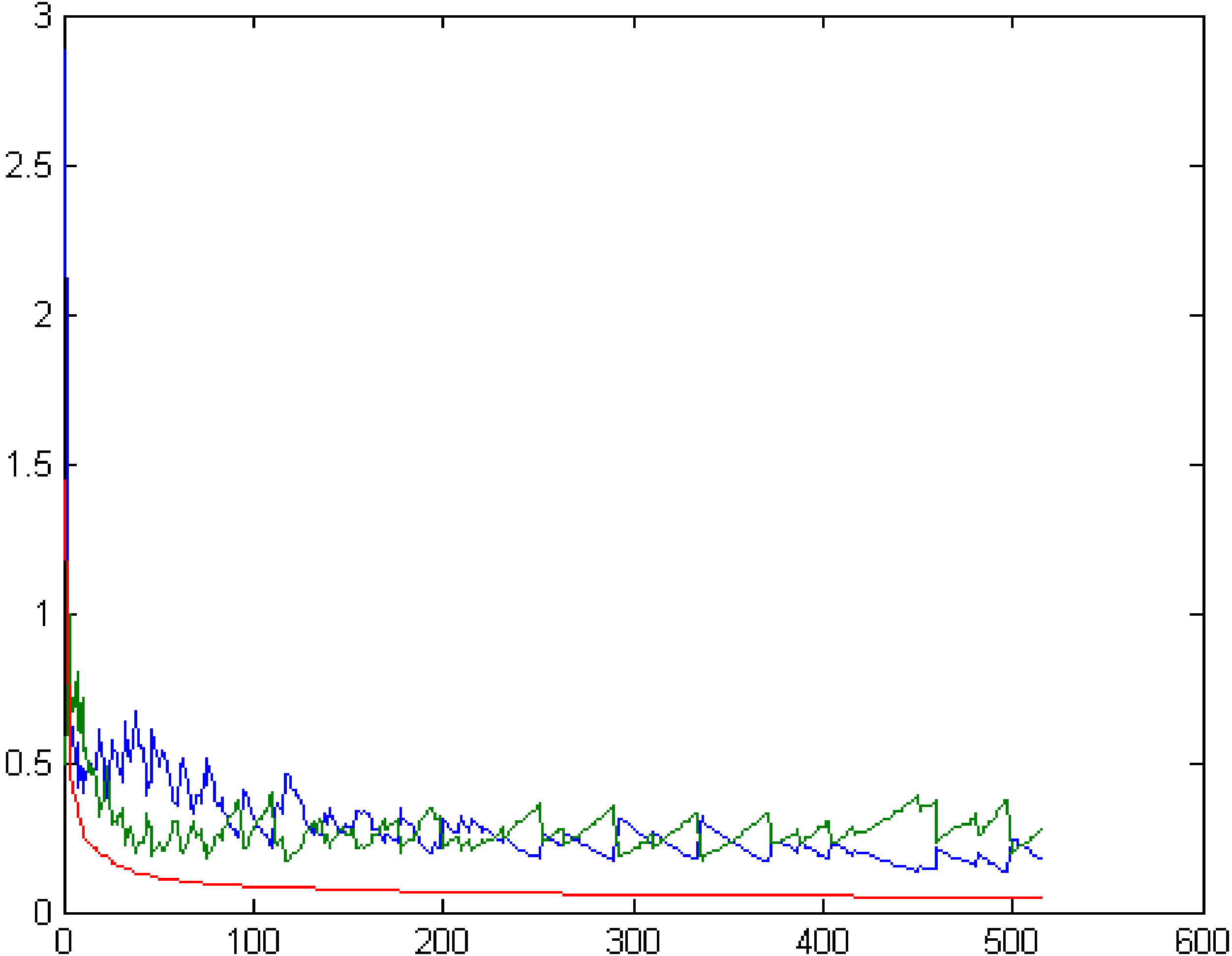

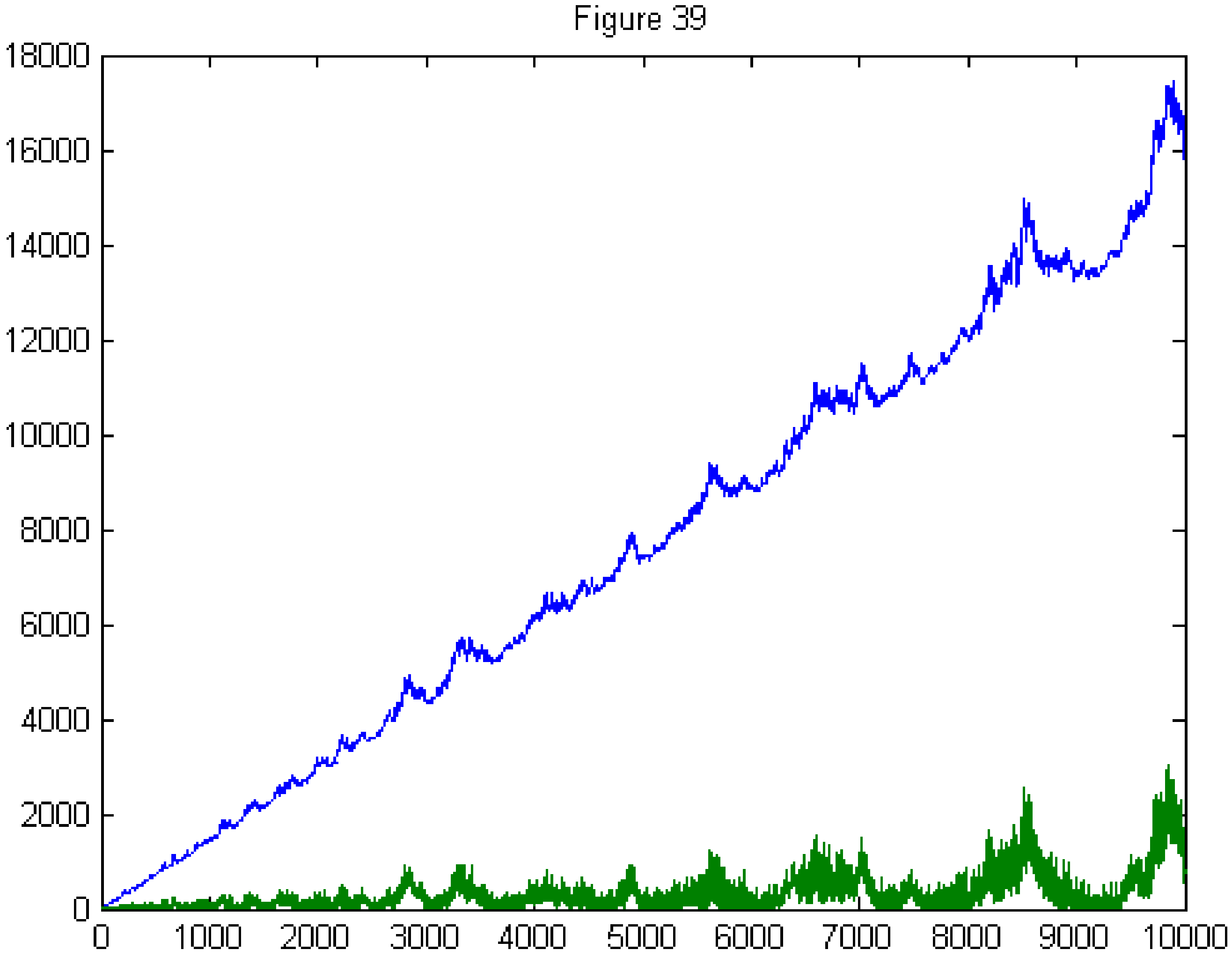
Figure 39
18000
16000
14000
12000
10000
8000
6000
4000
2000
0
0
1000
2000
3000
4000
5000
6000
7000
8000
9000
10000

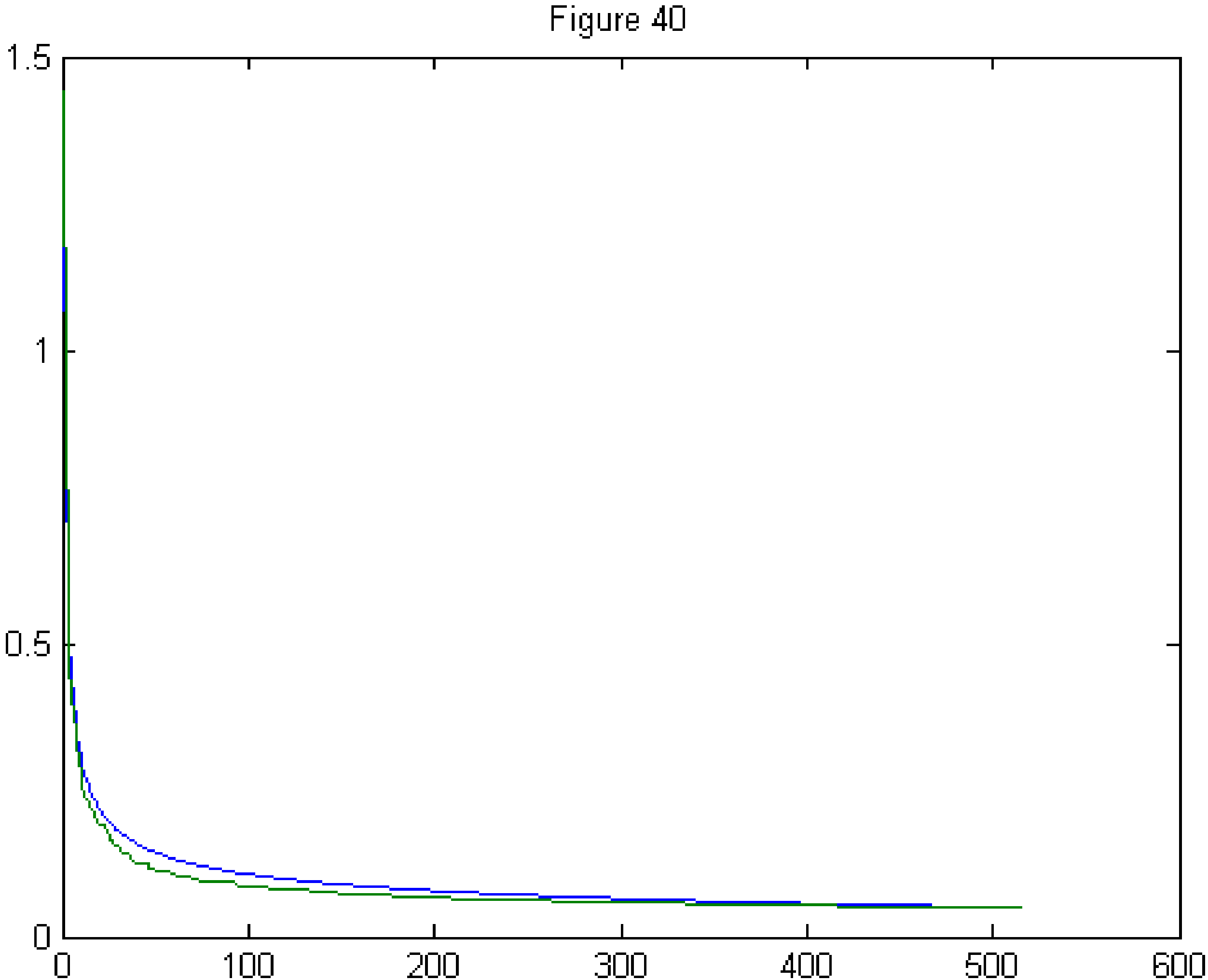

Figure 40
1.5
1
0.5
0
0
100
200
300
400
500
600

Figure 41

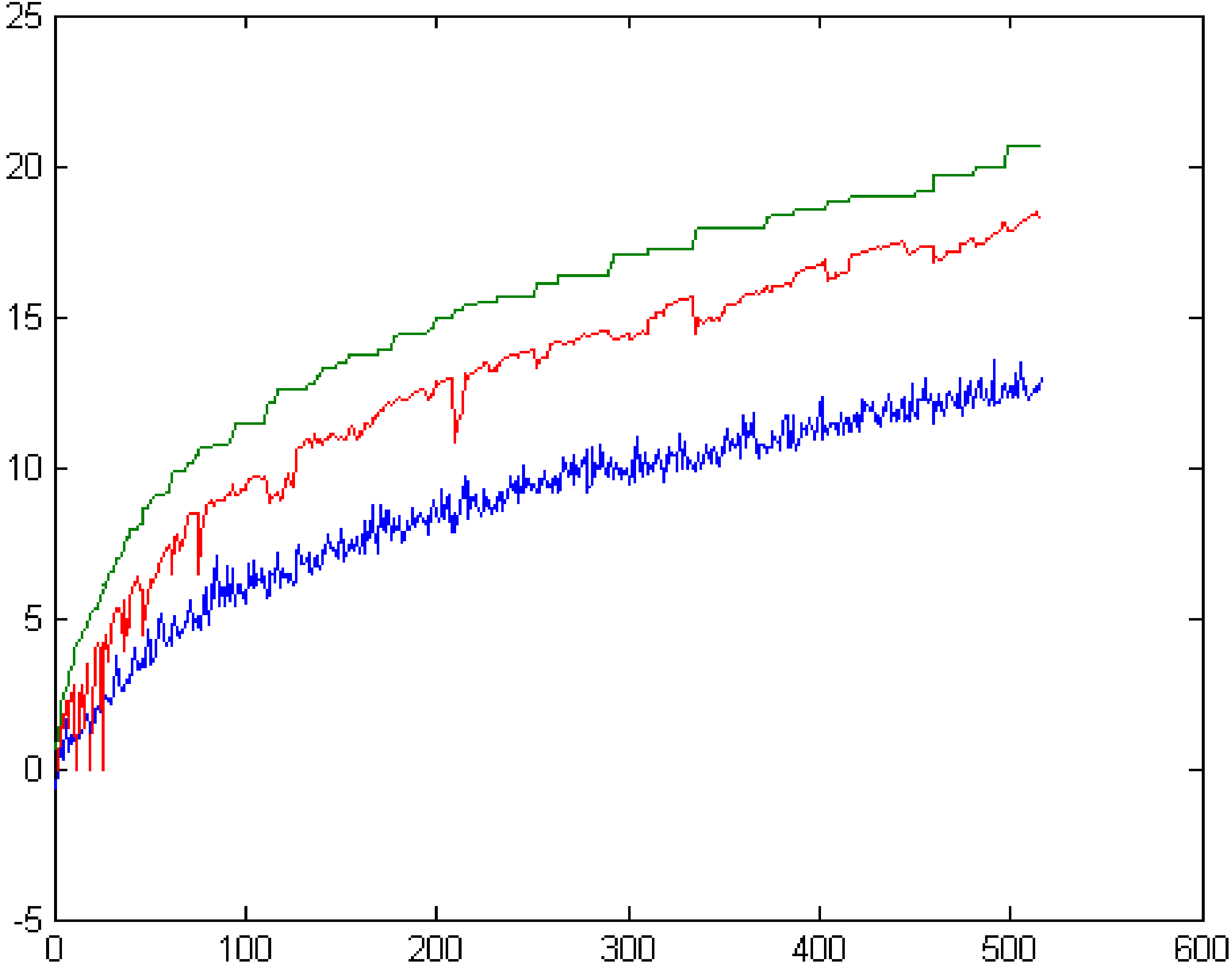

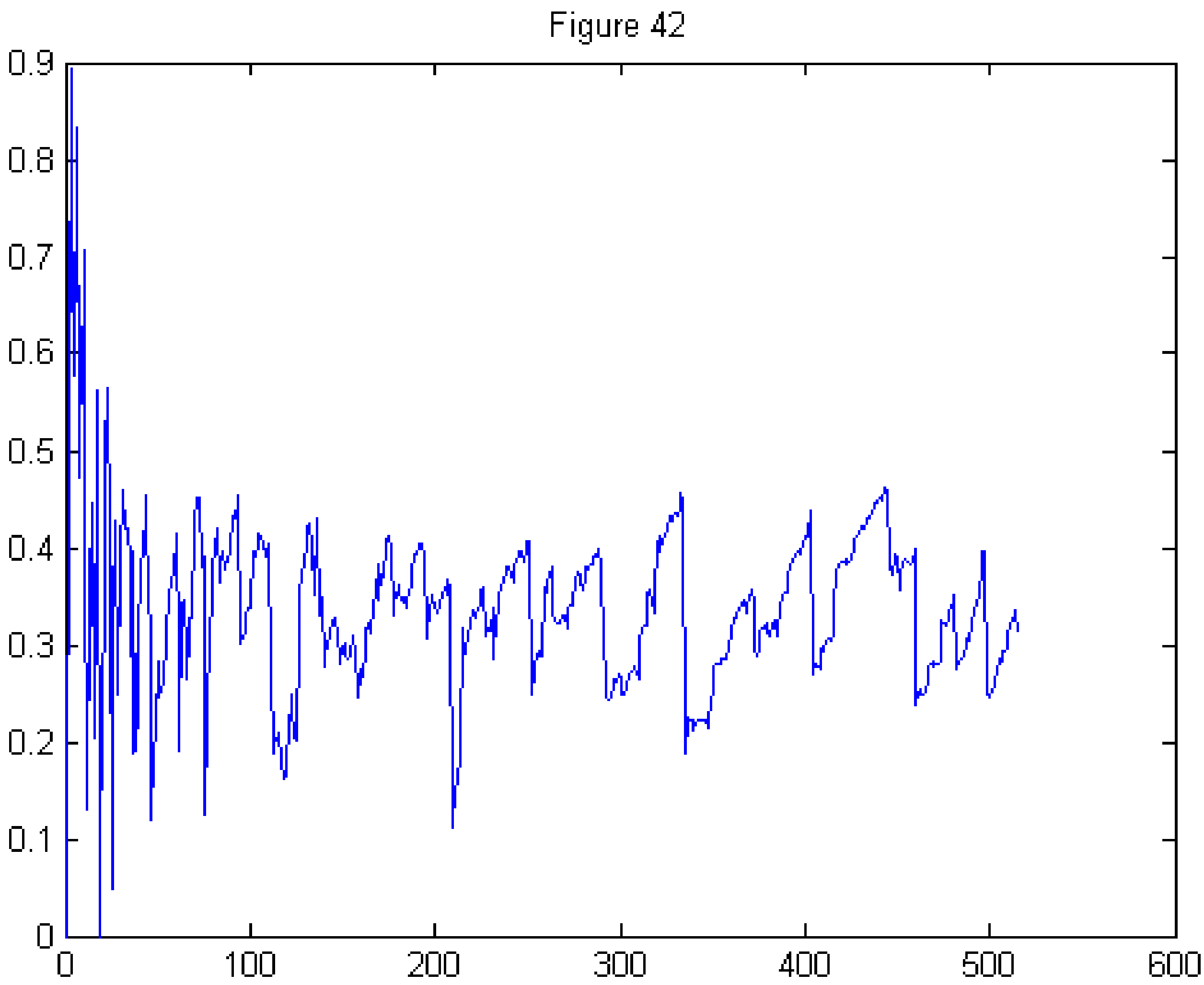
Figure 42
0.9
0.8
0.7
0.6
0.5
0.4
0.3
0.2
0.1
0
0
100
200
300
400
500
600

Figure 43

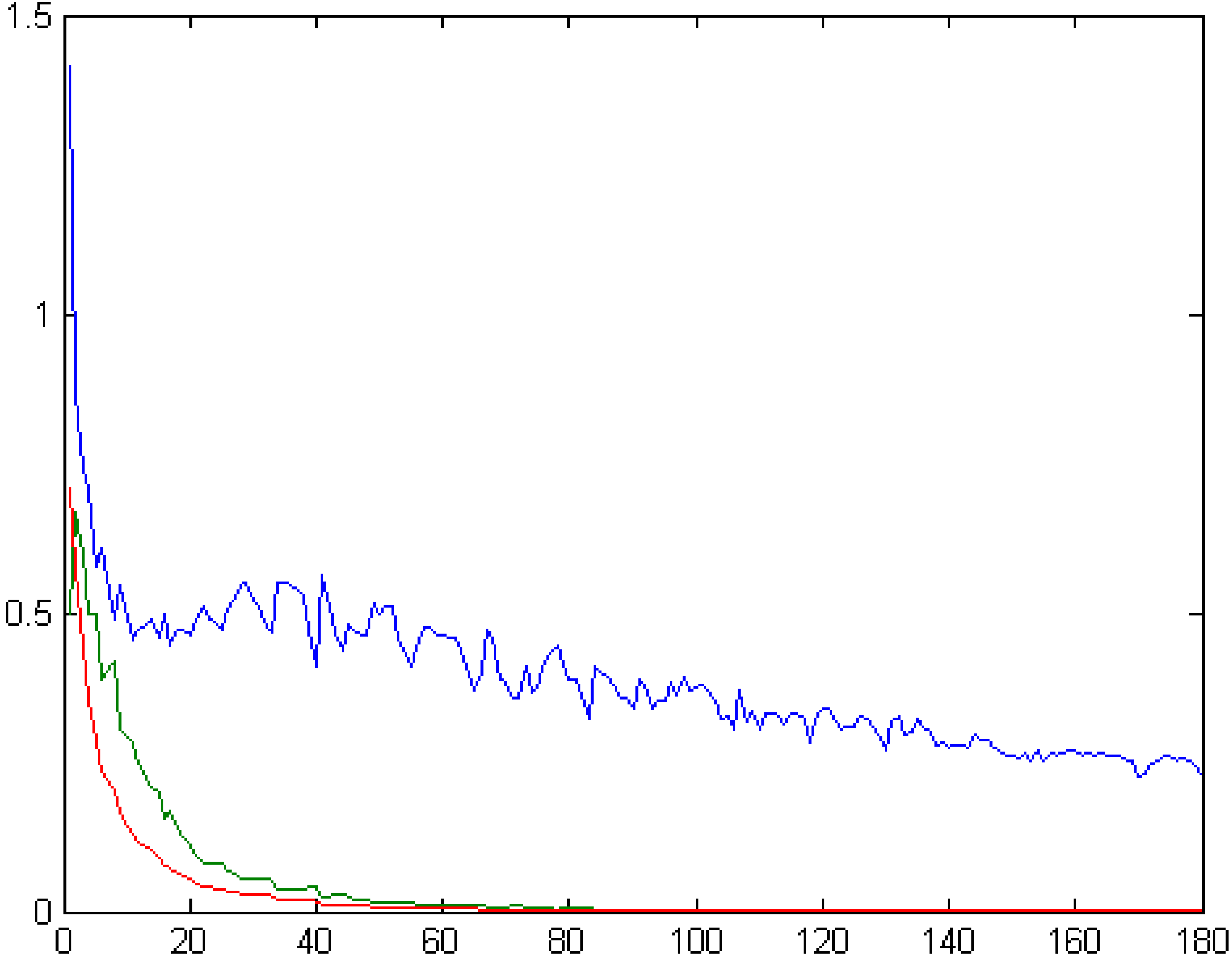

Figure 44

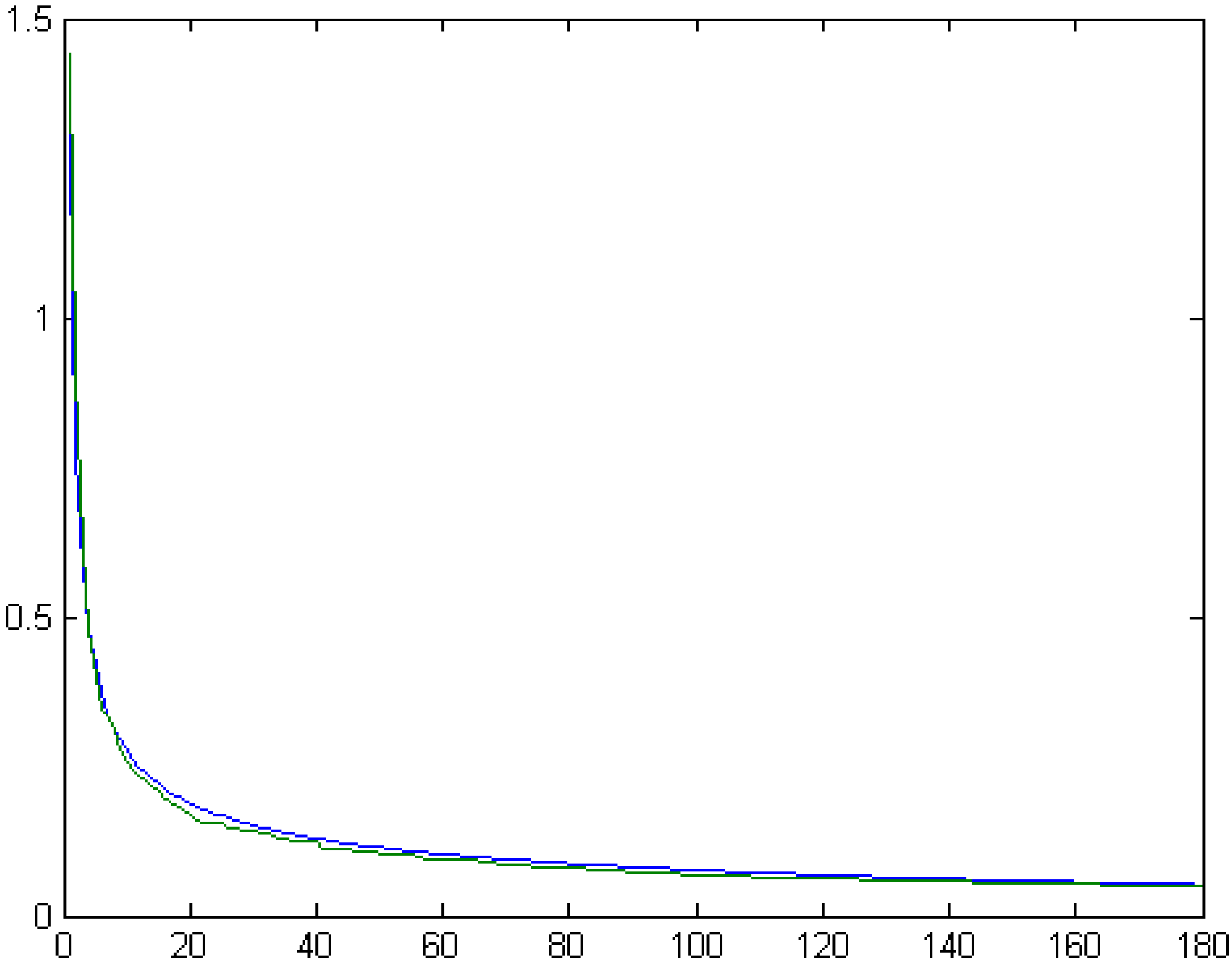

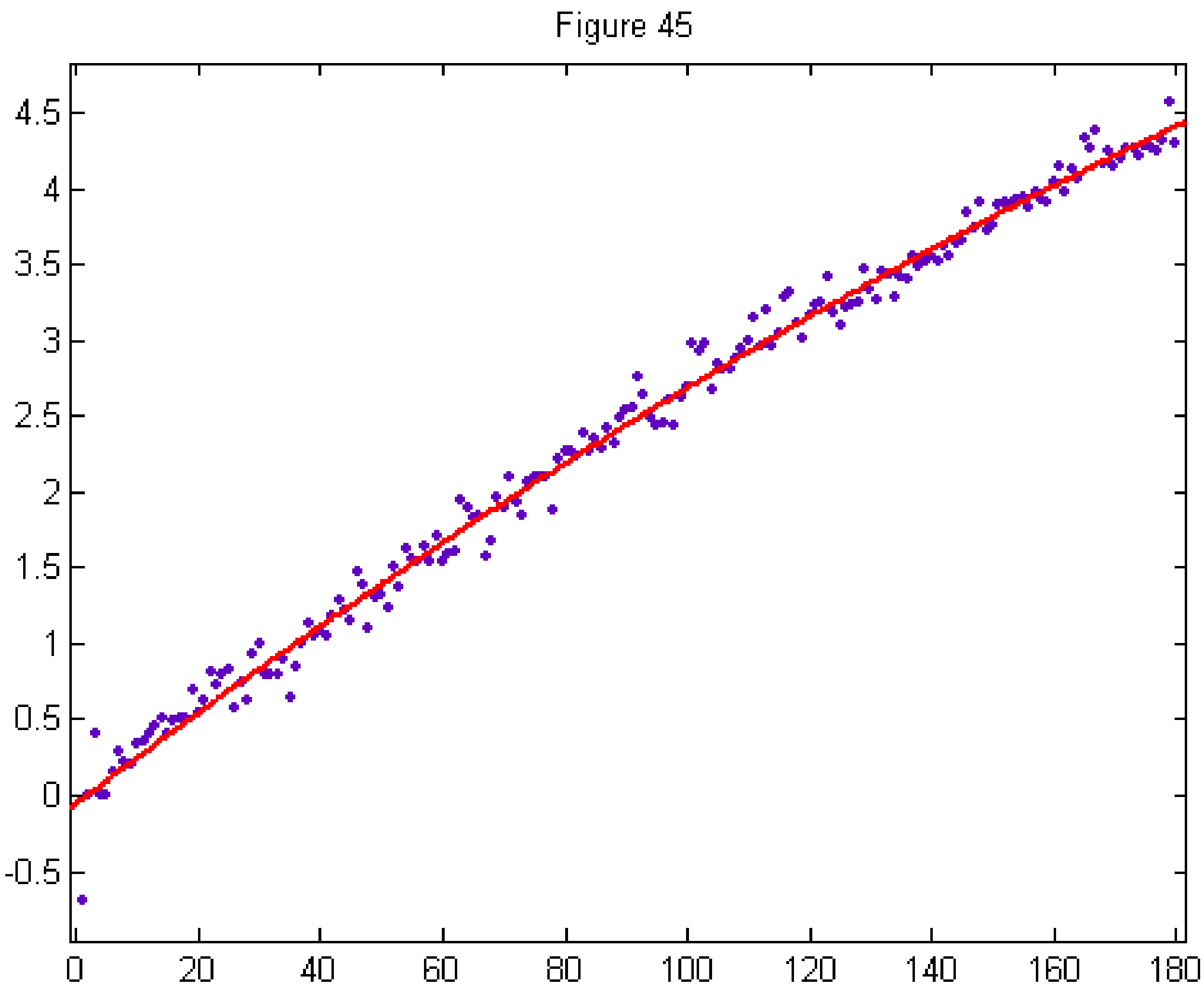

Figure 45
4.5
4
3.5
3
2.5
2
1.5
1
0.5
0
-0.5
0
20
40
60
80
100
120
140
160
180

Figure 46

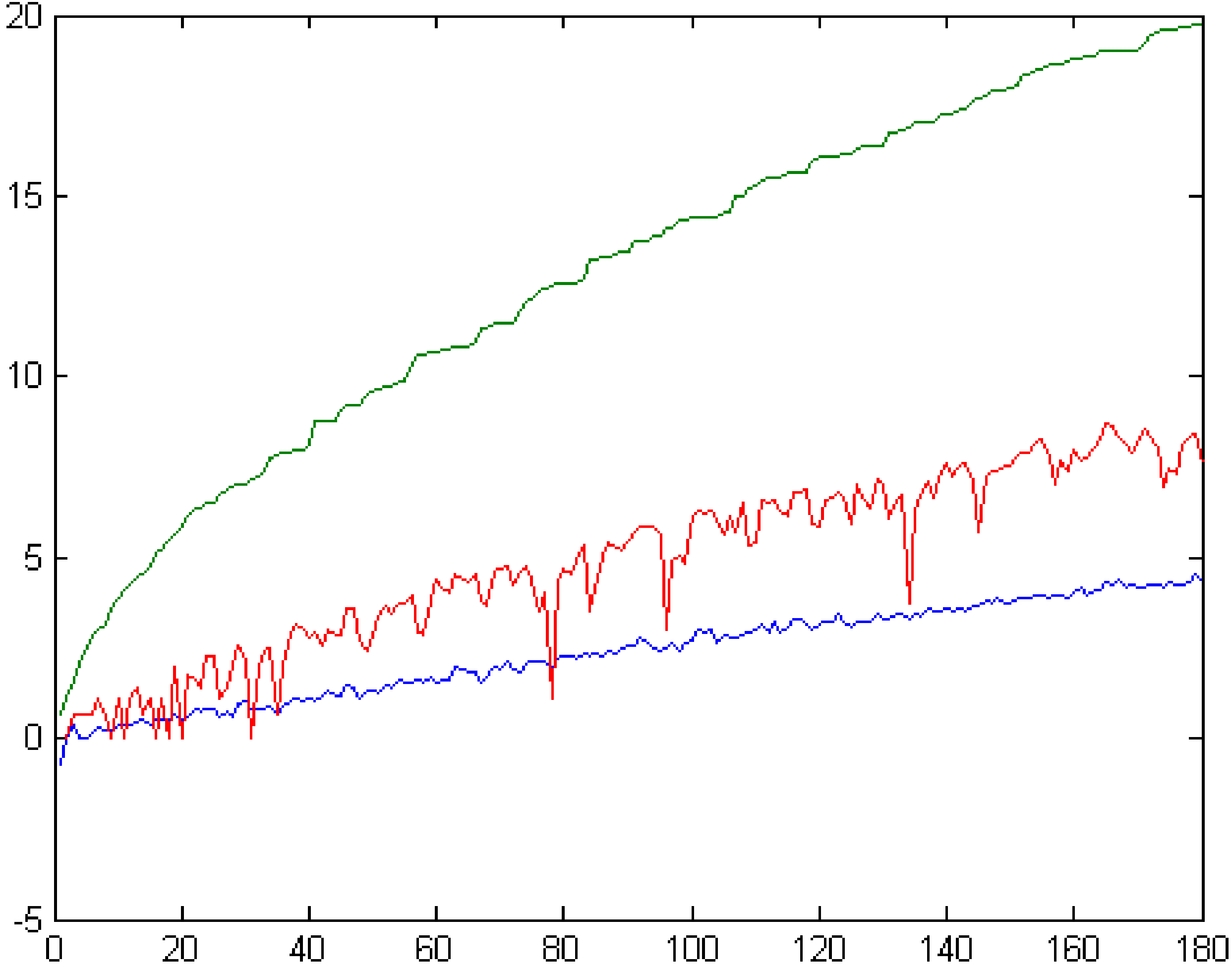

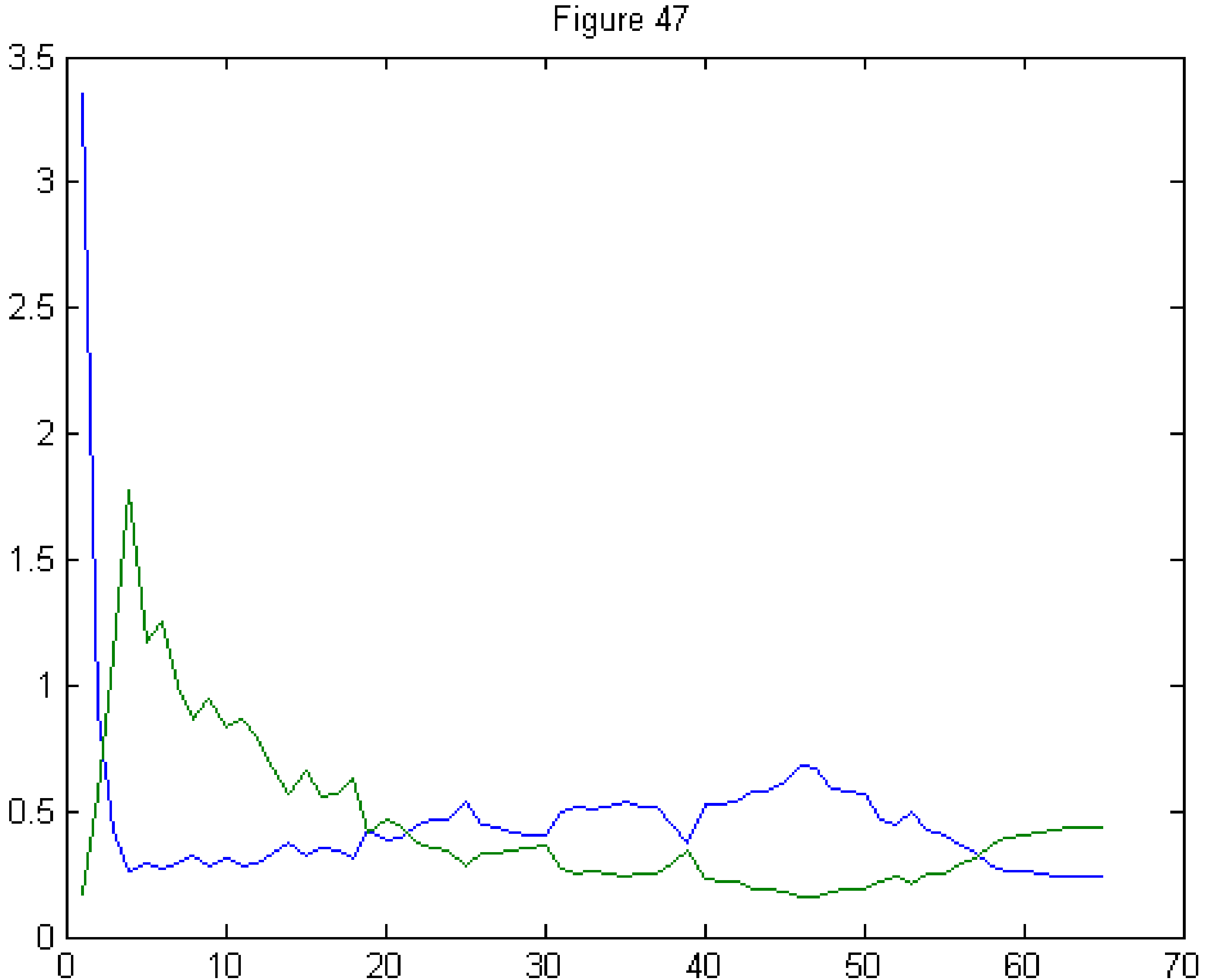
Figure 47
3.5
3
2.5
2
1.5
1
0.5
0
0
10
20
30
40
50
60
70

Figure 48

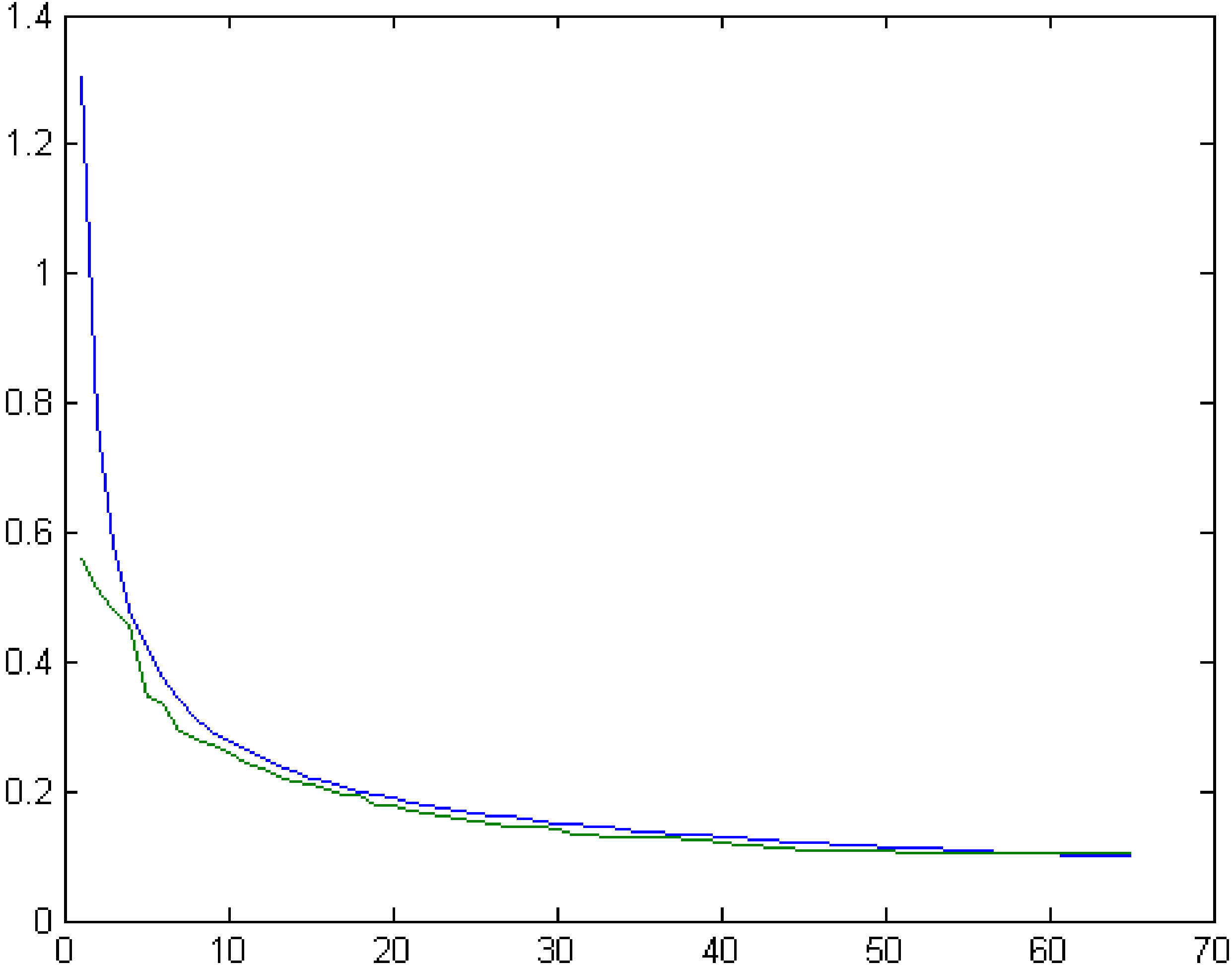

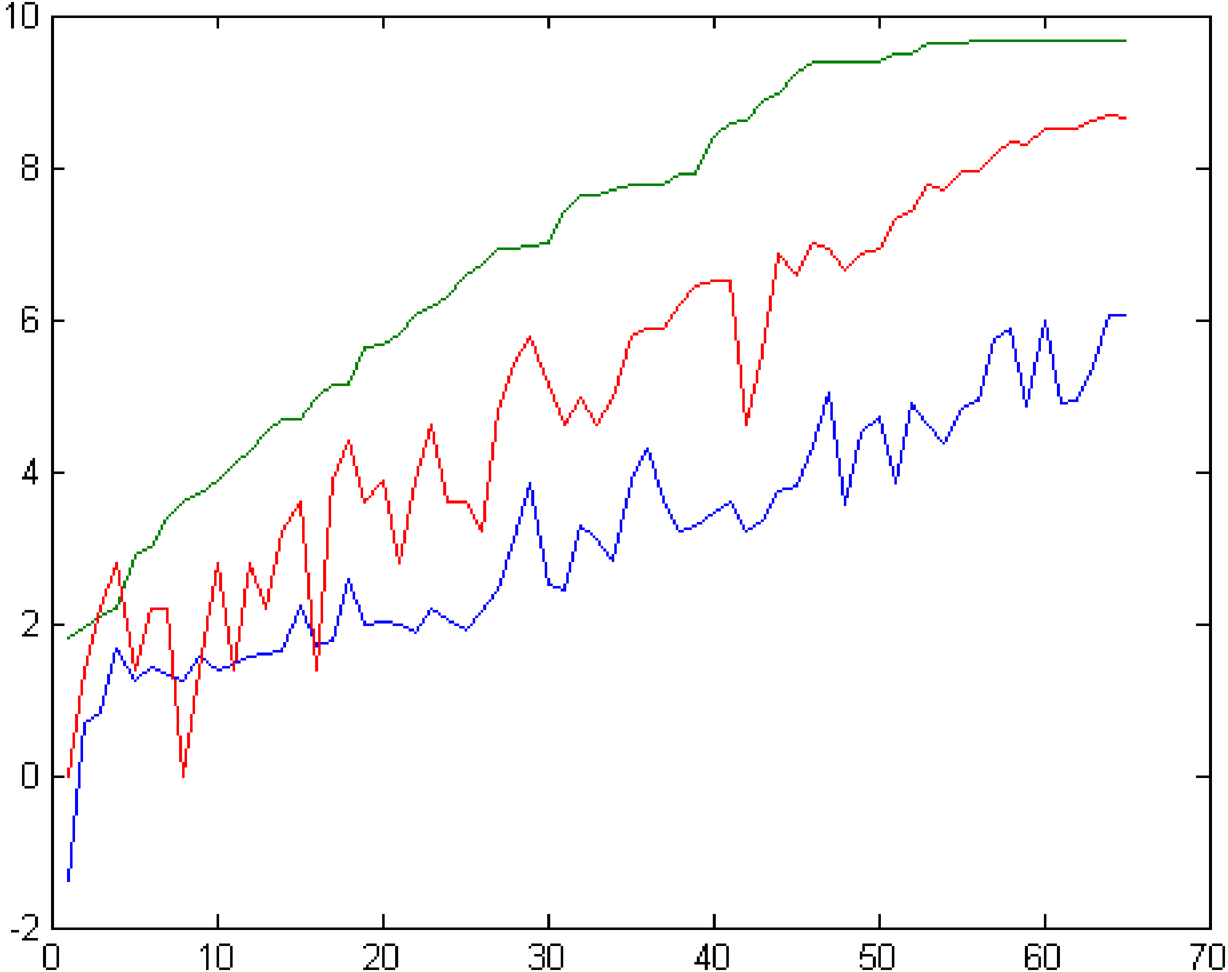

Figure 49

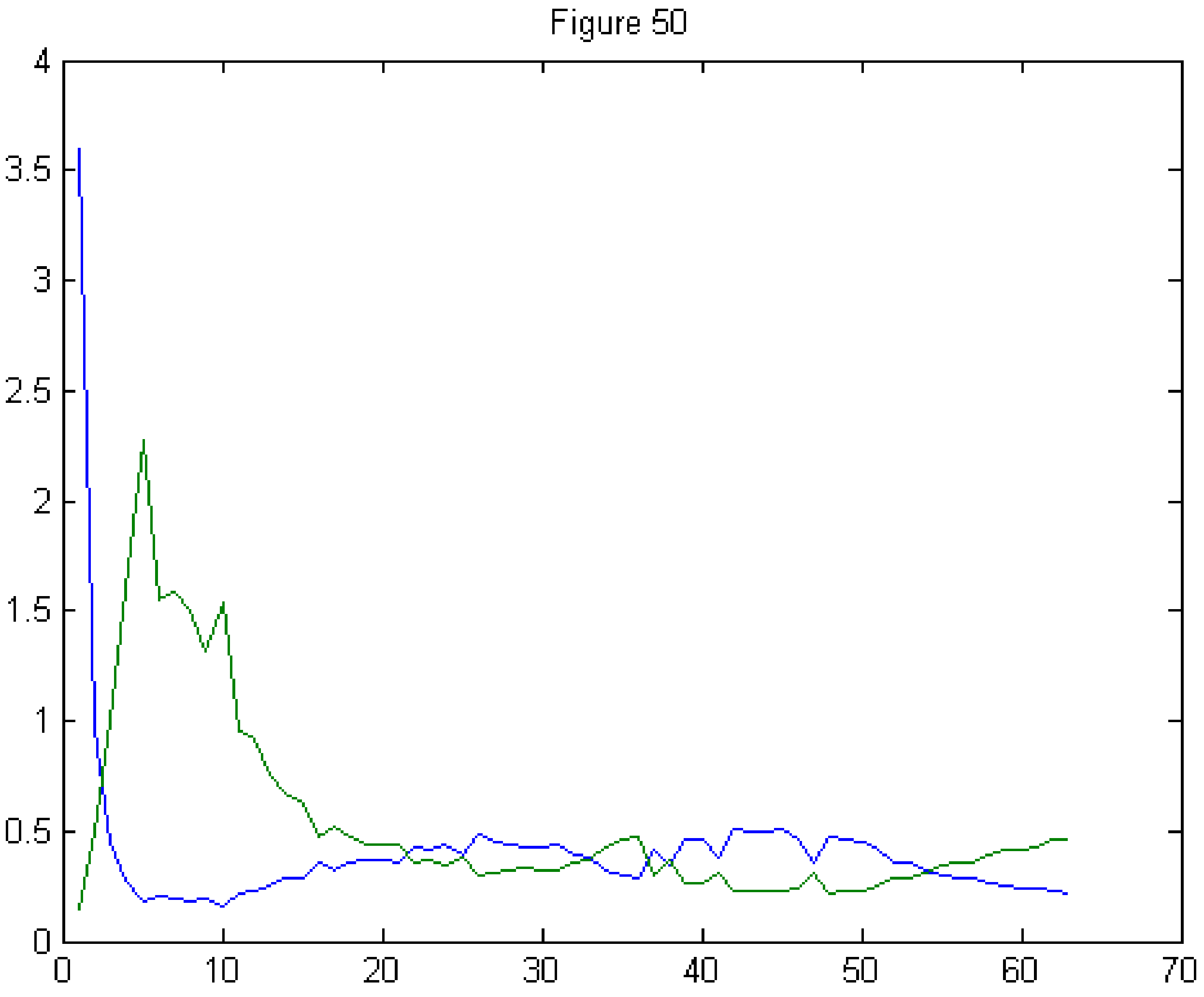
Figure 50
4
3.5
3
2.5
2
1.5
1
0.5
0
0
10
20
30
40
50
60
70

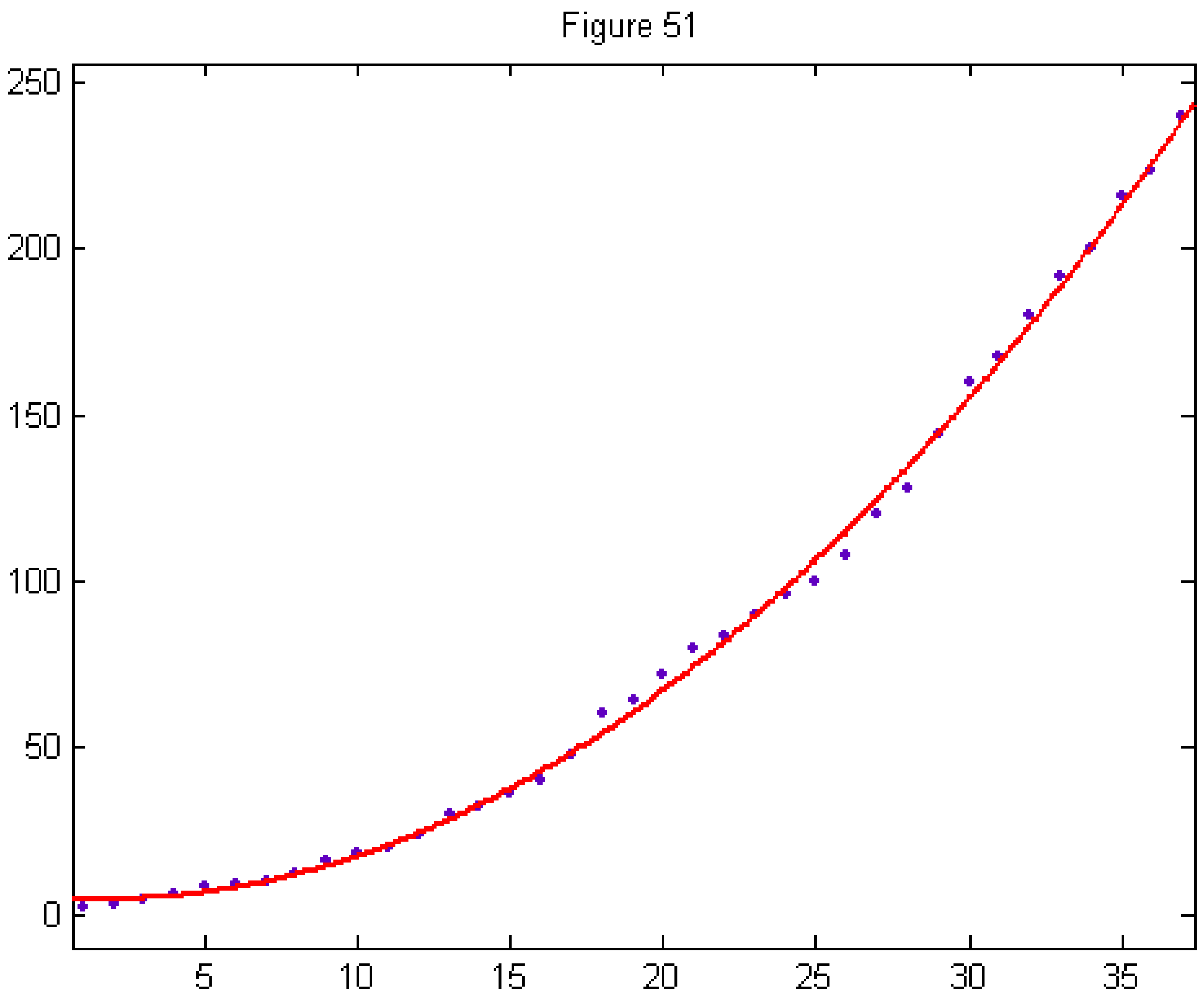

Figure 51
250
200
150
100
50
0
5
10
15
20
25
30
35

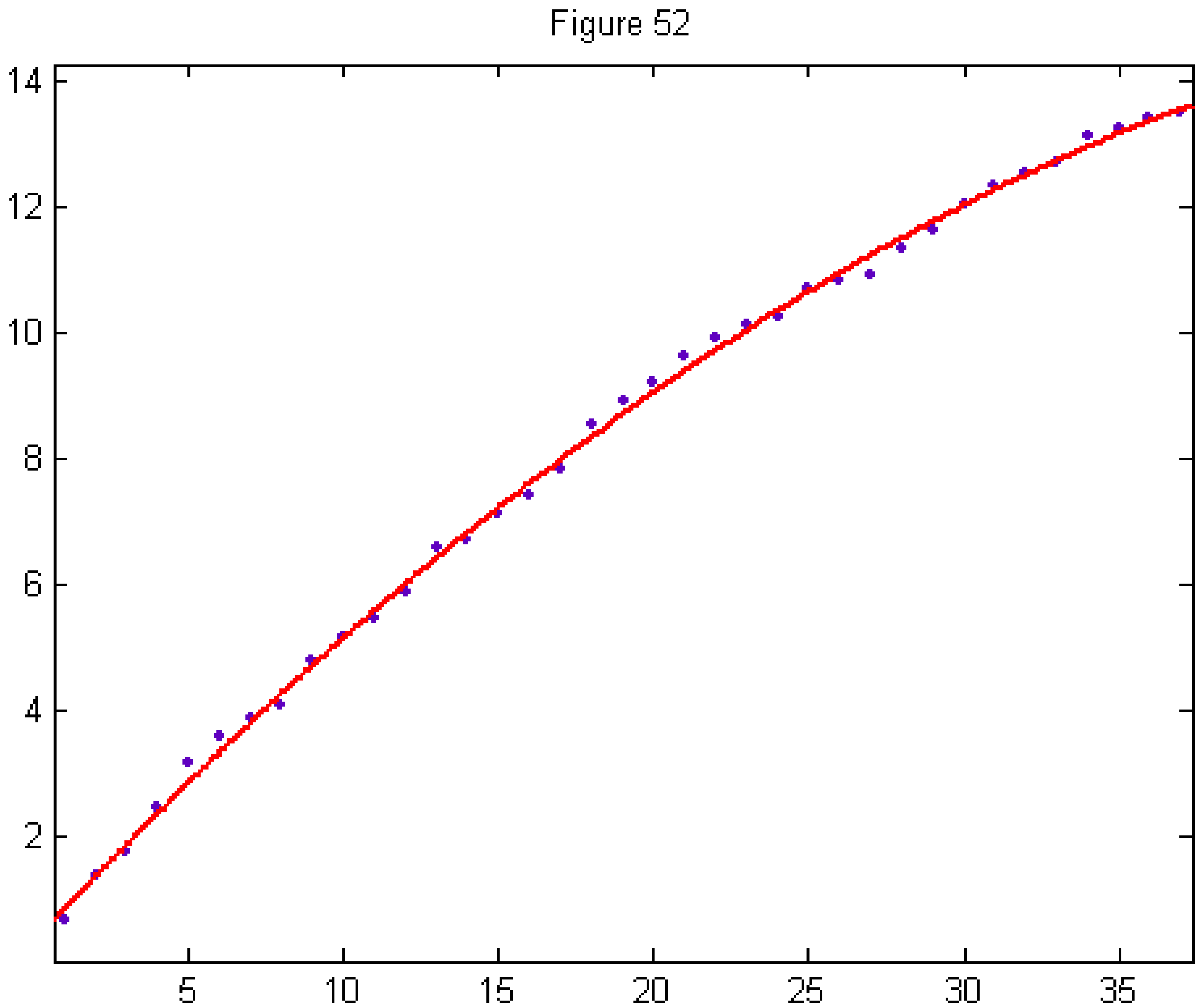
Figure 52
14
12
10
8
6
4
2
5
10
15
20
25
30
35

Figure 53

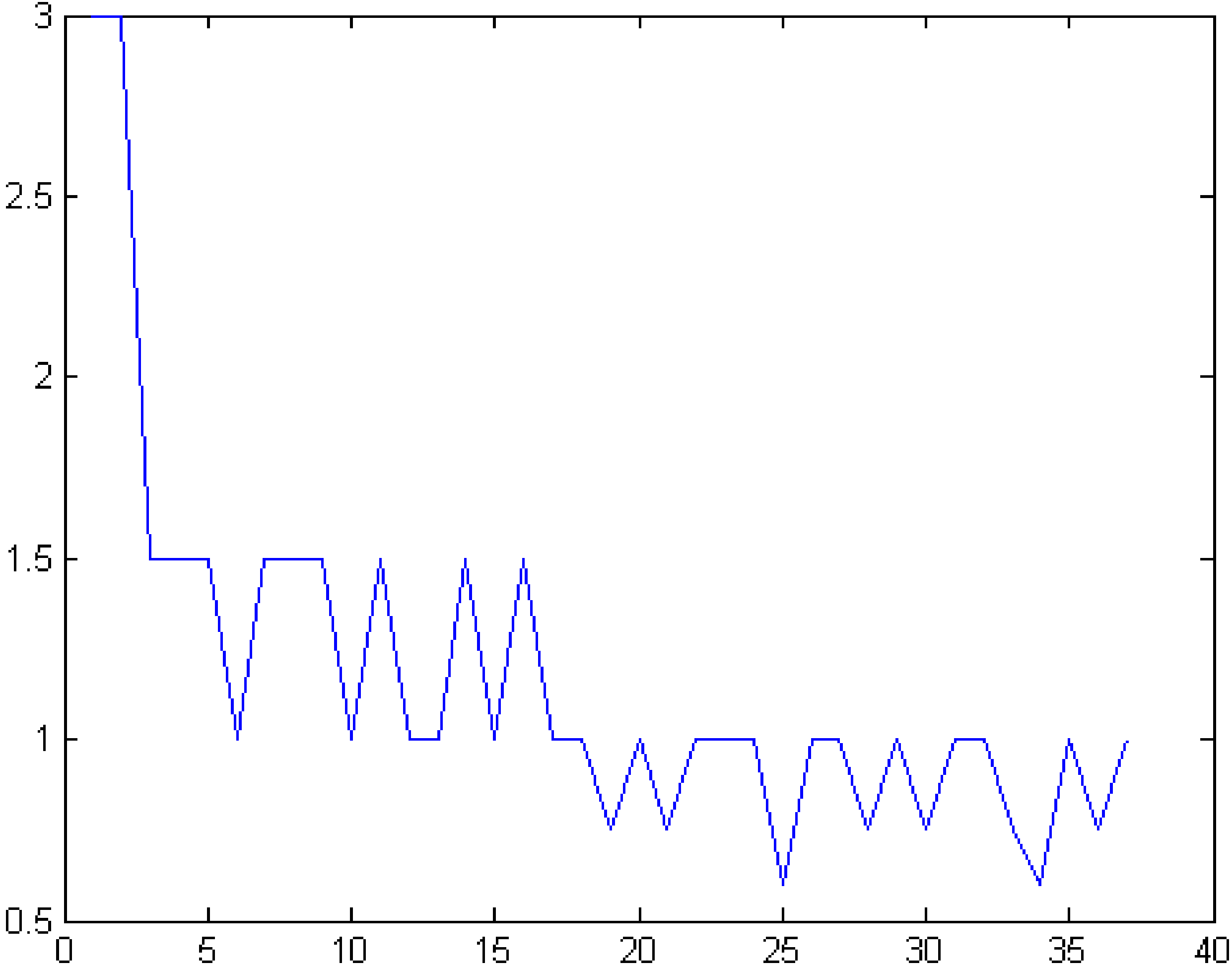

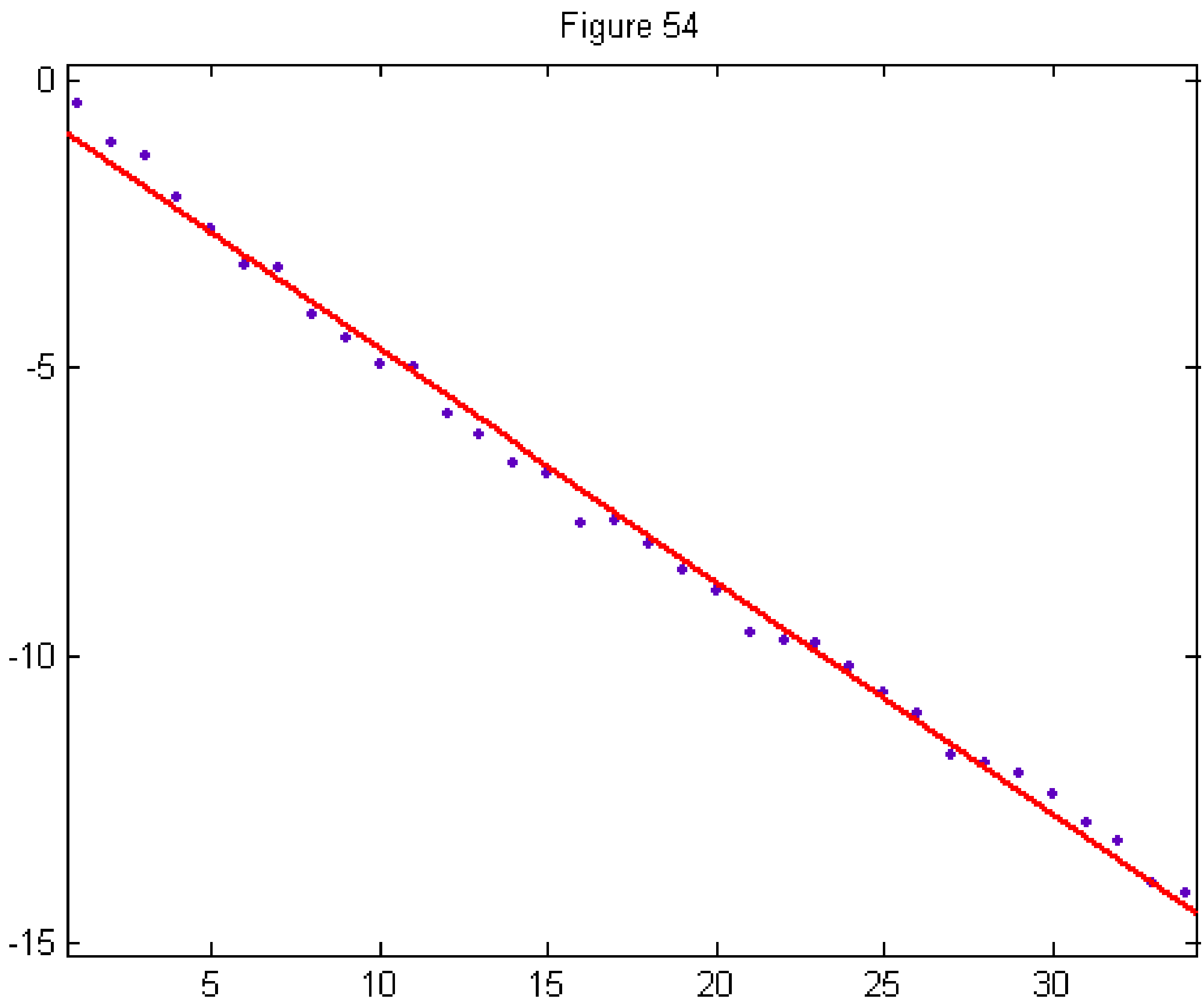
Figure 54
0
-5
-10
-15
5
10
15
20
25
30

Figure 55

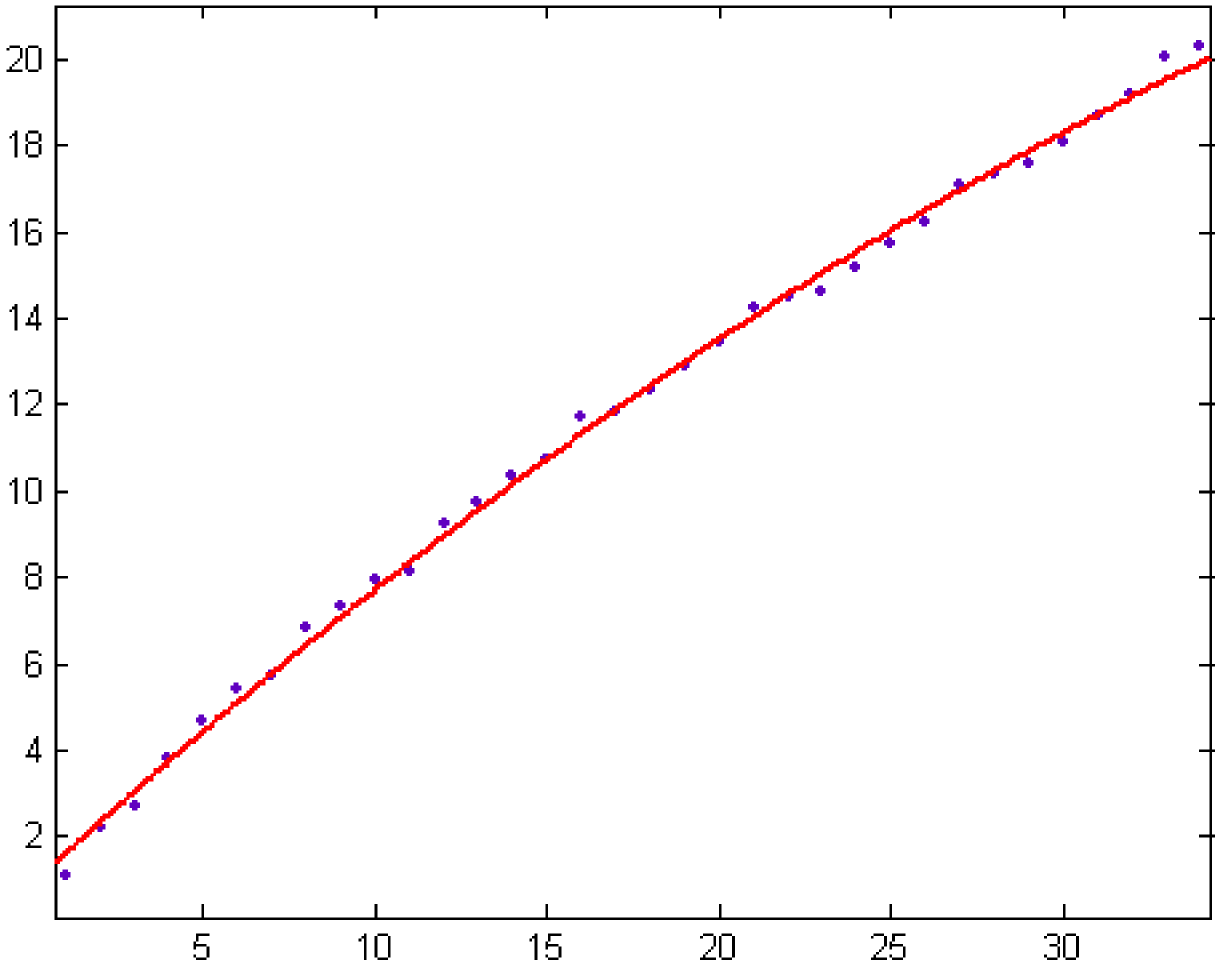

Figure 56

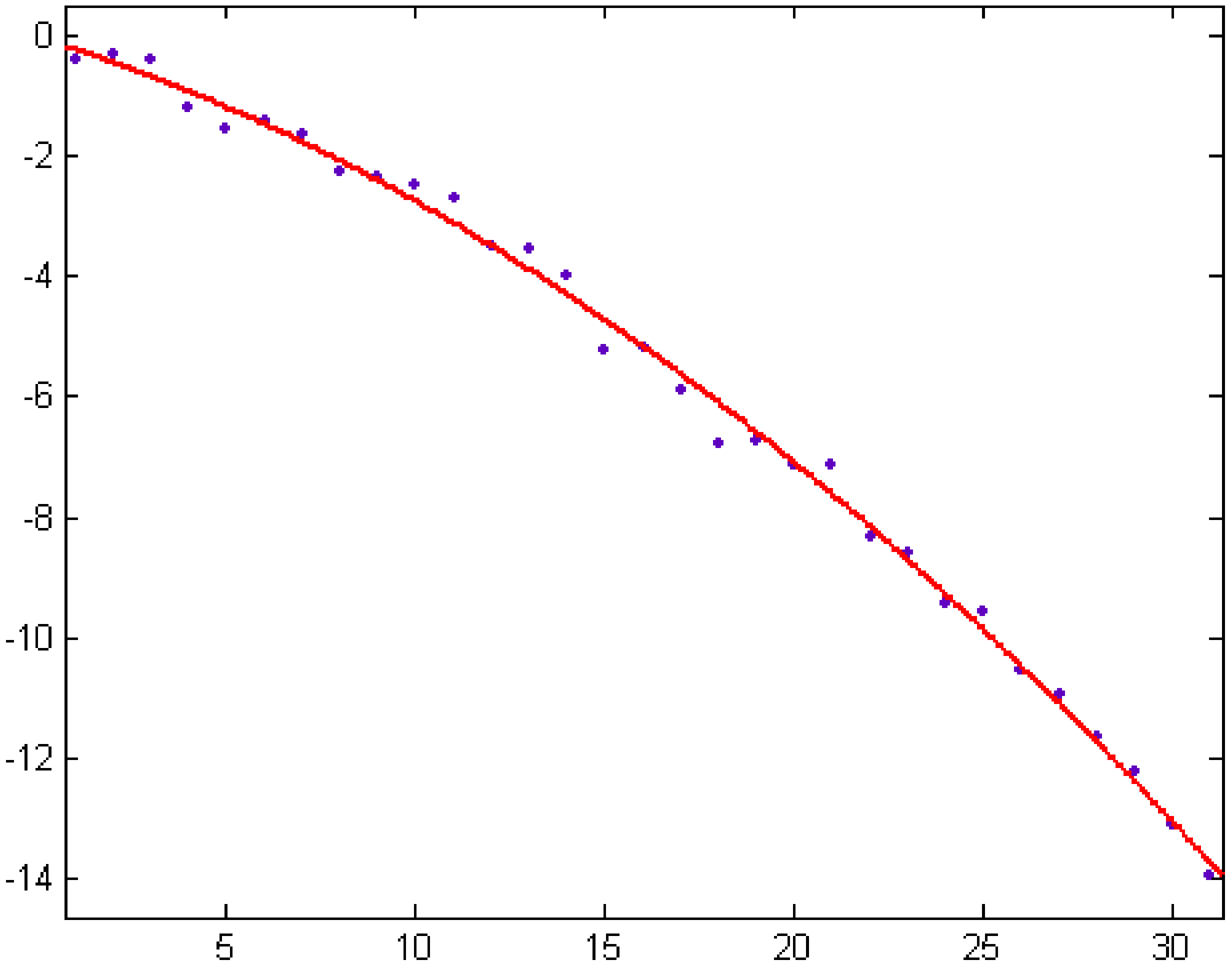

Figure 57

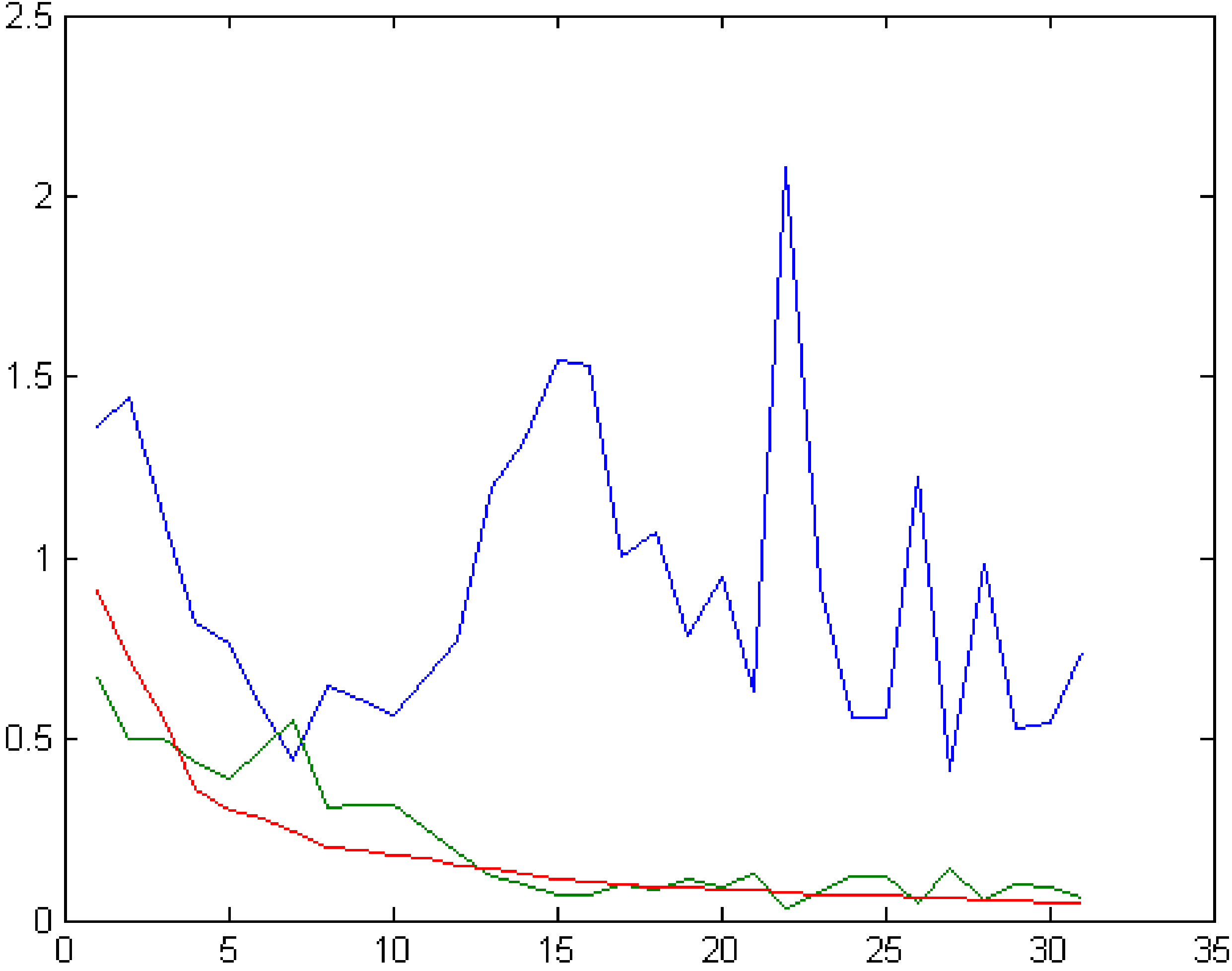

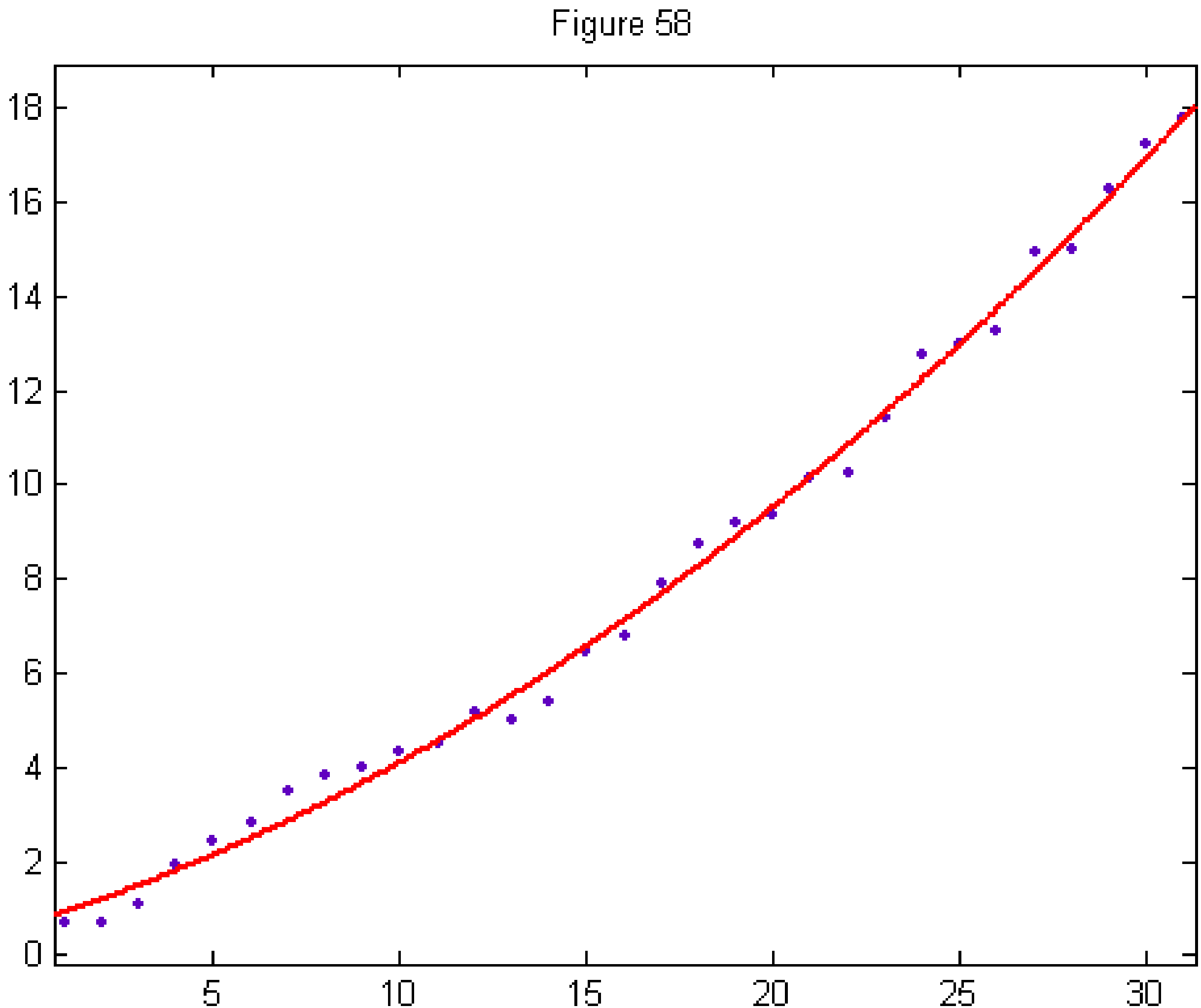
Figure 58
0
2
4
6
8
10
12
14
16
18
5
10
15
20
25
30

Figure 59

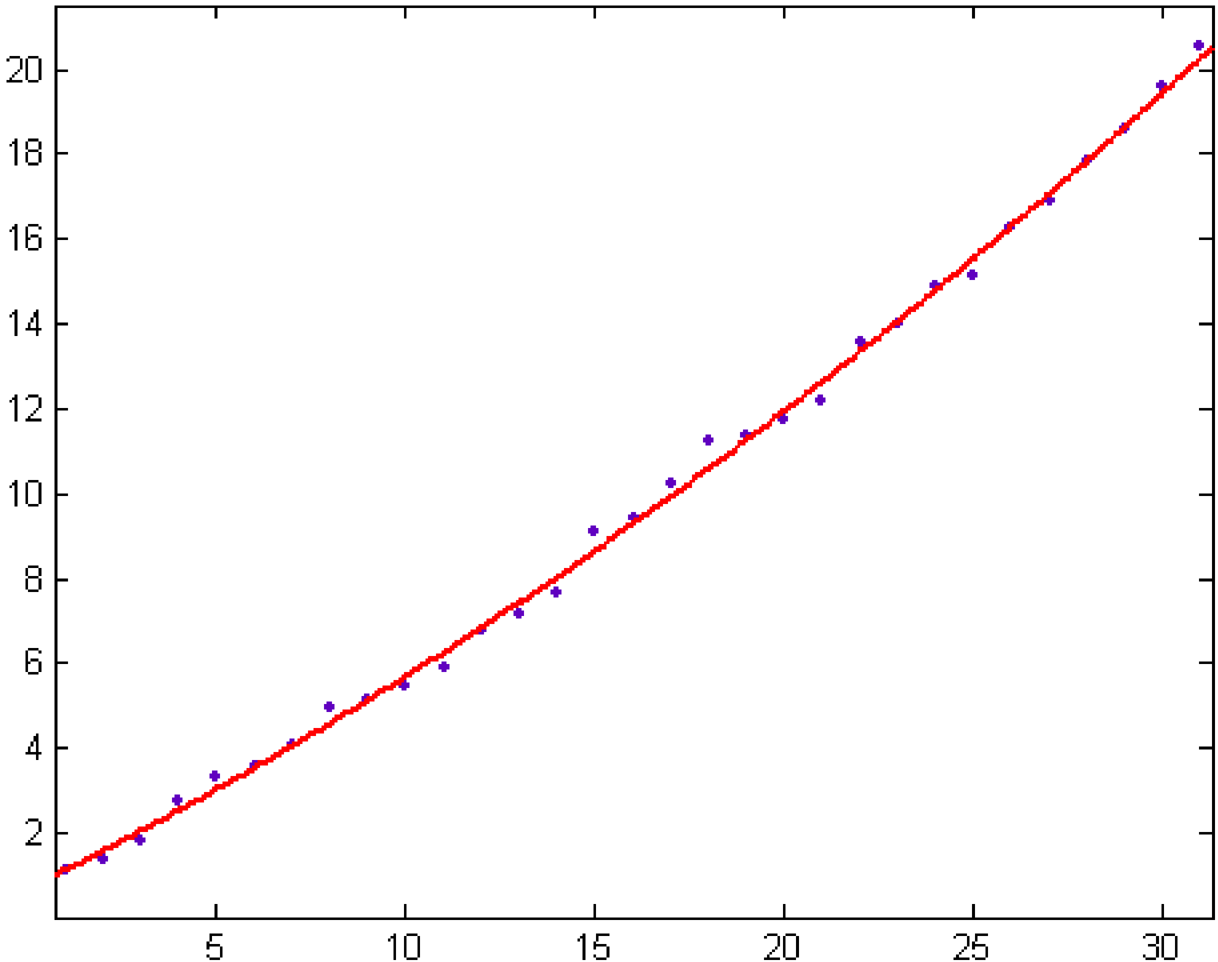

Figure 60

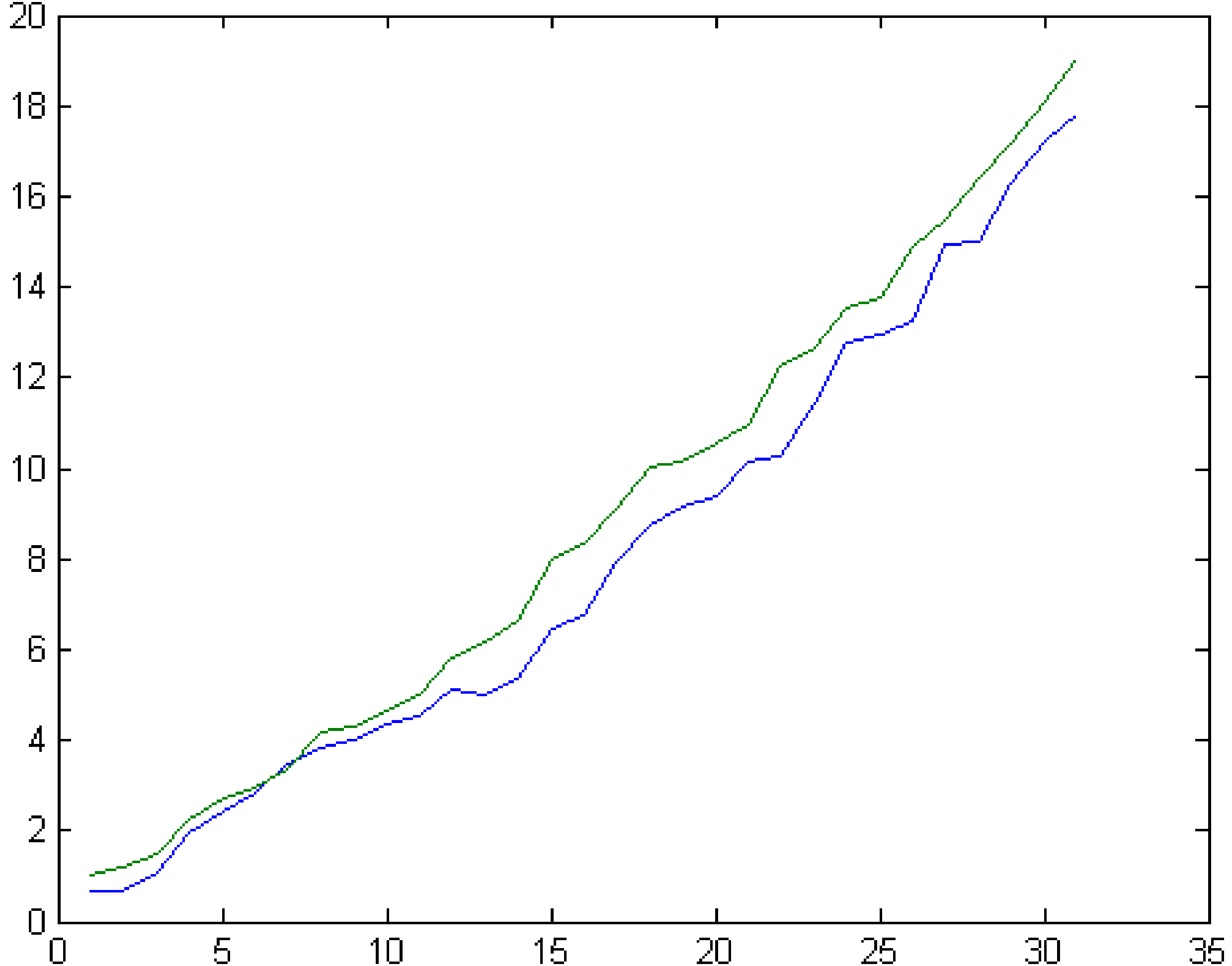

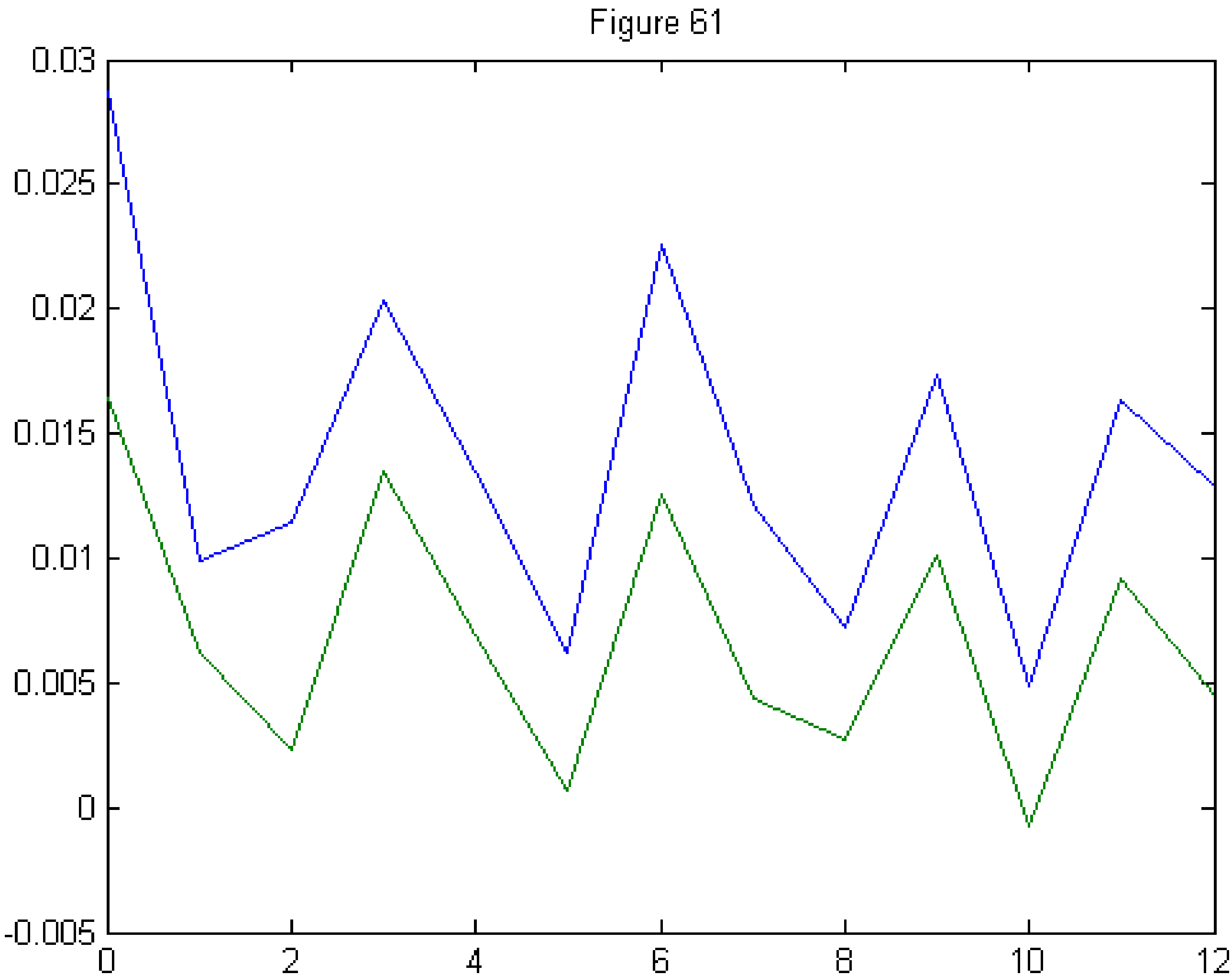
Figure 61
0.03
0.025
0.02
0.015
0.01
0.005
0
-0.005
0
2
4
6
8
10
12

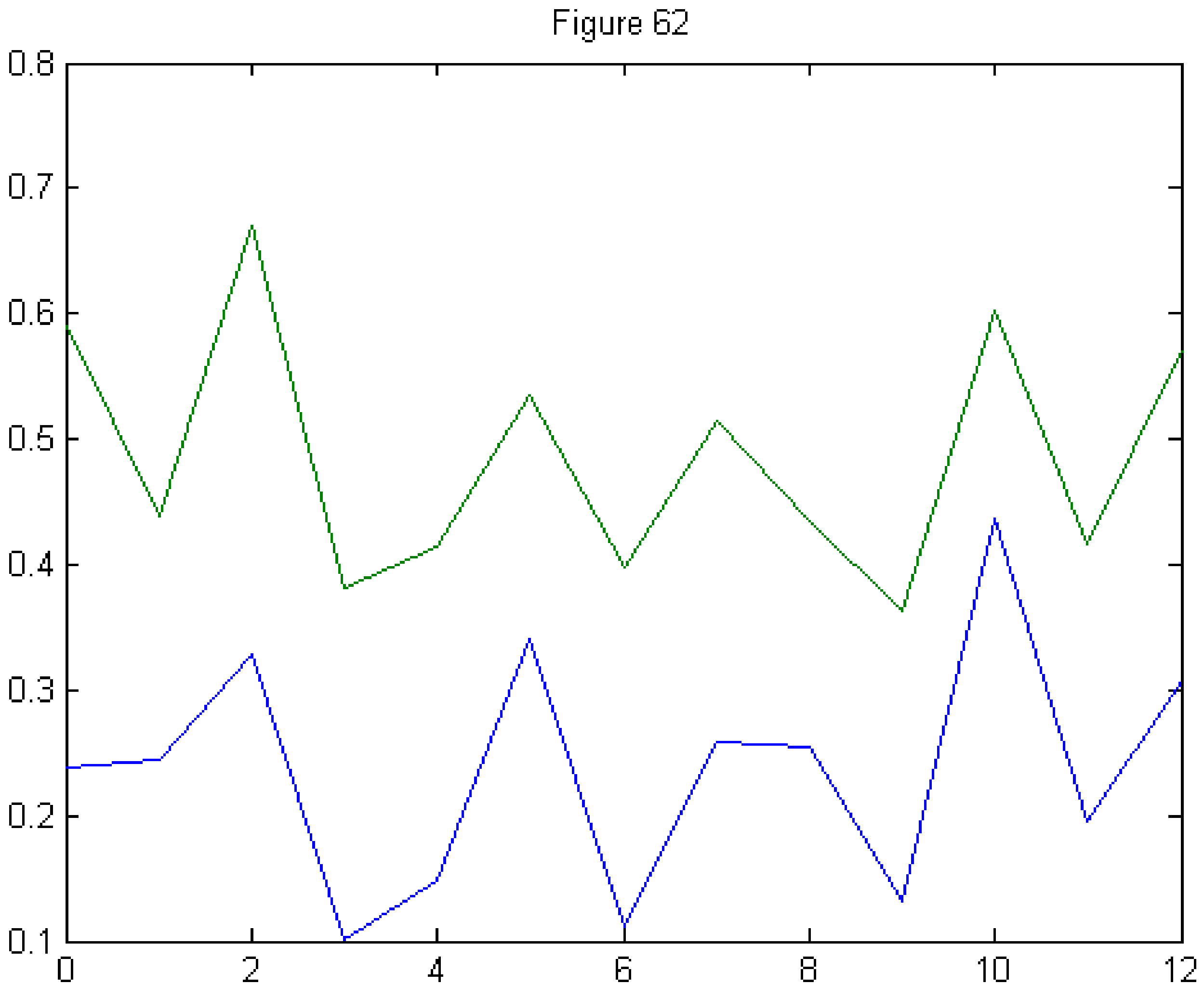
Figure 62
0.8
0.7
0.6
0.5
0.4
0.3
0.2
0.1
0
2
4
6
8
10
12

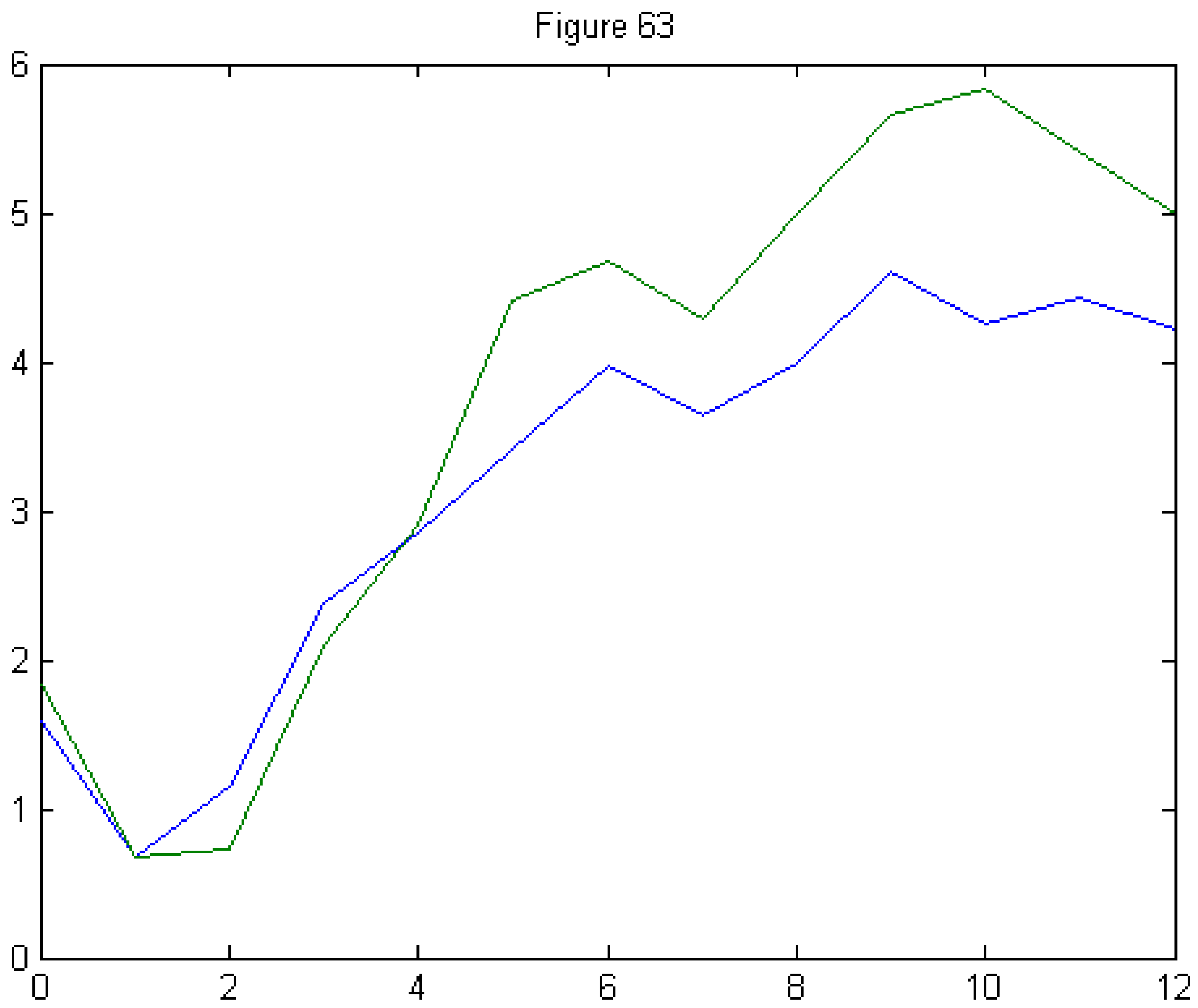
Figure 63
0
1
2
3
4
5
6
0
2
4
6
8
10
12

Figure 64

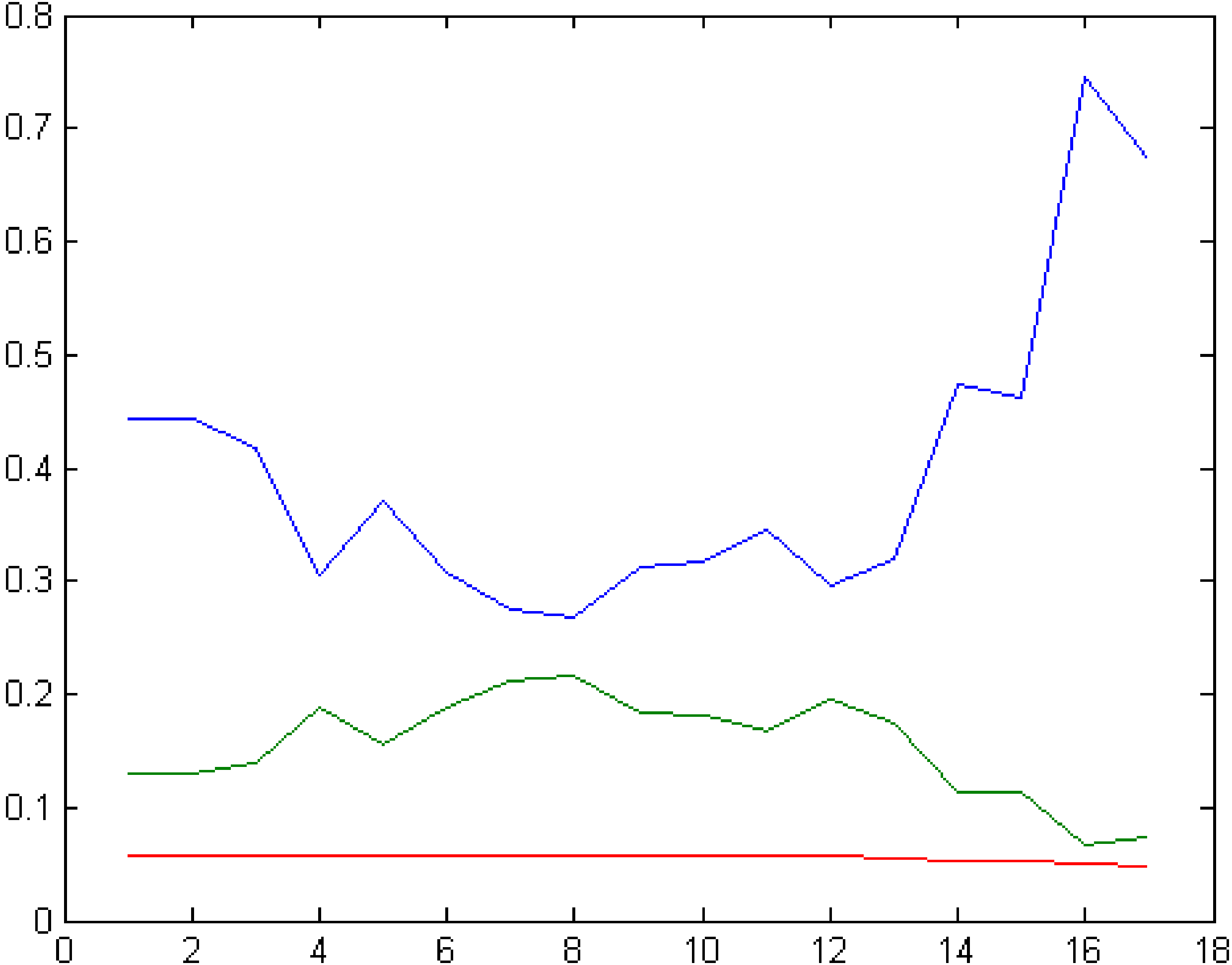

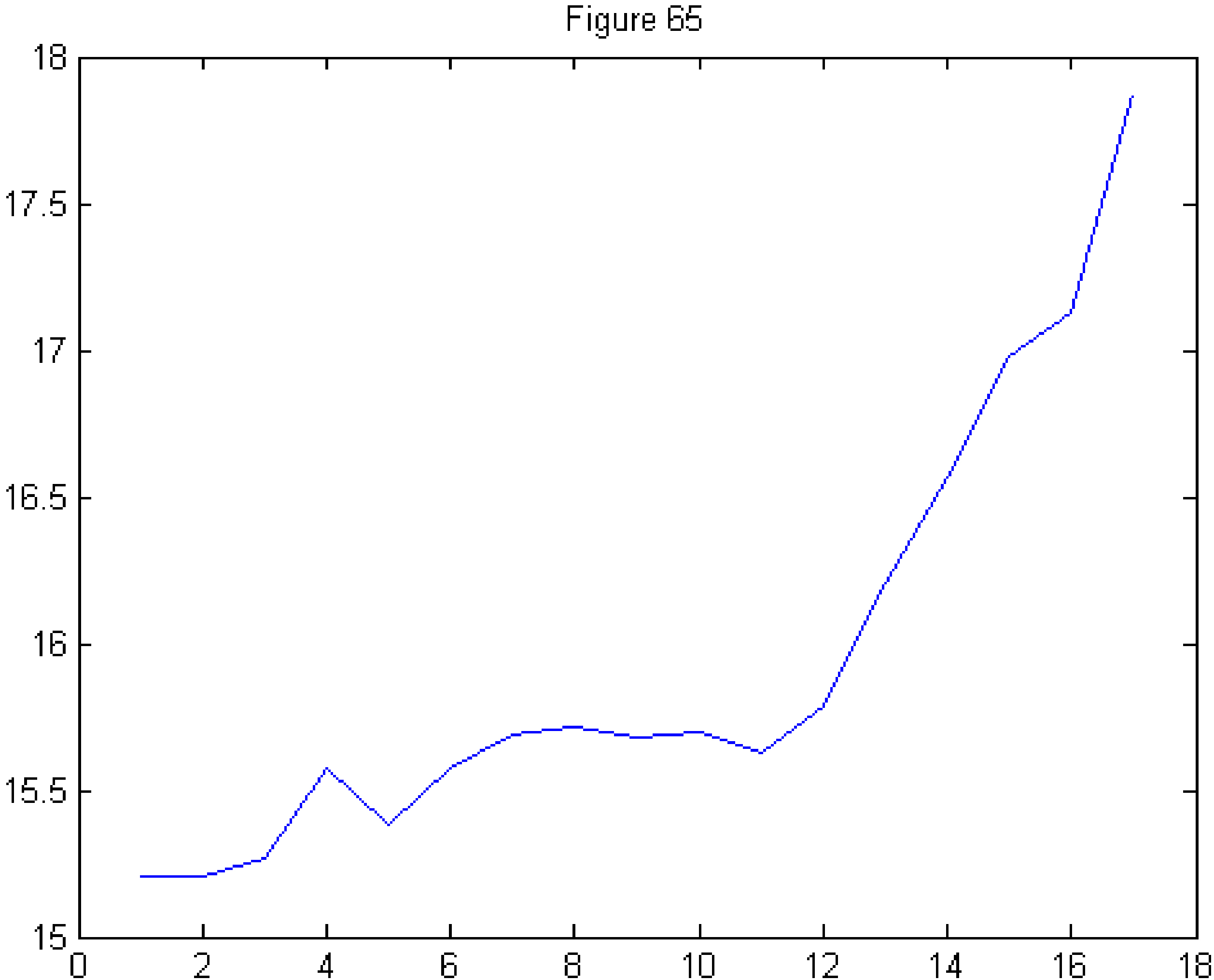
Figure 65
18
17.5
17
16.5
16
15.5
15
0
2
4
6
8
10
12
14
16
18

Figure 66

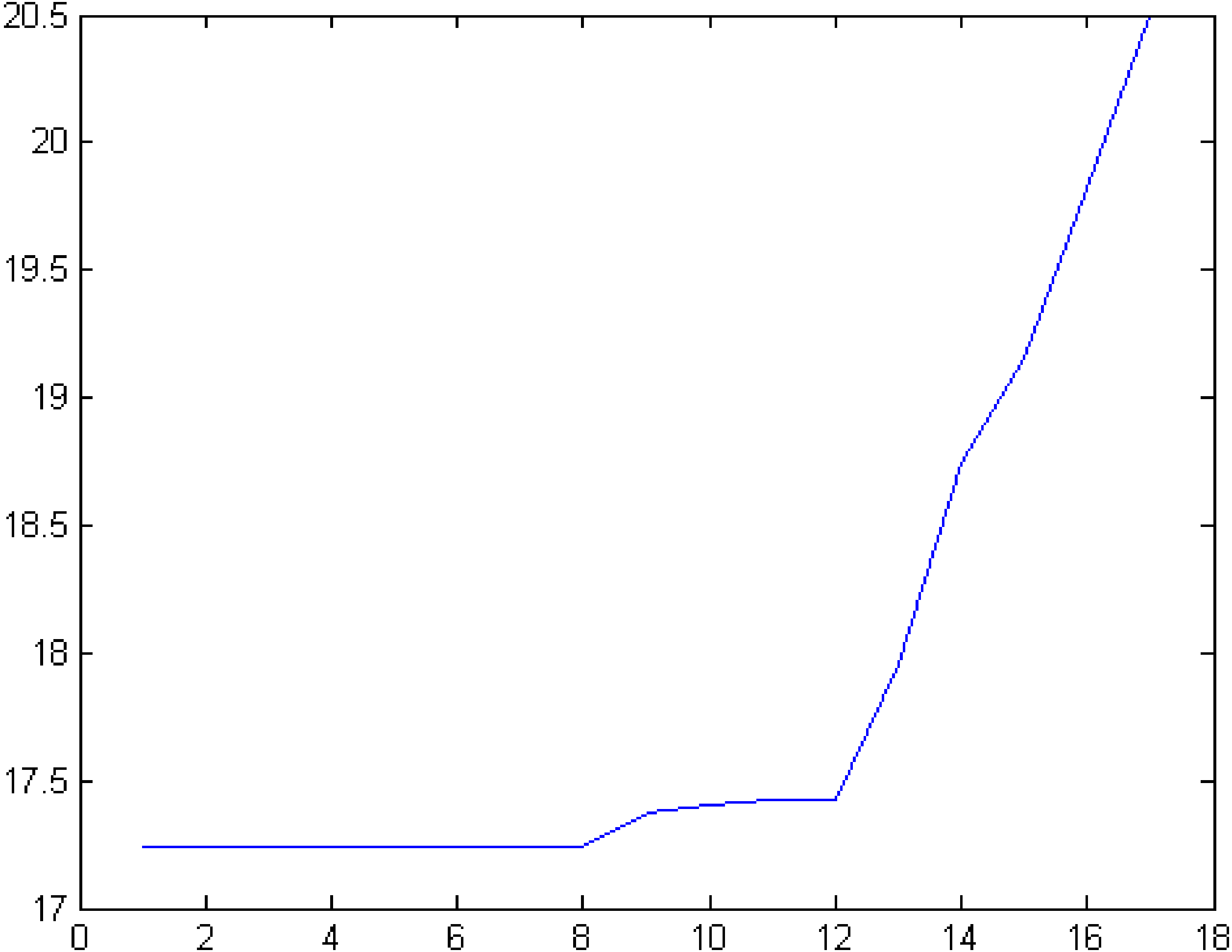

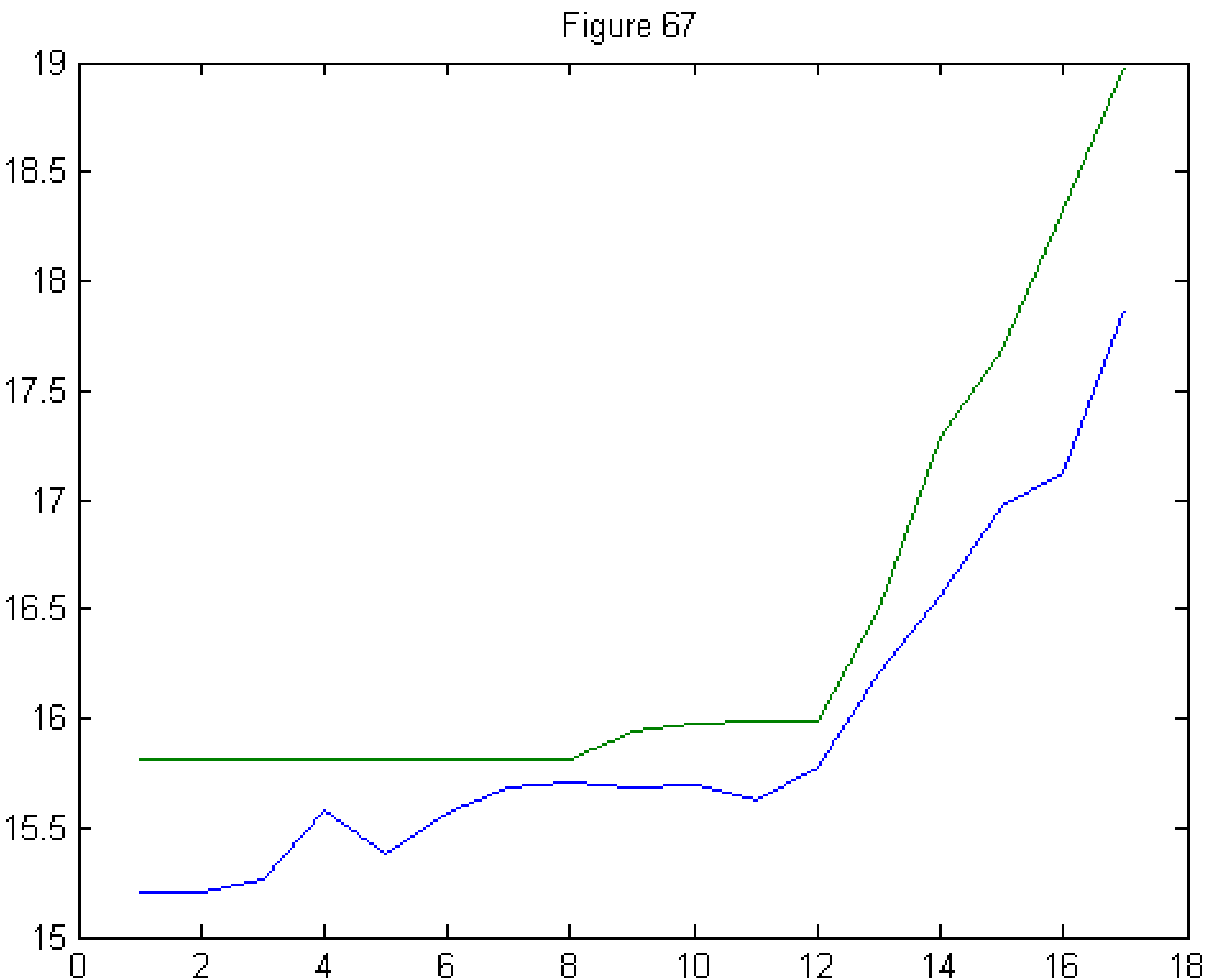
Figure 67
19
18.5
18
17.5
17
16.5
16
15.5
15
0
2
4
6
8
10
12
14
16
18

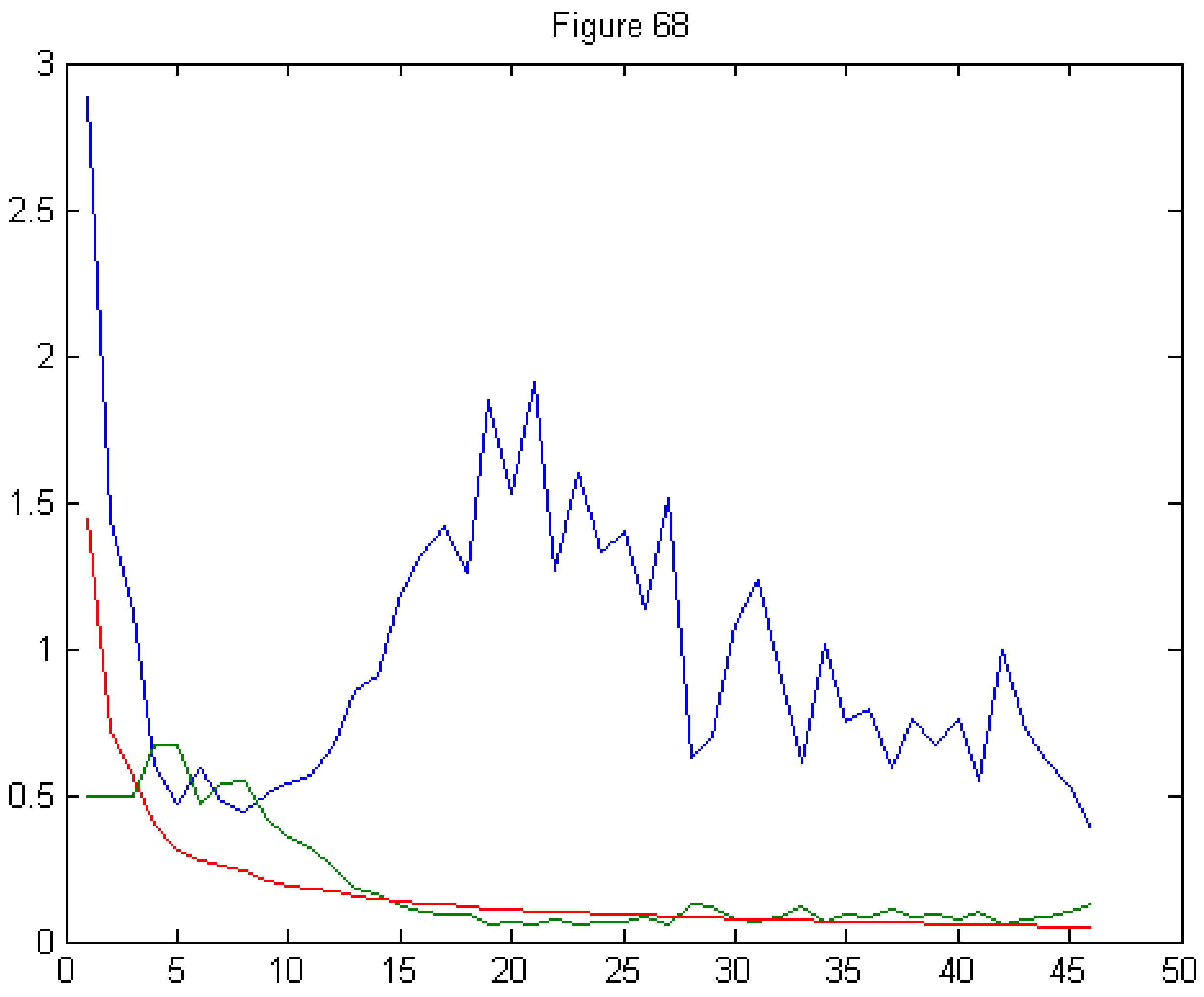

Figure 68
3
2.5
2
1.5
1
0.5
0
0
5
10
15
20
25
30
35
40
45
50

Figure 69

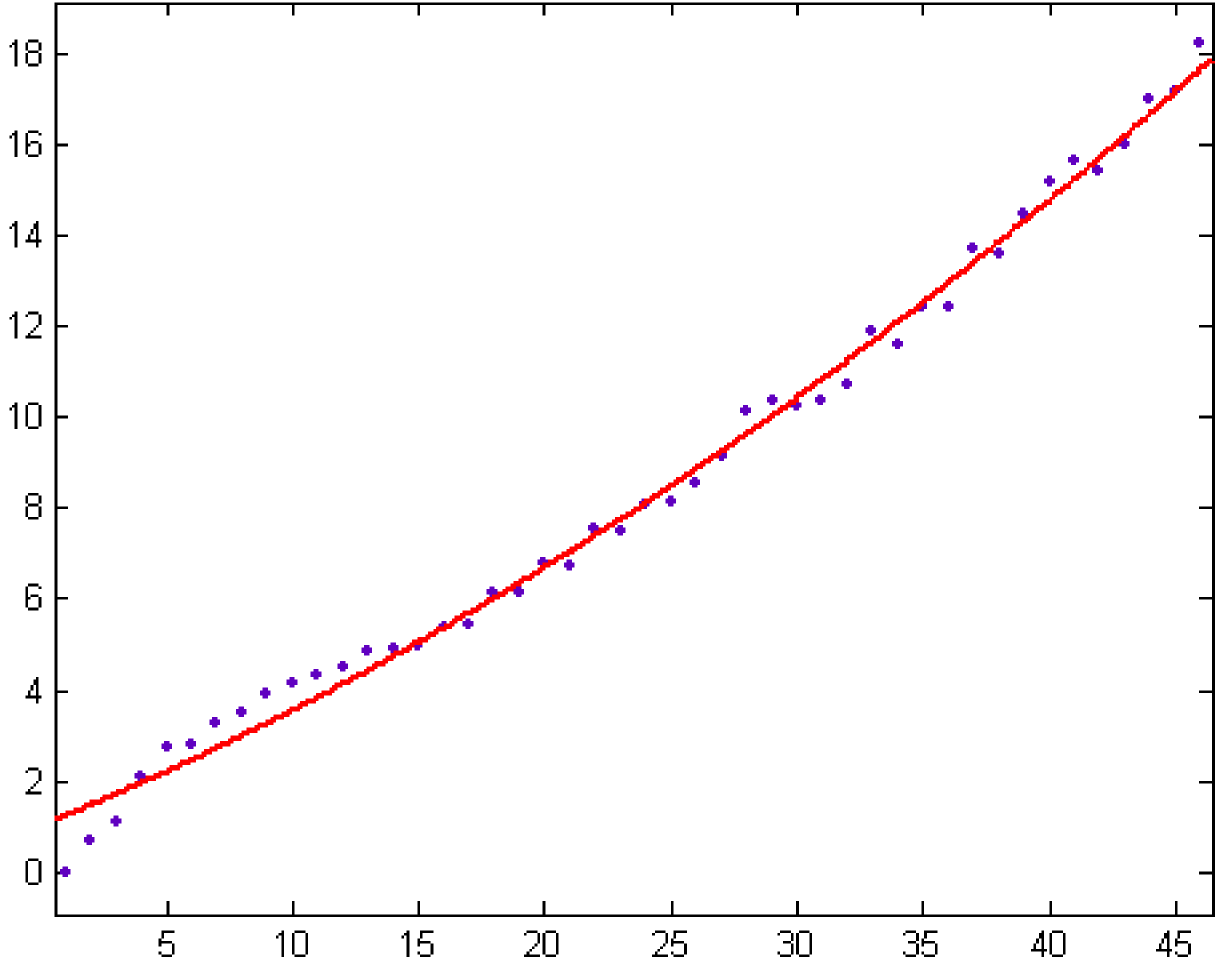

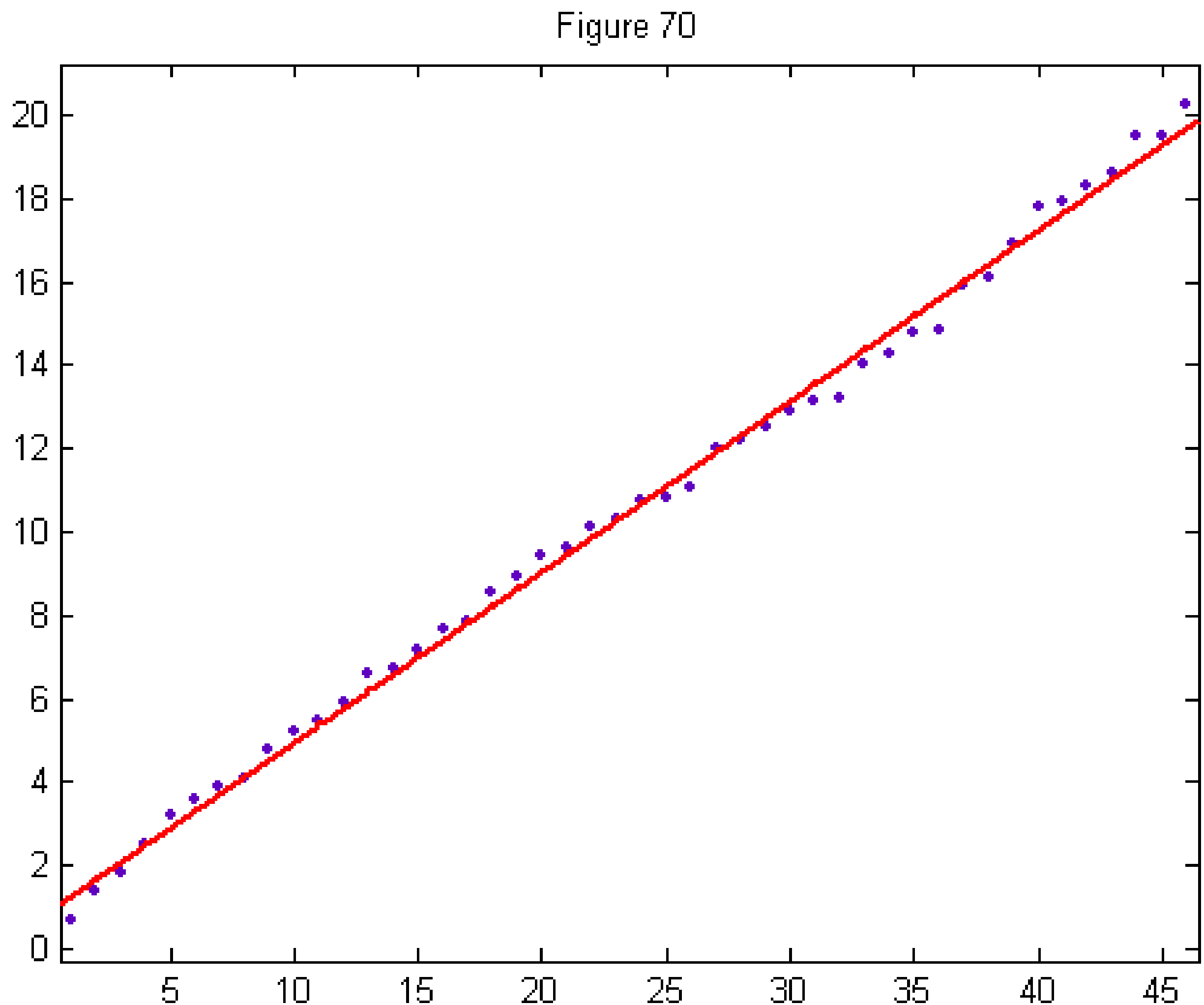
Figure 70
20
18
16
14
12
10
8
6
4
2
0
5
10
15
20
25
30
35
40
45

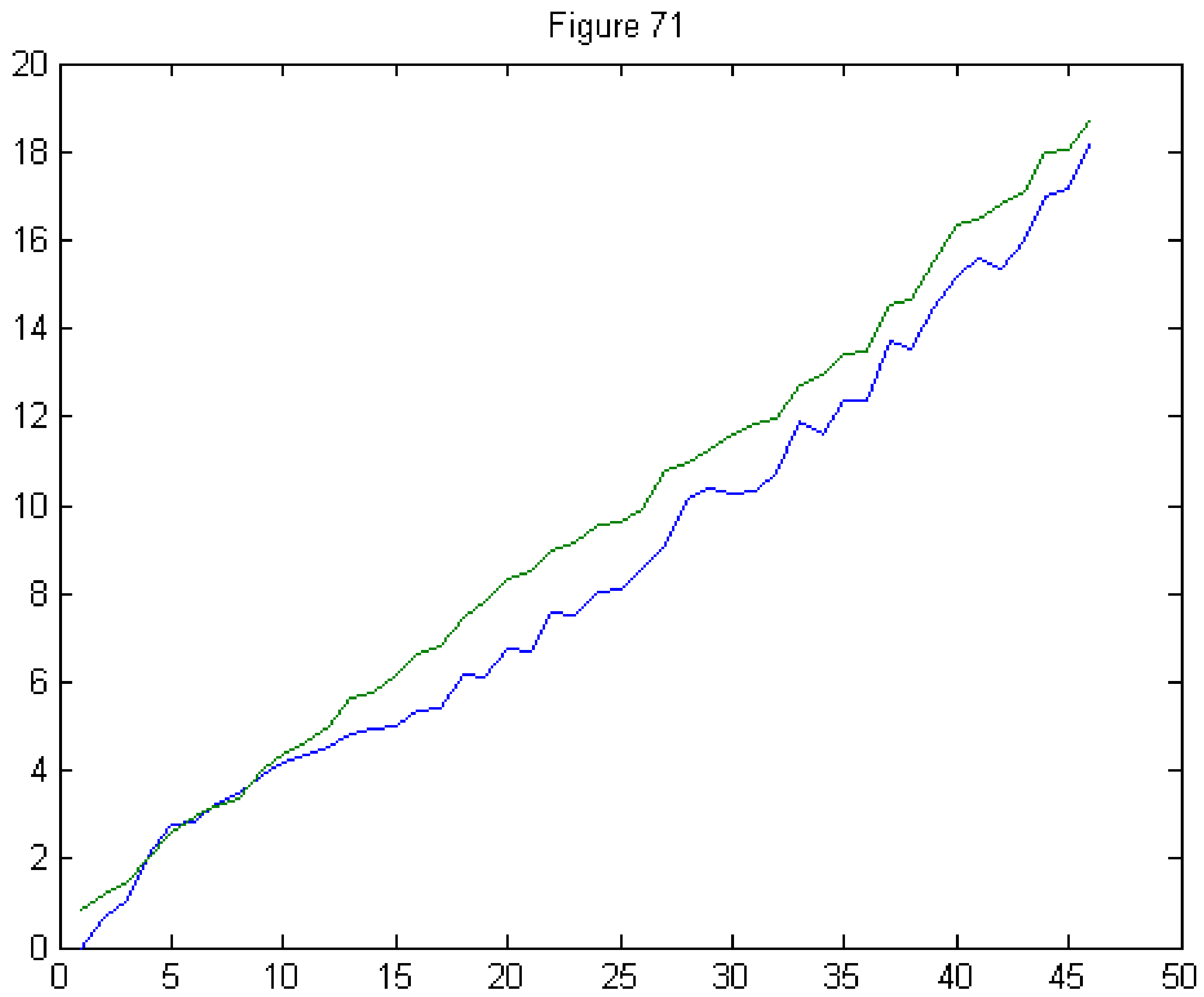
Figure 71
0
2
4
6
8
10
12
14
16
18
20
0
5
10
15
20
25
30
35
40
45
50

Figure 72

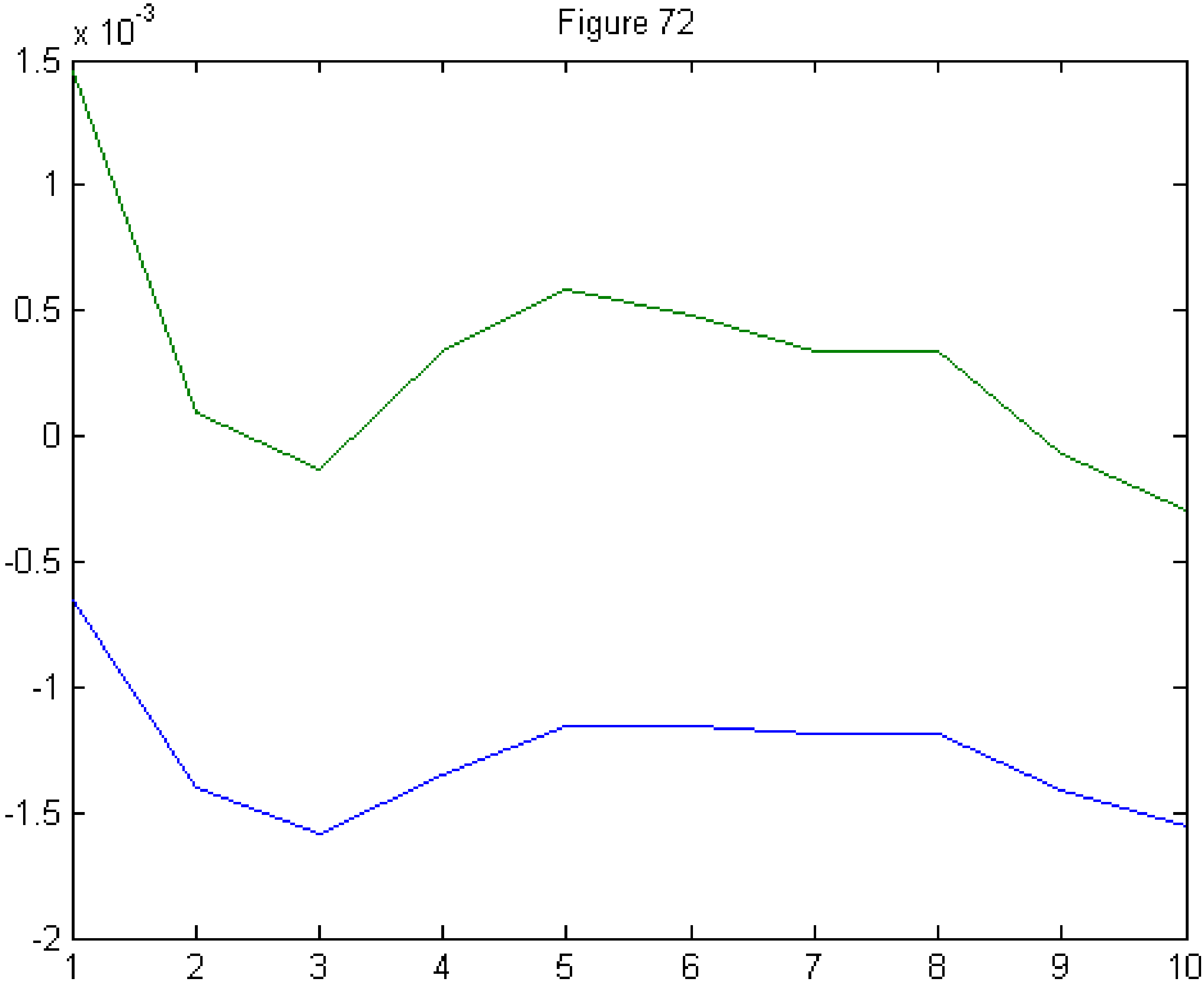

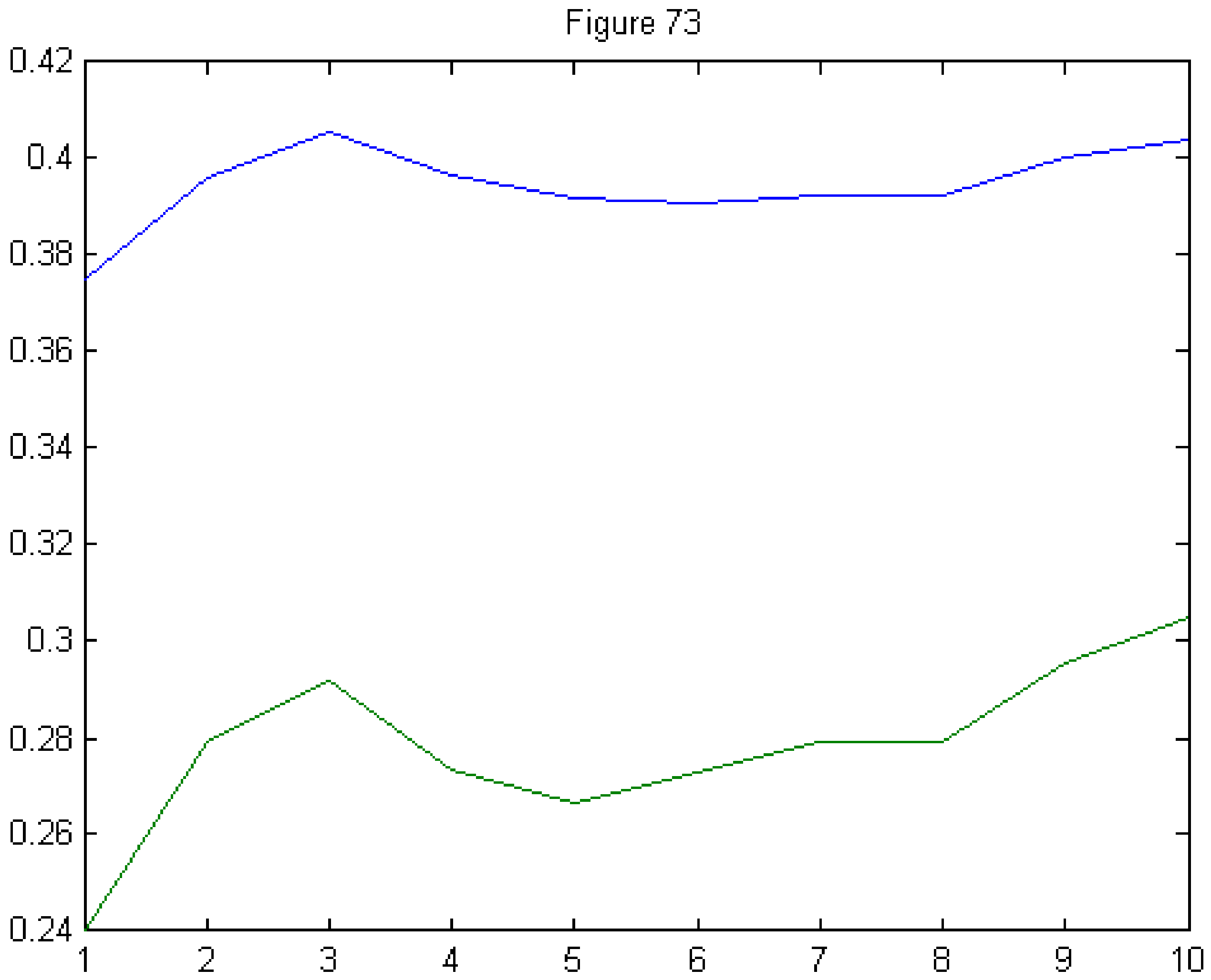
Figure 73
0.42
0.4
0.38
0.36
0.34
0.32
0.3
0.28
0.26
0.24
1
2
3
4
5
6
7
8
9
10

Figure 74

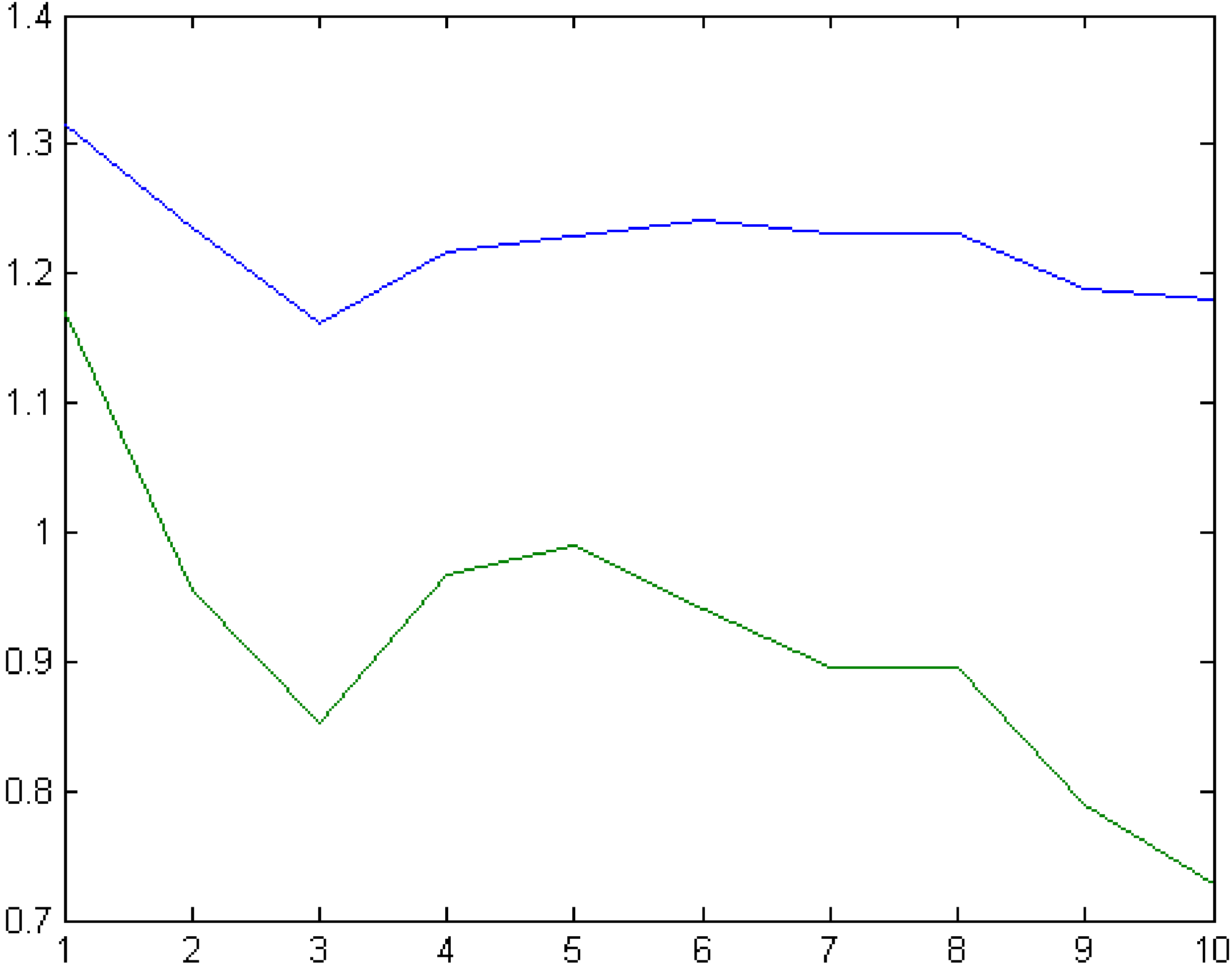

Figure 75

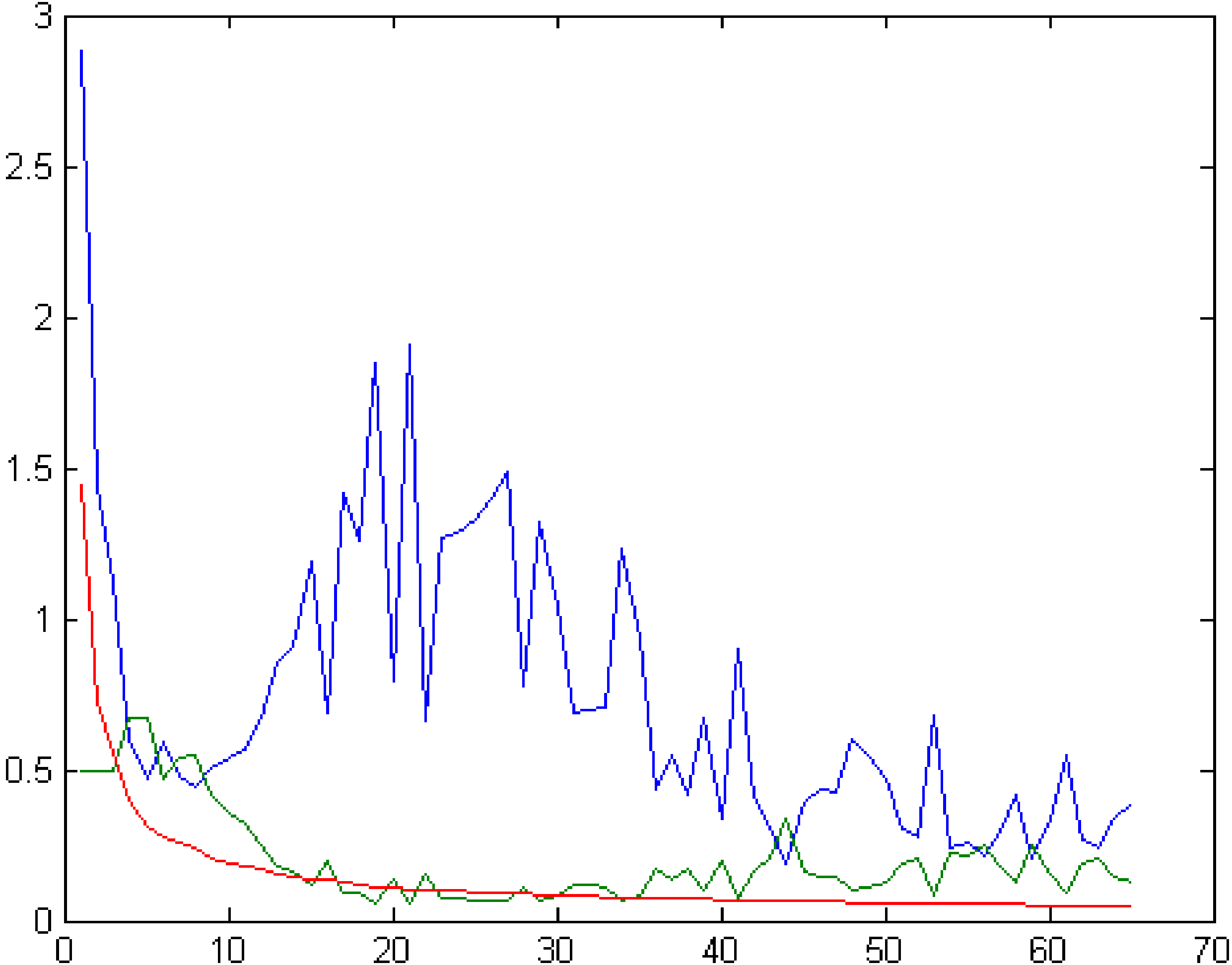

Figure 76

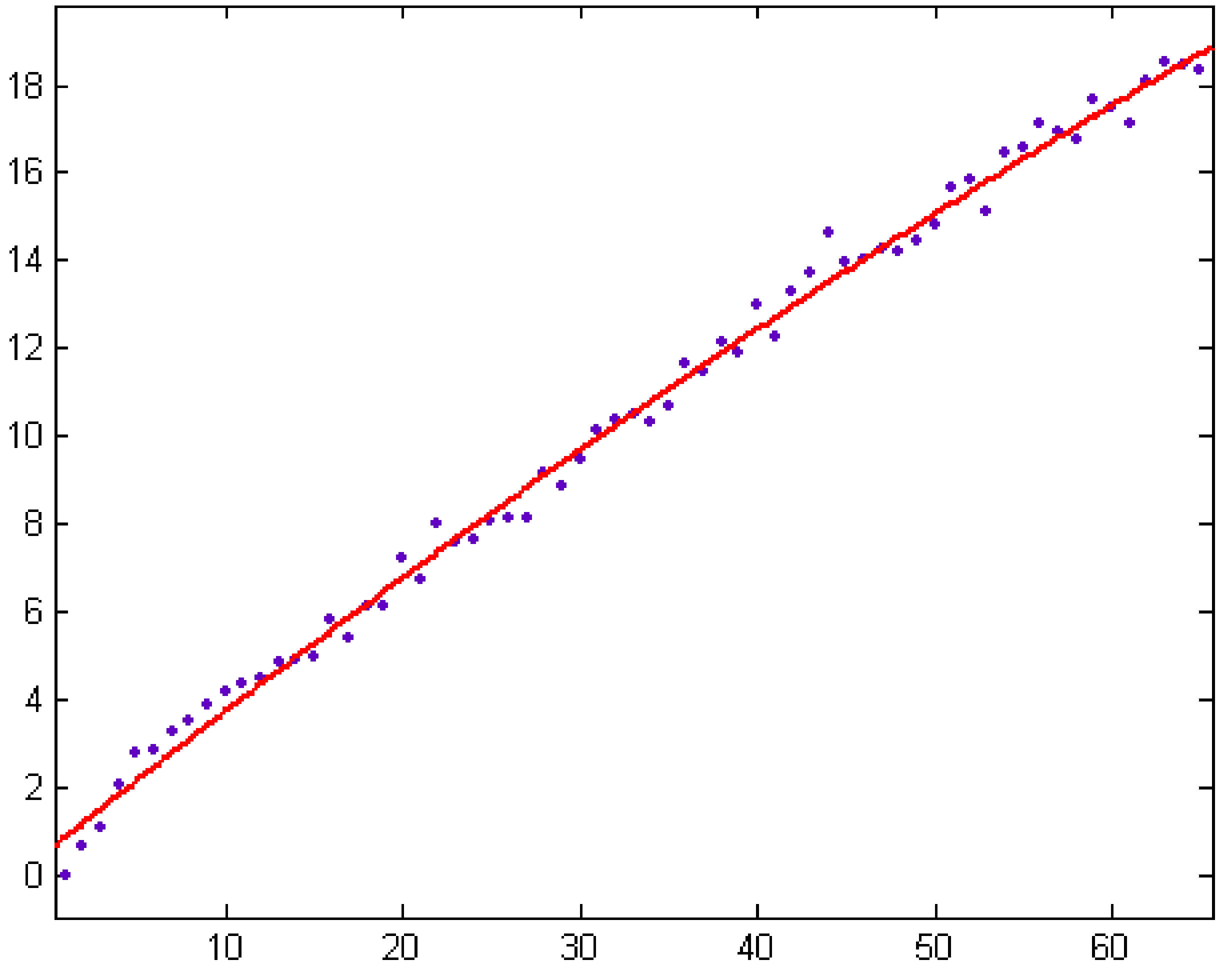

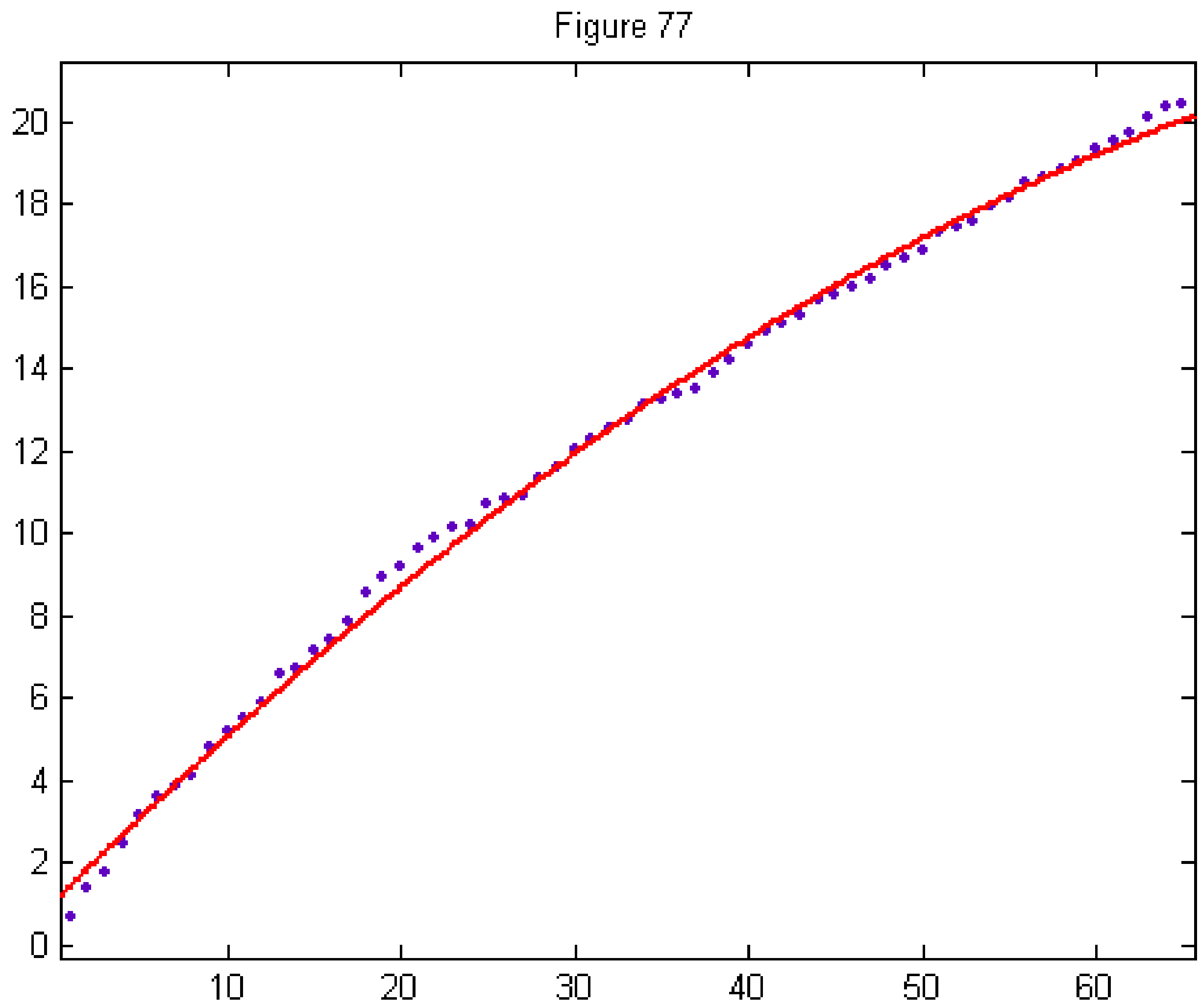
Figure 77
0
2
4
6
8
10
12
14
16
18
20
10
20
30
40
50
60

Figure 78

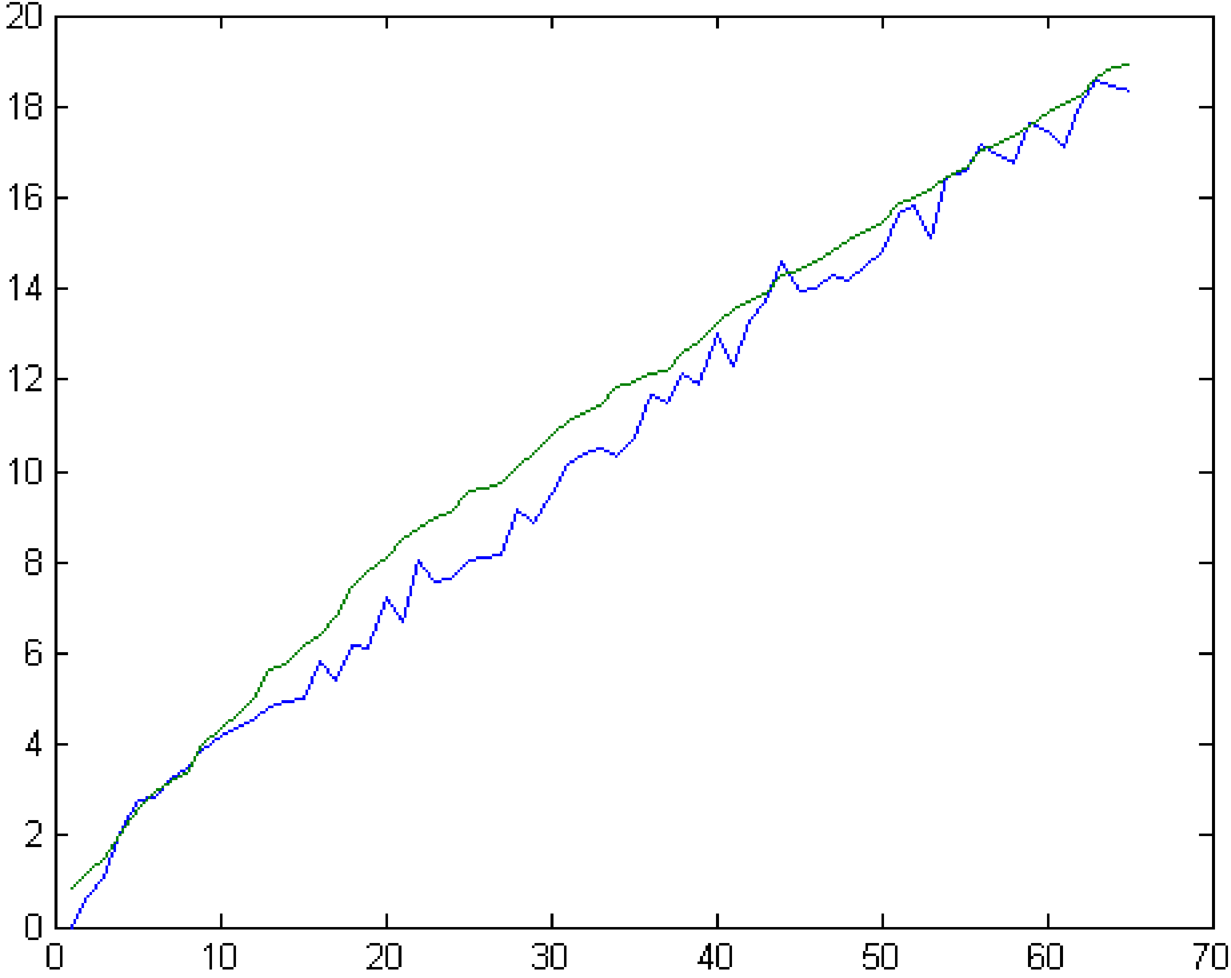

Figure 79

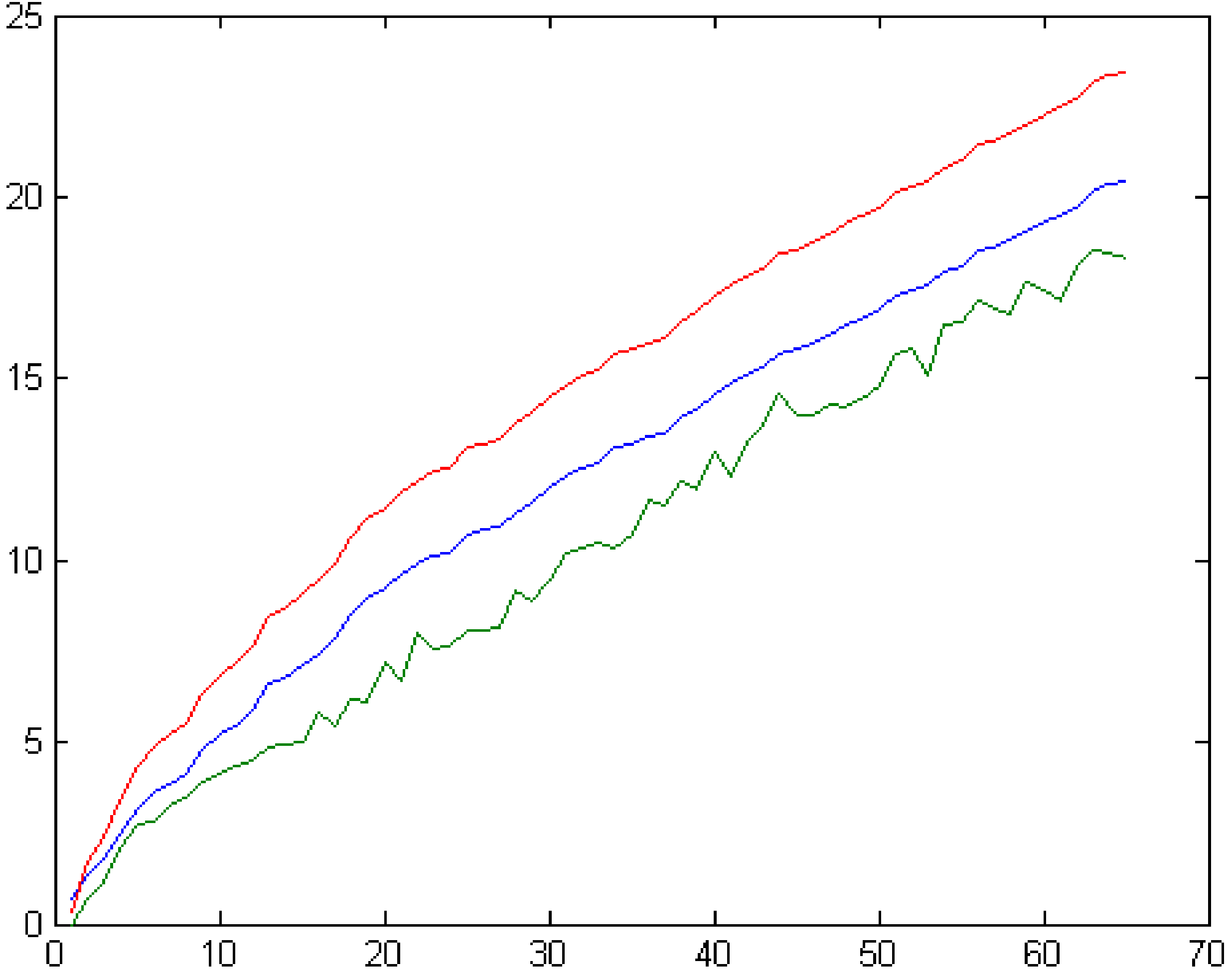

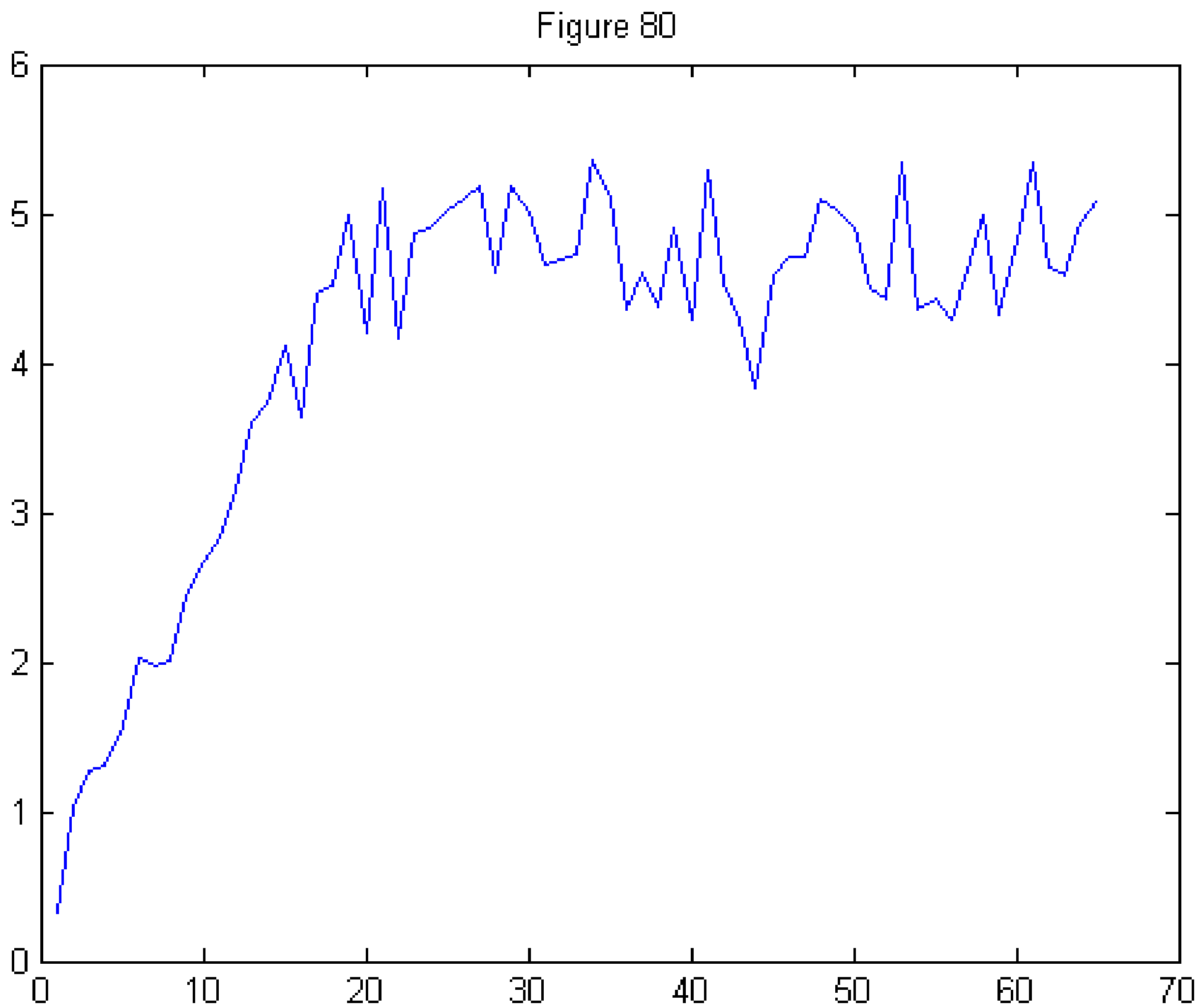
Figure 80
0
1
2
3
4
5
6
0
10
20
30
40
50
60
70

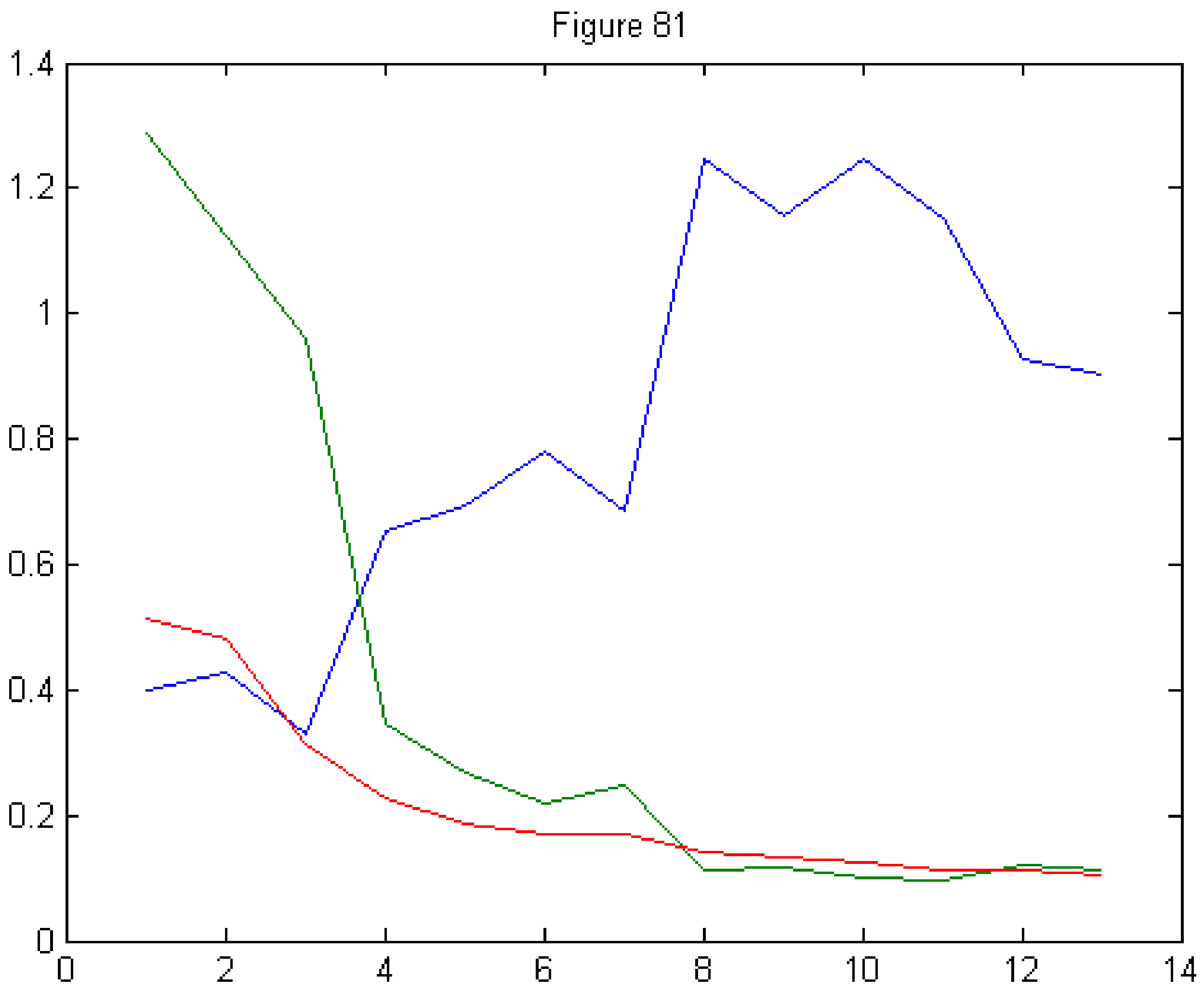
Figure 81
1.4
1.2
1
0.8
0.6
0.4
0.2
0
0
2
4
6
8
10
12
14

Figure 82

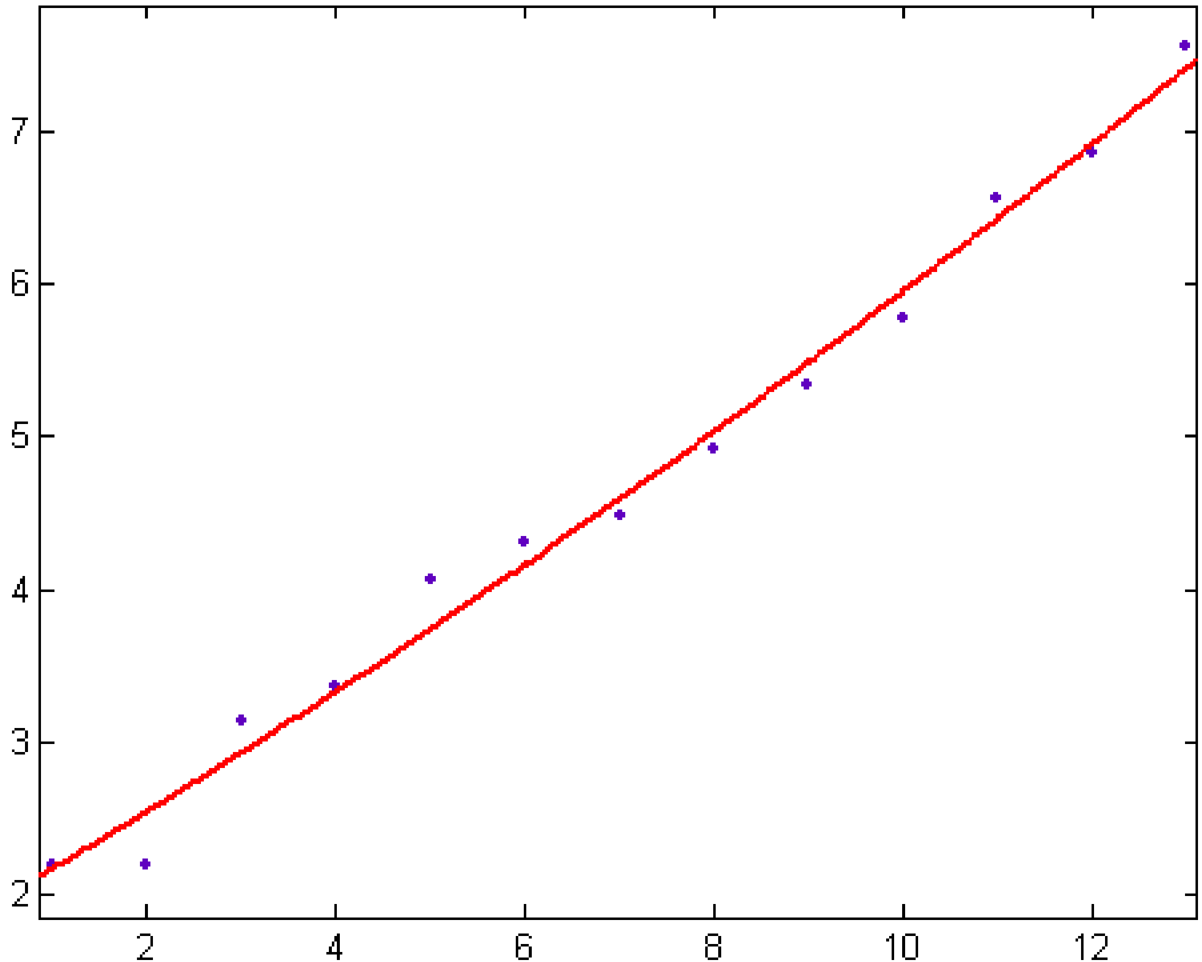

Figure 83

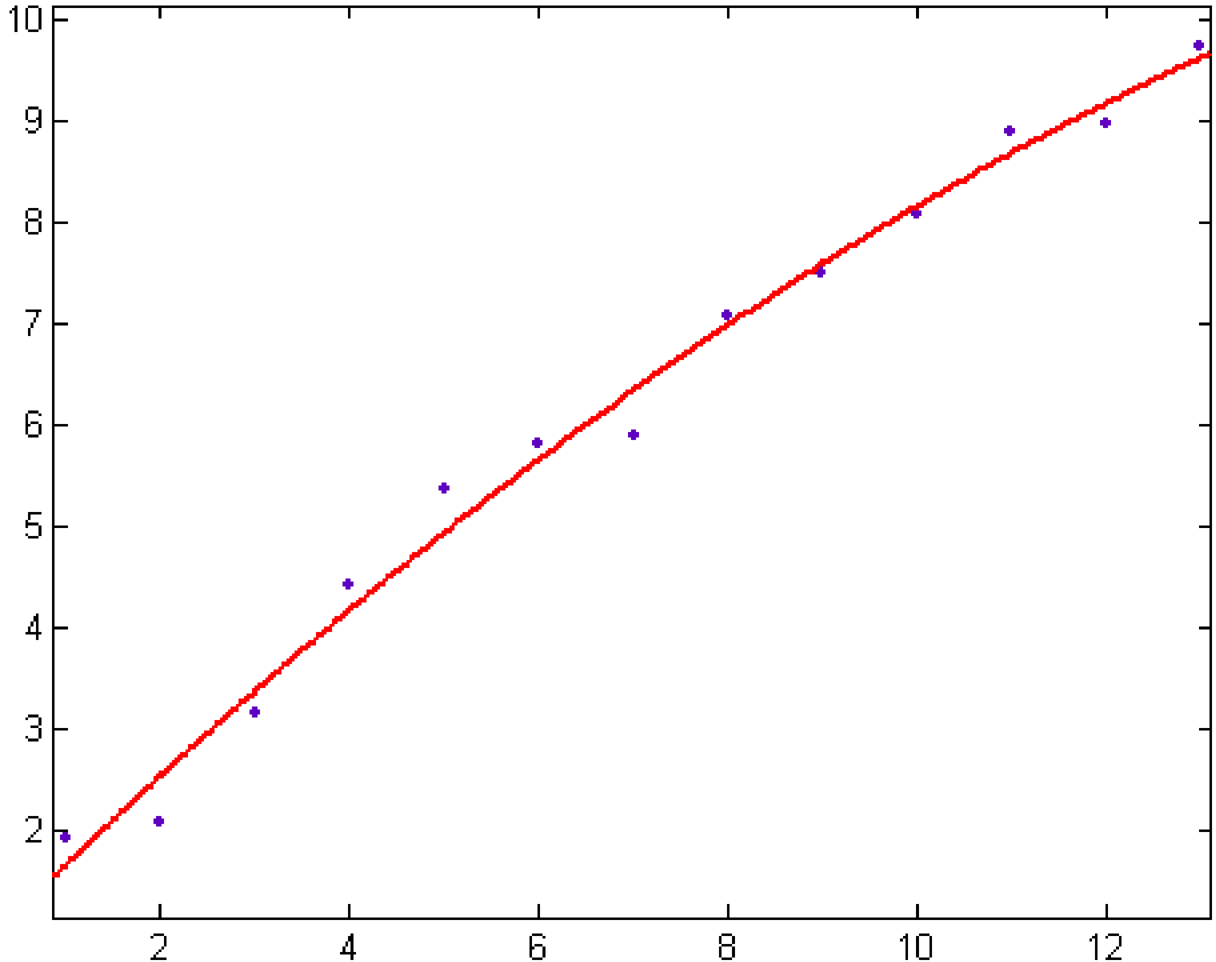

Figure 84